SANDIA REPORT
SAND99–8255
Unlimited Release
Printed October 1999

Using Indicators in Finite Termination Procedures

P. J. Williams, A. S. El-Bakry, and R. A. Tapia

Prepared by
Sandia National Laboratories
Albuquerque, New Mexico 87185 and Livermore, California 94550

Sandia is a multiprogram laboratory operated by Sandia Corporation, a Lockheed Martin Company, for the United States Department of Energy under Contract DE-AC04-94AL85000.

Sandia National Laboratories

Issued by Sandia National Laboratories, operated for the United States Department of Energy by Sandia Corporation.

Available to DOE and DOE contractors from
Office of Scientific and Technical Information
P.O. Box 62
Oak Ridge, TN 37831

Prices available from (703) 605-6000
Web site: http://www.ntis.gov/ordering.htm

Available to the public from
National Technical Information Service
U.S. Department of Commerce
5285 Port Royal Rd
Springfield, VA 22161

NTIS price codes
Printed copy: A12
Microfiche copy: A01

SAND99-2017
Unlimited Release
Printed August 1999

Advanced Blade Manufacturing Project
Final Report

Robert Z. Poore
Kamzin Technology, Inc.
425 Pontius Avenue North, Suite 150
Seattle, WA 98109

Sandia Contract – AN-0166

ABSTRACT

The original scope of the project was to research improvements to the processes and materials used in the manufacture of wood-epoxy blades, conduct tests to qualify any new material or processes for use in blade design and subsequently build and test six blades using the improved processes and materials. In particular, ABM was interested in reducing blade cost and improving quality. In addition, ABM needed to find a replacement material for the mature Douglas fir used in the manufacturing process. The use of mature Douglas fir is commercially unacceptable because of its limited supply and environmental concerns associated with the use of mature timber. Unfortunately, the bankruptcy of FloWind in June 1997 and a dramatic reduction in AWT sales made it impossible for ABM to complete the full scope of work. However, sufficient research and testing were completed to identify several promising changes in the blade manufacturing process and develop a preliminary design incorporating these changes.

Acknowledgments

The author would like to thank all of following people who have contributed to the successful completion of this research: Tom Ashwill, Dennis Harrison, Mike Zuteck, Dayton Griffin, Jerry Lafave, Jim Derosher, Billie Blades, Bill Bertelsen, Meade Gougeon, and Ron Roesler. While all of those listed made significant contributions, the author would like to particularly acknowledge the dedication and commitment of the ABM and AWT employees who spent many months completing this research under the constant cloud of uncertainty concerning the future of the organizations. Without their commitment and dedication it would not have been possible to complete this work.

Table of Contents

Table of Figures

Table of Tables

Appendices

Executive Summary

In January, 1997 FloWind Corporation was awarded a contract by the United States Department of Energy, through Sandia National Laboratories (Sandia), to develop improved manufacturing processes for wind turbine blades. The work was to be completed by Advanced Blade Manufacturing (ABM), a FloWind subsidiary. The objective of the Sandia Blade Manufacturing Program (BMP) was to "Promote the development of advancements in the manufacturing of utility-grade wind turbine blades in ways that significantly lower blade costs and improve their quality and reliability." This report documents the work completed by ABM on the FloWind BMP project.

The original scope of the project was to research improvements to the processes and materials used in the manufacture of wood-epoxy blades, conduct tests to qualify any new material or processes for use in blade design and subsequently build and test six blades using the improved processes and materials. In particular, ABM was interested in reducing blade cost and improving quality. In addition, ABM needed to find a replacement material for the mature Douglas fir used in the manufacturing process. The use of mature Douglas fir is commercially unacceptable due to a very limited supply and environmental concerns associated with the use of mature timber.

Unfortunately, due to the bankruptcy of FloWind in June 1997 and a dramatic reduction in Advanced Wind Turbines (AWT) sales, ABM was not able to complete the full scope of work. ABM was able to complete sufficient research and testing to identify several promising changes in the blade manufacturing process and develop a preliminary design incorporating these changes.

Baseline Turbine and Blade Description

The baseline turbine is the AWT-27. It is a downwind, free-yaw machine. The blades are lofted from NREL S825/S809/S810 thick-airfoil sections and are made of wood-epoxy laminates, reinforced with carbon fiber. The rotor is a teetered, two-bladed, fixed-pitch, stall-regulated design. It has a diameter of 27.4 m (90 ft) and has a nominal speed of 53 rpm. The rotor is connected directly to the gearbox mainshaft, and the gearbox increases the mainshaft speed to 1800 rpm, driving a three-phase, 60 Hz, 480 volt, induction generator.

The blades are constructed from wood/epoxy laminates with two shells bonded together with an inner vertical shear web. Carbon fiber is used in some of the laminations on the tension side, and the shells are sealed on the inner and outer surfaces with a layer of fiberglass. The outer surface is gelcoat. The number of laminations varies along the blade length in response to the load spectrum seen by each station on the blade. Due to the length of the blade, each laminate layer has multiple span-wise joints along the length of the blade. These joints are staggered between layers. In the most highly loaded layers, the ends of the veneer sheets are scarfed to improve the strength of the joints. In less heavily loaded veneer layers the veneer sheets are placed end-end, with no pre-treatment, to create butt joints.

Summary of Findings

The research completed identified several significant improvements to the blade design and manufacturing process. The most significant findings were:

1. Pre-sealing the scarfed joints in the blade shell sufficiently increased the joint strength to allow elimination of the carbon reinforcement from the design. This resulted in a significant cost savings.

2. Use of heat during the blade molding process will accelerate the epoxy cure sufficiently to allow the existing manufacturing facility to operate on two shifts rather than a single shift. This effectively doubles blade production with a modest capital investment.

3. The use of fumed silica as an epoxy extender will permit a 20% reduction in the amount of resin used in the blade and an associated cost savings.

4. Several additional improvements in the blade manufacturing process were developed which will increase manufacturing flexibility, improve blade quality and decrease the labor required to produce a blade.

5. Both Loblolly southern pine and new growth Douglas fir were tested as candidates to replace the mature Douglas fir currently used. Neither was found to be acceptable. Loblolly Pine may be a suitable candidate if it is used in conjunction with extended epoxy to reduce epoxy absorption. This was not tested due to resource limitations. An alternative second growth Douglas fir was identified late in the program which may be a suitable candidate as well.

6. The quality of the blade laminate produced is heavily dependent on material characteristics not generally published, such as their tendency to absorb epoxy. In addition, variables such as the age of the tree from which the veneer is made appears to have an impact. These variables, coupled with the inherent variability found when working with natural materials, dictate thorough testing of any change in the materials or processes used in manufacturing the blades.

Cost Reductions Identified

For single shift operation (750 blades per year or less) the project identified improvements which would reduce blade cost approximately $500 (8%) and would require a capital investment of approximately $103,500. At full single shift capacity this would provide a first year return on investment of approximately 366%. If the plant were operating at one third capacity there would be a positive return on investment in the first year.

For higher blade capacities and dual shift operation (1,500 blades per year) the project identified improvements which would reduce blade cost approximately $875 (14%) and would require a capital investment of approximately $507,000. At full single shift capacity this would provide a first year return on investment of approximately 260%. Operation at full two shift capacity would not be required to warrant the initial investment to move to two shift operation.

Conclusions and Recommendations

This project identified several significant improvements in the technology for manufacturing wood epoxy wind turbine blades which result in substantial reductions in the cost of the blades. However, the project was not successful in identifying an alternative material to replace the mature Douglas fir presently used in the blades. Several promising candidates beyond those tested were identified by the project, but resource limitations precluded testing them.

The wind turbine market has changed substantially since this project was originally proposed and the market for AWT and ABM products has decreased. This, together with the problems associated with FloWind's bankruptcy, have resulted in AWT and ABM being shut down.

Despite the failures of ABM and AWT, the technical potential for wood epoxy technology in wind turbine blade manufacture is significant. The wood epoxy material, when properly manufactured, offers a combination of light weight, relatively low cost and high strength not available in other known materials. As wind turbines continue to develop into larger diameters, these properties are expected to become even more desirable.

The technology also continues to have serious commercial limitations. These can generally be classified as a lack of market acceptance due in part to the technical limitations of the materials. It is therefore suggested that a careful assessment of the barriers to commercialization of the technology in the wind turbine market be completed prior to any further research on the technology. The technical advantages of the technology are very attractive; however, the commercial limitations of the technology should be understood and additional technical research directed toward addressing these limitations. Areas which may warrant further research include:

- Identification of a suitable wood species which is available in many parts of the world
- Examination of approaches to making blades with easily varied lengths
- Examination of techniques for making blades which will have round roots and be more readily accepted by existing turbine manufacturers
- Examination of the benefits available from wood epoxy as turbines increase in size.

If these limitations can be addressed, or the benefits of wood epoxy can be shown to be large enough, the market will accept it and the technology can play a major role in the world wind energy industry.

1. Introduction and Background

1.1 Background

Advanced blade Manufacturing (ABM) was established in 1995 to build wood-epoxy blades for the AWT-26 and AWT-27 wind turbines designed by Advanced Wind Turbines (AWT) and marketed by FloWind Corporation (FloWind). FloWind is the parent company of both ABM and AWT. During 1995 and 1996 ABM built almost 200 sets of blades for AWT turbines utilizing technology, equipment and methods originally developed by Gougeon Brothers Incorporated (Gougeon) in the 1980's. In January, 1997 FloWind was awarded a contract from the United States Department of Energy, through Sandia National Laboratories (Sandia), to have ABM develop improved manufacturing processes for wind turbine blades. The objective of the Sandia Blade Manufacturing Program (BMP) was to "Promote the development of advancements in the manufacturing of utility-grade wind turbine blades in ways that significantly lower blade costs and improve their quality and reliability." This report documents the work completed by ABM on the FloWind BMP project.

1.2 Project Purpose

Consistent with the objectives of the overall Sandia BMP project, the primary purpose of this project was to reduce the cost, and improve the reliability, of the blades used on the AWT-26 and AWT-27 wind turbine. Specifically, the project was to evaluate opportunities to reduce cost and improve reliability by examining two major areas:

1. Improvements to the manufacturing process though either changes in the process or changes in the process controls.
2. Changes in the blade material properties, through changes in the material or treatment of the materials in the manufacturing process, which would result in a reduction in cost or an increase in reliability.

1.3 Project Scope

The original project scope was to include the following steps:

- Research to identify candidate process and design improvements
- Testing and analysis to better quantify the potential benefits of the candidate changes
- Preliminary design of the factory equipment needed to implement the process improvements
- Preliminary design of a blade incorporating the most promising material and process changes
- Detailed design of the factory equipment needed to implement the process improvements
- Detailed design of a blade incorporating the most promising material and process changes
- Construction of six prototype blades incorporating the changes
- Laboratory and field testing of these blades.

Unfortunately, due to the bankruptcy of FloWind in June 1997 and a dramatic reduction in AWT sales, ABM was not able to complete the full scope of work. ABM was able to complete all of the work outlined above through the preliminary design of a blade incorporating the most promising material and process changes. At the completion of this work, it was apparent that ABM did not have the resources required to continue with the project and it was unlikely there would be a market for the improved blades being developed by the project. As a result, the project was canceled at the request of FloWind, AWT and ABM.

1.4 Report Organization

The remainder of this report is organized into five additional major sections. Section 2.0 describes the baseline turbine and blade which are the subject of this report. Section 3.0 presents the results of ABM's research into improvements in the manufacturing process. Section 4.0 presents ABM's work identifying alternative materials and material treatments. Section 5.0 presents the preliminary blade design developed under the project and Section 6.0 presents conclusion and recommendations.

2. Baseline Turbine and Blade Description

2.1 Baseline Turbine (AWT-27)

Advanced Wind Turbines, Inc. had two turbine designs, the AWT-26 and the AWT-27. Both turbine rotors used identical wood-epoxy blades, with the AWT-27 rotor including the addition of hub extenders to increase the diameter.

The configuration of the AWT-27 wind turbine is shown in Figure 2-1. The turbine is a downwind, free-yaw, fixed-pitch machine. Rotational energy is converted to electrical power in the nacelle, which contains a speed increaser (gearbox), generator, and a programmable logic controller (PLC).

The blades are lofted from NREL S825/S809/S810 thick-airfoil sections, and are made of wood-epoxy laminates, reinforced with carbon fiber. The AWT-27 rotor is a teetered, two-bladed, fixed-pitch, stall-regulated design. It has a diameter of 27.4 m (90 ft) and has a nominal speed of 53 rpm. The rotor is connected directly to the gearbox mainshaft, and the gearbox increases the mainshaft speed to 1800 rpm, driving a three-phase, 60 Hz, 480 volt , induction generator.

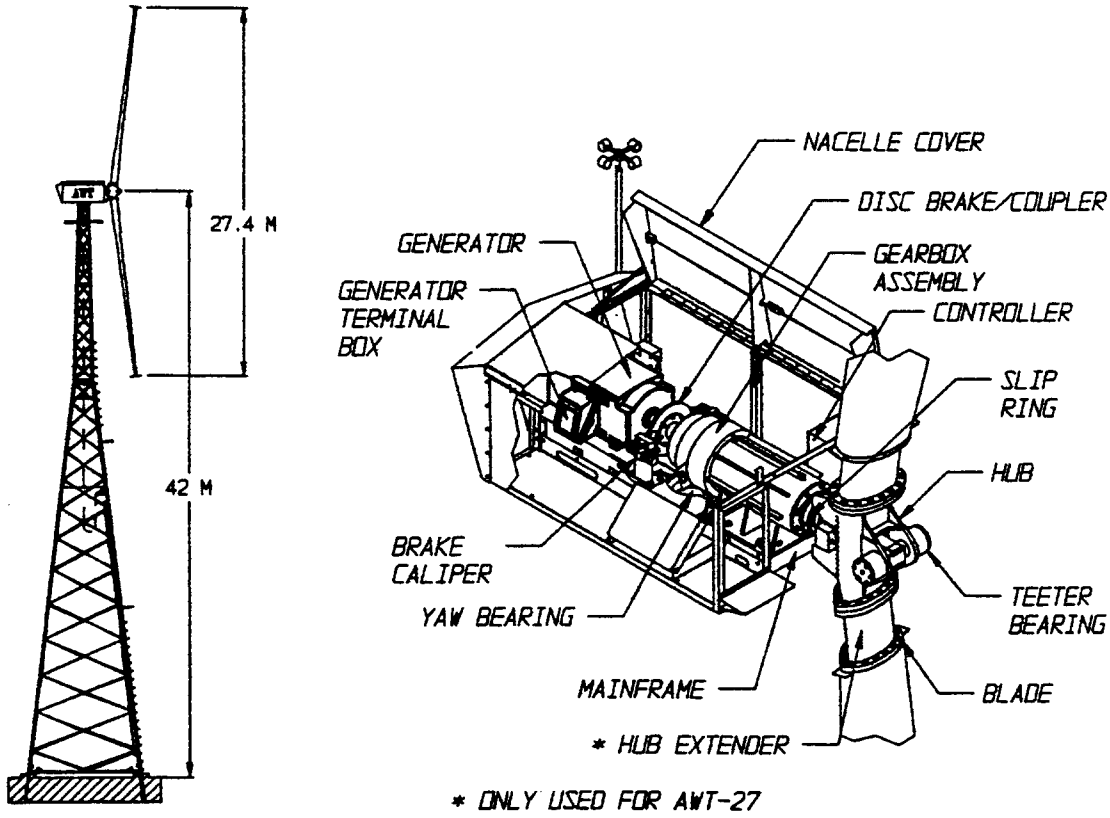

Figure 2-1 General Configuration of AWT-27 Turbine

The tower is a 42.7 m (140 ft) high free-standing, steel lattice structure. The machine is controlled by a PLC that is located in a control house adjacent to the tower. This PLC communicates with the PLC in the nacelle and also provides performance and maintenance diagnostic information. Connection to the grid is made at the switchboard enclosure in the control house.

2.2 Baseline Blade (AWT-26/27)

A drawing of the AWT-26/27 wind turbine blade cross section appears in Figure 2-2. The blades are constructed from wood/epoxy laminates with two shells bonded together with an inner vertical shear web. Carbon fiber is used in some of the laminations on the tension side, and the shells are sealed on the inner and outer surfaces with a layer of fiberglass. The outer surface is gelcoat.

The number of laminations varies along the blade length in response to the load spectrum seen by each station on the blade. Due to the length of the blade, each laminate layer has multiple spanwise joints along the length of the blade. These joints are staggered between layers. In the most highly loaded layers, the ends of the veneer sheets are scarfed to improve the strength of the joint. In less heavily loaded veneer layer, the veneer sheets are placed end-end with no pre-treatment to create a butt joint.

The blade is secured to the turbine hub with bolts which thread into steel studs bonded into the blade root.

The blade is 12.57 m (495 in.) in length and is lofted based on three basic NREL advanced airfoil sections: S815 on the inboard region, S809 on the midspan region, and S810 on the tip region of the blade. A smooth lofting process based on cubic splines was used to generate the intermediate airfoil shapes. The root region of the blade is governed by structural considerations peculiar to the wood/epoxy laminate system used to fabricate the blade shell. The anisotropic nature of the veneer limits the rate at which surface geometry can transition from an airfoil shape to a desirable shape for attachment to the hub. As a result the first basic airfoil station (S815 airfoil) is located 4.597 m (181 in.) from the center of rotation and the root shape approximates an oval.

Table 2-1 AWT-26/27 Blade Geometry

	AWT-26/27
Blade length	12,570 mm (495 in)
Hub station	533.4 mm (21 in)
Tip station	13,106 mm (516 in)
Total blade twist	6.10 degrees
Root (inboard) airfoil	S815
Midspan airfoil	S809
Tip (outboard) airfoil	S810
Furnished blade mass	447 kg (950 lb)
Maximum chord	1143 mm (45 in)
Maximum chord station	3,932 mm (154.8 in)
Tip chord	368 mm (14.5 in)
Root chord	774 mm (30.5 in)

Table 2-2 gives a summary of production costs and related figures of merit for the baseline blade. Note that a production rate of 3 blades/day may result in a 13% decrease in blade cost, relative to a 2 blades/day rate. For this report the 3 blade per day figures are used as the baseline.

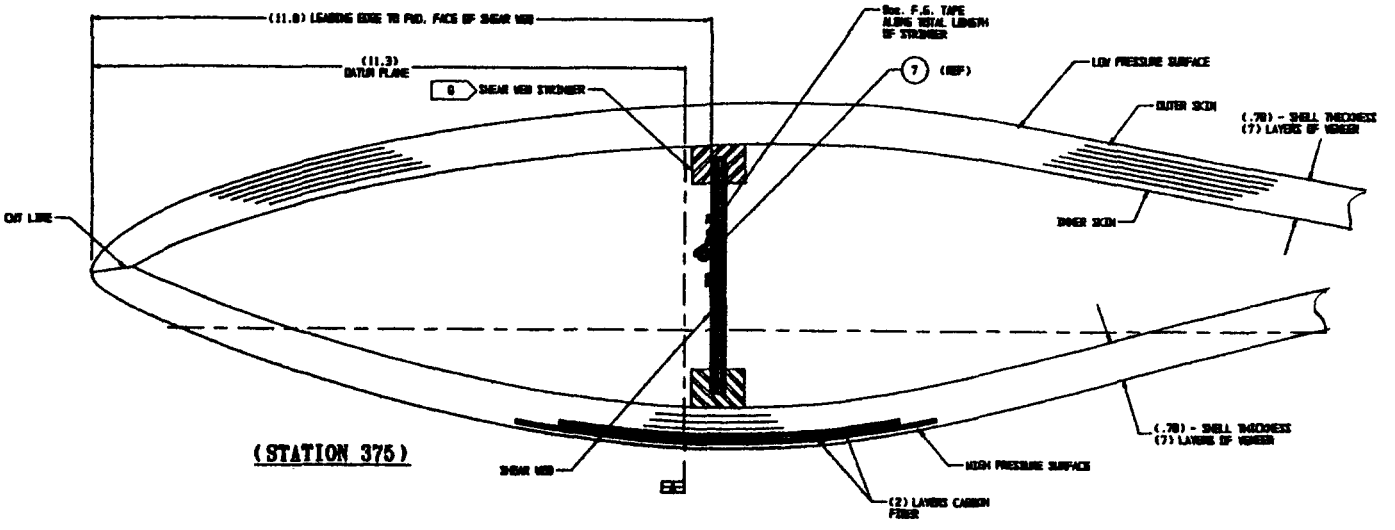

Figure 2-2 Typical Blade Cross Section

Table 2-2 Baseline Blade Costs

Cost/ Figure of Merit	Production Rate	
	2 blades/day (62.5 MW/year)	3 blades/day (94 MW/year)
Production Cost (per blade)	$7,091	$6,158
Weight (per blade)	950 lb.	950 lb.

3. Manufacturing Processes

The blades for the AWT-26/27 are constructed using a wood epoxy laminate system. High-grade, 2.5-mm (0.1 in.) thick Douglas fir veneer sheets are laminated in female molds using West System epoxy to form the high- and low-pressure half-shells. These two parts are then trimmed and bonded together, including a vertical shear web, as indicated in Figure 2-2, to form the basic blade shell.

The blade half-shells are laminated as follows:

1) outer gelcoat skin sprayed into molds (pigmented polyester gelcoat),
2) one layer of 0.75 oz/ yd^2 E glass veil cloth,
3) one layer of 12 oz/ yd^2 double-biaxial E glass,
4) laminating epoxy,
5) veneer layer,
6) carbon augmentation,

Repeat 5) & 6) as per local lay-up schedule

7) one layer of 12 oz/yd^2 double-biaxial E glass, and
8) two coats of resin/hardener to seal interior of blade shell.

Once the blade half-shells are complete and cured, they are removed from the molds, trimmed slightly and are ready for assembly with no further painting or sanding. After the shells and the shear web are bonded together, the epoxy lines at the leading and trailing edge seams are removed and the blade shells are complete with the exception of the installation of root and tip studs.

The blades are attached to the hub by steel inserts (studs) epoxied into holes bored into the end of the blade shell. The studs are tapered and contoured to effectively transfer the load from the wood/epoxy laminate blade shell through the thickened epoxy bond to the body of the steel insert without overloading any one of these three media. The studs contain pre-tapped holes accommodating bolts through the flange in the hub.

A plate for securing the tip vane mechanism is attached in a similar manner to the tip of the blade, except that the threaded studs are epoxied into the holes bored into the blade top. These threaded rods have stop nuts to provide a positive surface for the hardware to be bolted down against without pre-loading the epoxy /blade shell interface.

Carbon fiber reinforcement is used to augment the blade shells in certain locations. Only the high-pressure half of the blade shell is reinforced with carbon fiber tape along the longitudinal axis of the blade. By balancing the cross-sectional area of carbon with the cross-sectional area of wood and epoxy to ensure good load sharing, significant structural augmentation can be achieved with relatively small amounts of carbon.

The blade shell wall thickness is decreased along the span of the blade by using successively fewer veneers along the span of the blade. At the root, the shell wall is rapidly built up to a thickness of 89 mm (3.5 in.) to accommodate the load concentrations associated with the root stud inserts. The shell wall thickness at the tip of the blade is similarly built up to accommodate increased loads from the tip studs and the tip vanes.

This blade fabrication process can be summarized as the following ten principle steps, accomplished over four calendar days:

1. Laying the outer gel coat and fiberglass layers onto the blade mold.

2. Laying of the epoxy resin coated wood laminations onto the blade mold.
3. Vacuum bagging and curing the epoxy resin laminate.
4. Trimming of the newly formed blade shells, after removal from the molds.
5. Installing the shear web between blade shells and bonding of the blade shells together.
6. Machining the ends of the assembled blades and installing end caps
7. Installation of the blade root and tip stud bolts (boring, encapsulation with epoxy resin & curing).
8. Weighing and balancing blades into matched sets.
9. Finishing of the blades (edge seam finish sanding & painting, washing, final inspection).
10. Assembling and installation of the blade tip braking mechanisms

The improvements to this process evaluated as a part of the BMP were: changes in the process controls, reductions in the blade cure cycle time, use of a molded shear web, improvements in the methods used to drill the root stud cavities, and improvements in the blade machining process. Each of these are discussed in the following sections of the report. Each section includes subsections covering the baseline process condition, the research completed as a part of this project, a cost/benefit analysis of the improvements and the resulting conclusions.

3.1 Process Controls

During 1995 and 1996 ABM conducted an internal effort to ensure its quality system was in conformance with ISO 9000 requirements. During this process it became apparent that three aspects of the blade manufacturing process could benefit from more controls. These were:

1. The vacuum bagging process used during curing of the blade shells
2. Tests used to establish blade shell integrity
3. The process used to apply epoxy resin to the individual veneers

This section of the report documents the work which was completed to develop improved controls for these elements of the manufacturing process.

3.1.1 Vacuum Bag Process

After the laminated blade shells are placed into the mold a vacuum bag operation is used to compact the laminate, thus ensuring a strong bond between the laminations. The process specification requires that the blade shells be subjected to a vacuum of 18-22 Hg for an eight hour cure cycle. Excessive vacuum causes moisture to be pulled from the laminations, reducing bond strength. Insufficient vacuum also reduces bond strength due to insufficient compaction of the laminate. If the vacuum is not maintained throughout the curing cycle the laminate may pull apart, also reducing laminate strength.

In the current production process, the proper level of vacuum is established by an operator reading a mechanical gauge. The operator then sets a timer for the eight hour cure cycle and leaves the operation generally unattended. A significant portion of the cycle occurs at night, while the plant is not in operation.

To ensure process integrity and documentation it was necessary to develop process controls which would continuously monitor the status of the process, document out-of-specification conditions and alert an operator if the process falls out of specification.

To achieve this objective, an automatic vacuum monitoring instrumentation system was developed. This system provides a real time readout of the vacuum, continuously monitors and records the vacuum within

the molds and sounds an in-plant alarm and notifies off-site operators in the event of an out of specification condition. The system and its estimated costs are depicted in Figure 3-1.

3.1.2 Blade Shell Integrity

As a result of several tests conducted in conjunction with the National Renewable Energy Laboratory (NREL) ABM determined that there were some problems with the quality of the laminates it was producing. This resulted in an effort to identify a non-destructive testing technique for evaluating the condition of the blade shell.

These efforts resulted in ABM adopting stress wave testing as an NDT technique for the root portion of the blade shells. Stress wave testing is an NDT technique which utilizes accelerometers to measure the transit times of shock waves (stress waves) though the laminate being tested.

To better control the manufacturing process it was necessary to establish acceptance criteria for the blade laminate. An extensive data base of Stress Wave measurement and corresponding laminate quality was developed using a Metriguard model 239A Stress Wave Tester. This resulted in an acceptance criteria being established for the blade root. After the unit was sent to Metriguard for repair and returned to ABM it was found that the calibration of the unit was different than it had been when the original database was established. Subsequent testing developed a new standard. This experience resulted in ABM establishing a more frequent calibration interval for the Metriguard testing unit.

As part of this project standard testing procedures and data recording and analysis methods were also developed. Similar systems should be considered for any organization producing wood epoxy laminates where the quality of the laminate is a significant concern.

3.1.3 Resin Application Rate

In the current manufacturing process the epoxy is applied to the veneer sheets using a roll coating machine. As the veneer sheet is passed through this machine a pair of rollers, which rotate in a bath of epoxy, transfer a layer of epoxy to the veneer sheet. The amount of epoxy transferred depends on many variables including the spacing of the rollers, the viscosity of the epoxy, the condition of the veneer surface and the condition of the roller surface.

Examination of the historical blade production data showed that the standard deviation (sigma) of the application rate was approximately 1.66 grams per double glue line (g/dgl). The roll coater was typically set toward the mid point of the allowable standard of 24.5 - 30 g/dgl. When this is combined with a sigma of 1.66 g/dgl. it becomes apparent that at 3-sigma the amount of epoxy applied will be significantly outside of the allowed standard.

To address this problem it was necessary to evaluate the current process and implement changes which would ensure application rates within the standards.

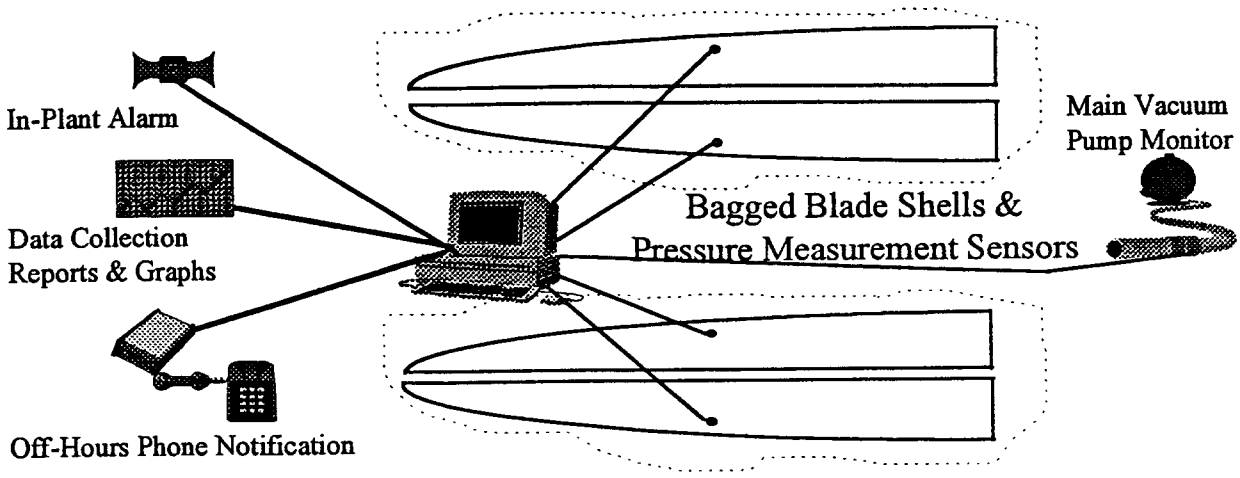

Cost Estimate

The Harrison proposal for the Honeywell recording unit:

1- HONEYWELL PROGENY RECORDER MODEL 031060-A0-200-0-0E00-00 RECORDER/ CONTROLLER	**$3,980**
7- HONEYWELL ST 3000 SERIES 900 SMART TRANSMITTERS, MODEL STA922-A1A--00000-MB-F1D3 is $1,173.25 @	**$8,213**

The Michigan I & C proposal for the Control Valve (Appendix page A30):

1 - 1/2" Baumann Control valve, 24000 SERIES, Little Scotty -	**$1,338**
Total Equipment Cost	**$13,531**

Installation cost estimate, including, materials, construction labor, coordination, and supervision:

Total Installation Cost	**$14,340**
Total Project Cost	**$27,871**

Figure 3-1 Automated Vacuum Monitoring Layout and Cost

The evaluation process showed that the rollers on the roll coater had become worn and glazed from many years of use. Discussions with the manufacturer indicated that resurfacing the rollers would significantly decrease the variability in the application rate of the epoxy. The evaluation also showed that while measurements of the resin application rates were being made periodically, the data was not being evaluated in any statistical manner. So long as the data recorded was within the prescribed limits, no adjustments to the machine were made. Measurements were taken several times during the production cycle but unless an out of specification operation occurred when a measurement was made the process was considered to be within specification.

As a result of this investigation it was concluded that the rollers on the roll coater should be recovered, a process control chart should be established at the roll coater and the machine operators and plant manager should be trained in its proper use. The mean and standard deviation of the measurements taken should be used to determine if the process is within specification. Data should be maintained for each blade manufactured to ensure traceability if problems occur in the field.

3.1.4 Conclusions

The wood-epoxy blade manufacturing process is one in which there are many variables affecting the quality of the finished blades. In particular, variability in the properties of the raw materials will result in high variability in the manufacturing process. For this reason, it is critical that appropriate process controls be in place during the manufacturing process. This portion of the BMP developed several significant improvements to the process controls at ABM which can be applied to any wood-epoxy blade manufacturing operation.

3.2 Reduction in Cure Cycle Time

3.2.1 Baseline Process

Steps 2, 5, and 6 of the blade manufacturing process outlined above require the use of epoxy adhesive. For these adhesives to achieve the required strength prior to successive manufacturing operations, an extensive cure cycle is required. The baseline manufacturing process employs ambient factory conditions during the curing cycle. Of the three process steps requiring epoxy resin, the blade lamination and cure cycle (step 3) requires the longest period. The present length of this cycle restricts the ABM factory to a single blade molding operation per 24-hour period. The specific steps in this process are shown in Table 3-1.

Table 3-1 Blade Molding Cycle Time

a)	preparation of molds for lamination	300 minutes (5 Hr.)
b)	epoxy resin coating of the wood veneers and placement in the mold (per mold basis)	45 minutes (3/4 Hr.)
c)	covering the filled mold with a plastic wrapper and placing under vacuum (nearly full atmospheric pressure is applied to the mold contents) (per mold basis)	15 minutes (1/4 Hr.)
d)	maintaining the mold and contents under vacuum, ambient temperature	480 minutes (8 Hr.)
e)	vacuum bagging complete, mold & contents setting until blade shell removal	420 minutes (7 Hr.)
	Total Cycle Time	24 Hours

If the duration of this process could be reduced to a maximum of 12 hours it would be possible to operate the factory on a two production shift per day basis. This would result in a reduction in blade cost through better utilization of the equipment, facilities, and labor. The production rate would be doubled without

requiring a corresponding increase in factory tooling or overhead costs. Discounting the "wait" period, which is not required to ensure product quality, the mold preparation, placement of veneer and resins into the mold, and the vacuum bagging steps require 17 hours to complete. To reduce the duration of this cycle to 12 hours will require that the vacuum duration be reduced from 8 hours to 3 hours, as the other steps are already optimized.

3.2.2 Research Completed

The following research process was followed to evaluate the potential for reducing the cure cycle time of the blade molding process.

1. Determine epoxy resin cure time vs. temperature for epoxy mixtures used in ABM operations. This was expected to allow a determination of the temperature required to sufficiently shorten the cure time.
2. Determine epoxy hardness vs. temperature profiles. This is required to ensure that the blade is not removed from its mold until the epoxy is sufficiently cured to preclude a change in blade shape when removed from the mold.
3. Utilizing the data obtained, complete preliminary engineering of the equipment required to achieve the desired reduction in cycle time.

3.2.2.1 Cure Rate Curve Determination

The Gougeon Brothers, Inc. (GBI) provided data on the cure rates of the 105 epoxy resin and 206 "slow" hardener used in the blade lamination process. This data is shown in Table 3-2.

Table 3-2 Cure Rate Data for 105 Resin / 206 Hardener

	CYCLE	CURE TIMES (min)		
		65°F	75°F	85°F
	START	0	0	0
POT LIFE	POT	24	18	11.5
GELLATION	GEL	300	48	42
VITRIFICATION POINT	SET	330	90	72
VITRIFICATION COMPLETE	SOLID	420	150	90

Inspection of the cure rate data indicates that the time required to reach full vitrification is strongly temperature dependent. It also indicates that at typical ambient factory temperature of 65 °F the epoxy will have achieved full vitrification prior to the end of the vacuum bagging process. An increase in vacuum bagging operating temperature to 85°F from 65°F, would result in a decrease in vacuum time required for full vitrification from seven and a half hours to one and a half hours. Since increasing the factory production to two production cycles per day is dependent on the completion of the vacuum bagging cure cycle in a maximum of three hours, it appears that performing the vacuum bagging at elevated temperatures will accomplish the objective. However, it was not clear whether the cure time information provided by Gougeon was representative of the relatively isothermal conditions experienced in much of a blade where relatively thin films of epoxy are used.

A concern with elevating the temperature during the curing cycle is that the elevated temperature of the partially cured epoxy would result in epoxy whose properties were insufficient to preclude changes in blade shape if the blades were removed from the mold before the blade had cooled sufficiently. Hardness, as

measured by a Durometer reading, is used as a criteria for determining whether an epoxy resin laminate has developed sufficient strength to withstand typical handling forces after removal from the mold. Data concerning the hardness of the epoxy resin/hardener mixture used by ABM as a function of cure time and temperature was not available.

To address these questions, a series of tests to measure the hardness of the epoxy as it cured under thin film conditions were developed.

3.2.2.2 Hardness Testing

Three series of laboratory tests were completed, one at 65°F , one at 90°F, and one at 100°F. The tests performed at 65 °F were used as the base case, duplicating the conditions normally found in the factory during the colder winter months. The tests were performed at ABM using existing temperature controlled refrigerators and ovens. Hardness was measured utilizing a Durometer to obtain values on the Shore D hardness scale. Special sample containers were fabricated for testing purposes to insure that the test results modeled the isothermal conditions experienced in the curing cycle of the blade laminate. The sample containers were constructed from 1 ½ inch thick aluminum plate six inches square. These plates had a 3/16" Garolite sheet containing a 3" diameter hole bonded to the top surface of the aluminum plate. The large aluminum plate served as a heat sink to assure isothermal conditions and the Garolite formed platen cavity contained the epoxy sample. Data (temperature and Shore D hardness) were recorded at one hour elapsed time intervals. The results of these tests are shown in Figure 3-2.

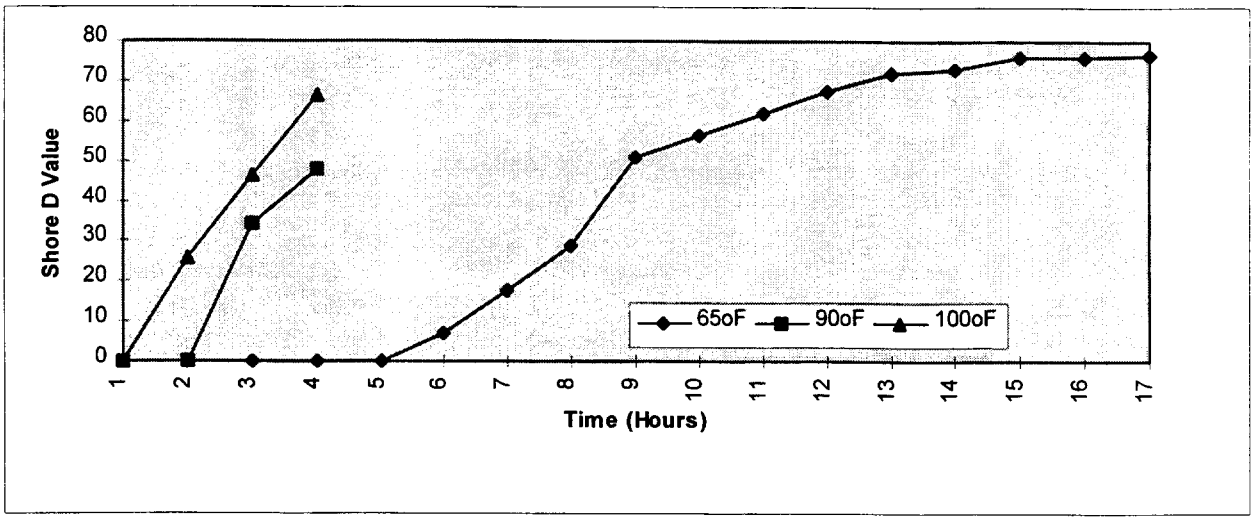

Figure 3-2 Shore D Hardness Testing Results

Examination of the data in Figure 3-2 for 65 °F result in the following observations:

- The epoxy resin remains very soft (< 1 on Shore D value) for a 5 to 6 hour period following mixing of the epoxy resin and hardener system. At the time the vacuum is released (8-9 hours after mixing the epoxy) it attained a Shore D value of 30-50. At the time the blades are removed from the molds (15-16 hours) the Shore D value is approximately 76.

- An accelerated production curing cycle must produce the Shore D values of 30 to 50 by the end of the vacuum forming step and 70 by the unloading of the blade shell from the mold if the physical properties known to be successful in producing blades are to be maintained.

While the precise Shore D values required to ensure high blade quality after removing the blade from the mold are not known, maintaining the values currently achieved in production was considered a conservative approach.

Examination of the data obtained in the elevated temperature test series result in the following observations:

- Between 2.5 and 3 hours were required with the 90 °F samples before they reached a Shore D hardness value of approximately 30. Upon rapid cool-down the sample hardness increased to 70+. This would reduce the blade vacuum forming cycle time from eight hours to 3 hours if Shore D harnesses at the time of removal of the vacuum are maintained. Since the heat-up and cool-down cycles of the blade and mold fixture are estimated to require a minimum of 1/2 hour each, the elevated temperature of 90 °F would require at least a 4 hour cycle, which was determined to be inadequate to achieve a 12 hour cycle time.

- Two hours were required with the 100 °F samples, before they reached a Shore D hardness value of approximately 30. Upon rapid cool-down the sample hardness increased to 60+. With the heat-up and cool-down cycles of the blade and mold fixture estimated to require 1/2 hour each, the elevated temperature of 100 °F would be adequate to yield the required shortening of the overall blade vacuum forming and cure cycle reduction of 15 hours to 3 hours.

- Note that the heat-up and cool down times may be longer than the estimated 0.5 hours. However, the curing process in the molds is not a purely isothermal cycle and it is believed probable that the blades could be removed from the molds, without damage before returning to ambient temperature.

3.2.3 Cost/Benefit Analysis

3.2.3.1 Blade Cost Reduction

The baseline cost for blade manufacture used for this project is the $6,158 estimated for a 3 blades per operating day rate.

For a 3 blades per 12 hour period or 6 blades per operating day rate variable costs/blade remained unchanged and fixed costs/month also remained unchanged, but were spread over the increased production.

This analysis resulted in a reduction in the cost per blade to $ 5,785. A 6% reduction.

3.2.3.2 Capital Costs

The current factory operation provides a floor area of approximately 30 feet in width by 50 feet in length (1500 sq. ft.) for the vacuum forming operation. As each of the six blade shell molds (3 each high pressure and low pressure blade halves) are filled with the wood veneer/epoxy resin matrix, they are moved into the area and enveloped in plastic wrap to create a sealed enclosure surrounding the mold and contents.

To shorten the time required for the blades to cure during the vacuum forming process, three methods of heating the molds and contents were evaluated: (a) direct radiant heat of the wood epoxy laminate, (b) conduction heating of the laminate through the mold, and (c) radio frequency excitation. The result of the evaluation was selection of radiant heating. Convection heating of the molds is not recommended because incorporating heating elements into the mold shells would require the fabrication of new molds. Radio frequency excitation of the mold and contents is also not recommended, since radio frequency excitation of epoxy resin and/or molds created using epoxy resins would be inefficient due to the low concentration of hydrogen bonds in the epoxy resin and wood veneer. Hydrogen bond excitation is the preferred means of heat generation for radio frequency systems. Radiant heating was selected since this method of heating is currently used successfully in the molding industry to provide accelerated curing cycles for fiberglass composites. Fostoria Industries, Inc., a vender of radiant heating systems for the composite industry, provided a preliminary design for a system and a budgetary cost estimate.

In reviewing the requirements with Fostoria Industries, Inc., it was recommended that the area used for the vacuum forming operation be enclosed. This would create a curing room that could be divided into three separate heating zones using curtain wall dividers. Each zone would contain independently controlled electric infrared heater modules. The heater modules consist of quartz lamps which have the capability of rapid heat up and cool down cycles. The separation of the curing area into three zones would allow the staging of filled molds into the area as they are filled, providing additional time for mold heat up and curing. Ventilation of the new curing room was also recommended to provide for a rapid cool down following the cure cycle.

The cost estimate for the electrical infrared heating system was $ 39,925 and estimated delivery for the components was 10 to 12 weeks following placement of the order.

The cost estimate for the construction of the new curing room, installation of the electric heating system, and construction of the new curing room ventilation system was estimated by ABM at $173,550 with completion of the construction estimated to require four weeks following receipt of the heating system components. Total cost of the completed facility is therefor estimated to be $213,475 .

To accomplish an orderly start up of a multiple shift factory operation, a significant investment in technician training will be required. The original ABM factory startup required a period of eight weeks to reach the designed capacity operation. Startup of a multiple shift factory operation, which basically requires duplication of the original factory crew component, is estimated to require the same period to reach capacity operation. During this training period, the average production rate can be assumed for cost estimation purposes to be one half design rate. Using the monthly ABM Production Cost Standard for the expanded production rate of 126 blades per month, the training cost is estimated at one month of fixed operating costs = $190,210.

3.2.3.3 Simple Economic Analysis

Assuming the cost savings and production rates discussed above, the yearly cost saving achievable through implementation of a shortened cure cycle time is:

Cost Reduction = $372.61/Blade * 126 Blades/Month * 12 Months/Year = $563,386 per year

Total capital cost + startup cost = $213,475 + $190,210= $403,685

Calculated Yearly Return on Investment = $563,386/$403,685 * 100% = 140% (about a nine month pay-back)

Note however that this analysis is dependent on achieving the full assumed production rate of over 1,400 blades per year. This is equivalent to 700 wind turbines per year. Without reducing the cycle time, the plant is capable of producing blades for 350 wind turbines per year.

3.2.4 Conclusions

The use of radiant heating to accelerate the curing time of the blades in the molds is a practical way to substantially increase the capacity of the ABM facility and reduce blade cost. However implementing this change requires a significant initial investment in capital equipment and personnel training. Therefore, the demand for blades from the facility would have to be carefully evaluated prior to implementing the change.

3.3 Molded Shear Web

The shear web in the AWT blade is a strengthening spar, spanning the internal gap between the two blade halves. The current shear web manufacturing process is labor intensive and results in significant variations between individual shear webs. This variation increases the time required to install the shear web in the blade shell during step 5 of the blade manufacturing process. The purpose of this portion of the BMP project was to examine ways to reduce the variability between shear webs and thus decrease cost and increase blade quality.

3.3.1 Baseline Process

The shear web assembly spans the internal gap between the two blade halves and runs nearly the entire length of the blade. Figure 2-2 shows the shear web assembly in a typical blade cross section. Note that the shear web assembly consists of the shear web itself and a top and bottom shear web stringer. Due to the length of commonly available raw materials and the length of the blade, both the shear web and the stringer are made from multiple lengths of material joined by scarf joints. The shear web is hand fabricated using Finland Birch plywood, 5/4" Douglas fir "clear" board stock, and epoxy resin, with the individual "piece" components produced in batches. Individual shear webs are assembled the day before they are to be installed in an actual blade. The overall process of manufacturing the individual components and their assembly into a shear web unit ready for blade installation is labor intensive, requiring ten (10) man-hours per shear web. Since the shear web is assembled from fabricated components, themselves made with basic hand power tools, there are a number of measurement tolerances and adjustment allowances in each piece and the resulting shear web assembly. The current shear web construction procedures result in "unique" one of a kind shear web units, none quite identical to one another. This shear web "uniqueness" increases the labor required to custom fit each shear web during installation into the blades.

3.3.2 Research Completed

At the start of this research, the idea of molding the shear web from alternative materials such as fiberglass and foam were considered. These ideas were rejected because of concerns over the material costs and their structural compatibility with a wooden blade shell. In order to accomplish the objectives of this portion of the project it was determined that the basic material of the shear web should remain unchanged but the design of the components would need to be modified to allow the use of a mold to form the shear web assembly.

The design of the hand fabricated shear web piece components and the overall shear web assembly were reviewed to determine which elements required redesign to fit a molded design. In addition the design was examined to determine if other additional design revisions would gain production or material cost efficiencies. Recommendations resulting from this study were:

1. The shear web stringer design, employing 5/4" Douglas fir board stock that is fabricated into 1" x 3/4" strips with 1/4" dado grooves had to be redesigned for use with a mold. A new design was developed which replaced each stringer with two (2) 3/8" x 3/4" strips. Figure 3-3 shows the proposed configuration.

2. Replacement of the scarfed joints in the shear web and stringer with "butt" joints was proposed.

3. A new molding fixture would be designed and constructed to allow fabrication of a pre-molded shear web. This would create shear web units that were identical to one another. This would reduce the time required to fit shear webs into blades and allow a reduction in the tolerance allowed between the shear web and blade shell. The reduced tolerance will result in a better fit and an improved quality blade.

These recommendations were reviewed with the ABM blade design consultant, Mr. Michael Zuteck. Mr. Zuteck concluded that the first and third proposals were acceptable but the scarfed joints could not be replaced with "butt" joints.

Following approval of this approach, the tooling which would be required was designed. A total of three molds would be required to support the present factory production capacity. The molds would be produced by ABM technicians utilizing the same propriety technology now employed in manufacturing ABM molds for the blade laminations. This technology uses epoxy resins, Verticel® cardboard honeycomb, and fiberglass cloth materials to produce molds using a "master plug" of the desired dimensions.

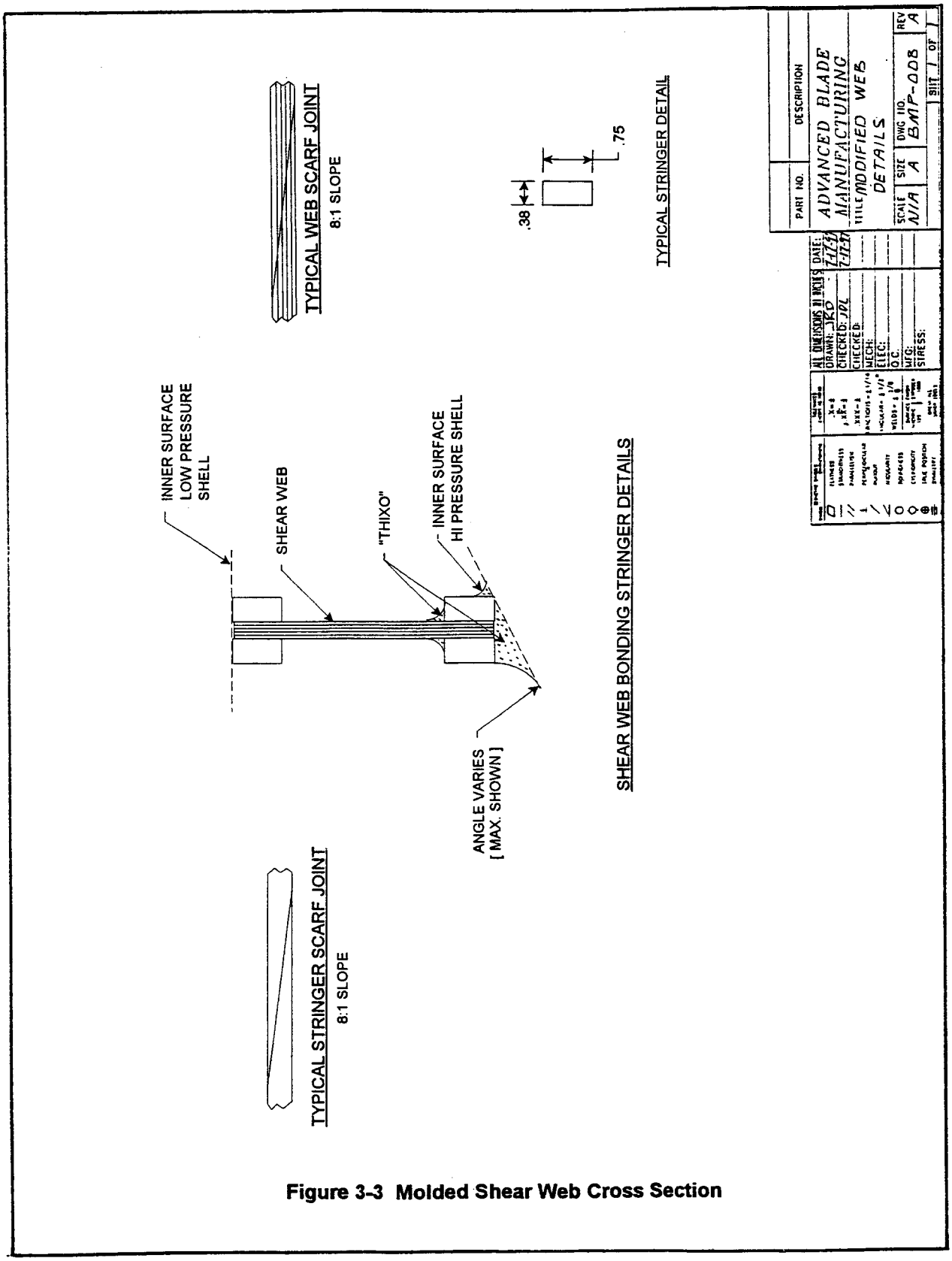

Figure 3-3 Molded Shear Web Cross Section

3.3.3 Cost/Benefit Analysis

3.3.3.1 Capital Equipment Costs

A summary of the total costs to implement the Molded Shear Web proposal is presented in Table 3-3.

Table 3-3 Molded Shear Web Capital Costs

DESCRIPTION	QUANTITY	MATERIAL	LABOR	CONTINGENCY	TOTAL
Shear Web Plug	(1)	$132	$2,070	$440	$2,642
Shear Web Mold	(3)	$2,215	$9,318	$2,307	$13,840
Cutting Template	(1)	$71	$414	$ 97	$582
Clamping Plates	(12)				$444
TOTAL SHEAR WEB PROPOSAL					$17,508

3.3.3.2 Cost Reductions

Manufacturing man-hour utilization studies were completed for both the current and proposed methods of constructing and installing shear webs during the blade assembly operations. The results are shown in Table 3-4.

Table 3-4 Molded Shear Web Labor Estimates (man-hours)

OPERATION	CURRENT	PROPOSED	REDUCTION
Shear Web Fabrication	10	8	2
Shear Web Installation	4	2	2

In addition to the expected reduction in man-hours from the use of a molded shear web, a small reduction in material costs can be achieved. However, since the reduction is quite small on a per blade basis, it has not been included in the analysis. Use of the new shear web design will also improve the overall function, quality and subsequent reliability of the present blade.

3.3.3.3 Simple Economic Analysis

The economic analysis for this portion of the study was conducted assuming the present plant capacity of 3 blades per day was fully utilized.

Economic savings = 4 man-hours * ($ 10.00/Hr. + $.3.50/Hr. {employee overhead}) = $ 54.00 / blade

$ 54/blade * 3 blades/day * 253 worked days per year = $ 40,986 / year.

Using the estimated capital equipment costs of $17,508 with these savings results in a simple first year return on investment of 234% (R.O.I. = $40,986 / $17,508 * 100% = 234%)

3.3.4 Conclusions

A change in the design of the blade shear web to utilize a design capable of being molded results in a modest reduction in the cost of the blades but an attractive return on investment if the capacity of the plant

is utilized. In addition to the cost reduction achieved, use of molded shear webs can increase the quality of the blades by reducing the variability in the dimensions of the shear webs.

3.4 Stud Cavity Drilling Process Improvements

Following the blade root machining and capping operation, the next operation is the drilling of the 15 root stud cavities into the blade root and subsequent bonding of the studs into the root. This operation is currently accomplished by the root stud crew which uses non-automated tooling to drill the cavities.

The purpose of this portion of the project was to determine ways to reduce the time and cost associated with forming the root stud cavities.

3.4.1 Baseline Process

The baseline cost estimates used in this report were developed using data from the 1995 blade manufacturing campaign at ABM. During this campaign, the factory used a drilling station equipped to drill 15 root stud cavities at one time; however, only five cavities were ever drilled simultaneously. The drilling station capacity was limited by the ability of the operator to manually drive the tapered end mill bits into the blade. The technician could only apply enough force to "drive" five bits simultaneously into the blade.

However, during a blade qualification test completed in 1996 following the production campaign it was determined that using the tapered end mill bits to drill the cavities had resulted in a cavity whose internal surface was incompatible with the formation of a high strength bond between the blade and the adhesive. The cavity inner surface was very smooth with only minimal fiber exposure for epoxy resin bonding. This resulted in the root studs failing the blade qualification test.

Following identification of the cause of root stud failure observed in the blade qualification test, the design of the drill bit used to drill the root stud cavity was revised to increase the amount of exposed wood fiber on the cavity inner surface. The "improved" drill bit was similar to a previous experimental prototype originally used in early blade development work. This drill bit exposes a large amount of wood fiber, but is not "self-cleaning". The bit requires a high pressure air sweep to continuously remove cutting chips from the cavity during the drilling operation. This is to prevent burnishing of the internal wood surface which would also result in inadequate bond formation. The air sweep to remove wood chips causes the drilling bit to have a flattened tip. As a result an initial pilot drill hole must be drilled into the blade. Even with a pilot hole, the drill bit requires considerably more pressure to penetrate the blade shell than the tapered end mills used in the production process. It is currently estimated that the present design of the drilling station would only allow a total of three "improved" drill cavities to be simultaneously drilled. This will result in a net increase in the costs of the blades as the number of cavities drilled per drilling operation will decrease from five to three. In addition, the new drill bits require two different drilling bits to be used in conjunction with high pressure air to remove drilling chips. Note that ABM only had one of the improved drill bits when the research was conducted.

3.4.2 Research Completed

The research on this task focuses on ways to increase the number of root stud cavities which could be made in a single operation. Three separate approaches were evaluated:

1. Purchase two (2) additional improved drill bits and the necessary accessories to increase the present drill station capacity to the limits imposed by manually "driving" the bits into the blade root. In addition, the current factory compressed air system will require up-grading to include a compressed air dryer. The air dryer is required to avoid the possibility of entrained water droplets "wetting" the cavity surfaces since wetted surfaces will inhibit bonding of the epoxy resin mixtures used to bond the studs. An air manifold piping system around the drilling station will also be provided to allow connection of multiple bits to the compressed air supply. This approach results in a higher cost stud drilling operation than the baseline because the overall drilling capacity will have been reduced from five (5) to three (3) cavities per drilling cycle and the improved bits require two separate bits to be used instead of the single formerly used "self-cleaning" tapered end mill boring bit.
2. Purchase four (4) additional improved cavity drill bits, necessary accessories, compressed air dryer & manifold system, and convert the drill station to hydraulically driving the bits into the blade roots. This approach also requires redesign of the blade support bunks to withstand the greater forces applied to drive more than three improved bits into the blade roots. The hydraulic drive used to drive the drill bits into the blade will be required to provide a variable controlled forward feed rate, as well as a quick reverse function to produce a cavity with the required surface quality. High rates may produce excessive bit "wobble" as well as excessive pressures to the blade support stand while slow rates may result in cavity surface "burnishing" due to excessive heat formation during drilling. This approach results in nearly returning the root stud drilling operating costs back to the base line capacity.
3. Purchase fourteen (14) additional improved cavity drill bits and all other features as described in option No. 2. In addition redesign the hydraulic system and the blade support bunks to withstand the higher pressures resulting from using fifteen "improved" bits instead of five.

To determine the feasibility of each of these scenarios, designs for the required modifications to the present root stud drilling station were developed for each scenario. Due to the similarity of the scenarios, the modifications were similar for each, only executed to varying degrees. The changes required included :

1. developing an air manifold system to supply compressed air to multiple improved drill bits
2. modifications to the present drill station to use a hydraulic system to drive multiple improved bits into the blade root
3. modifications to the blade support bunks to withstand the increased pressures associated with driving a larger number of bits simultaneously into the blades

The portions of the resulting designs which would be subcontracted were submitted to local vendors for budgetary pricing and ABM personnel estimated the costs of the installation work which would be completed by ABM.

3.4.3 Cost/Benefit Analysis

3.4.3.1 Capital Equipment Costs

A summary of the total costs for the three cases is presented in Tables 3-5, 3-6 and 3-7.

Table 3-5 CASE 1 - Three Drill Bit Capacity

DESCRIPTION	QUANTITY	COST ESTIMATION BASIS	TOTAL
Boring Bits	(2)	Rose Tool & Die - low bid ($825 ea.) received	$1,650
Modify Drill Chuck Shafts	(3)	Rose Tool & Die - low bid ($58 ea.) received	$174
Bronze Air Collars	(3)	Rose Tool & Die - low bid ($37.50 ea.) received	$113
Air Manifold System	(1)	ABM Cost Estimation	$3,206
Compressed Air Dryer Sys.	(1)	Compressor Engineering - low bid received	$3,033
Installation of Air Dryer	(1)	ABM Cost Estimation	$4,831
Total Case 1 Cost			$ 13,007

Table 3-6 CASE 2 - Five Drill Bit Capacity

DESCRIPTION	QUANTITY	COST ESTIMATION BASIS	TOTAL
Boring Bits	(4)	Rose Tool & Die - low bid ($800 ea.) received	$3,200
Modify Drill Chuck Shafts	(5)	Rose Tool & Die - low bid ($58 ea.) received	$290
Bronze Air Collars	(5)	Rose Tool & Die - low bid ($37.50 ea.) received	$188
Air Manifold System	(1)	ABM Cost Estimation	$3,206
Compressed Air Dryer Sys.	(1)	Compressor Engineering - low bid received	$3,033
Installation of Air Dryer	(1)	ABM Cost Estimation	$4,831
Hydraulic Cylinder Mounts	(2)	Rose Tool & Die - low bid ($225 ea.) received	$450
Hydraulic Drive System	(1)	ABM Cost Estimation	$6,301
Install Hydraulic System	(1)	Rose Tool & Die - low bid received	$1,075
Fabricate Bunk Braces	(4)	Rose Tool & Die - low bid ($90 ea.) received	$360
Install Bunk Braces	(1)	Rose Tool & Die - low bid received	$395
Total Case 2 Cost			$ 23,329

Table 3-7 CASE 3 - Fifteen Drill Bit Capacity

DESCRIPTION	QUANTITY	COST ESTIMATION BASIS	TOTAL
Boring Bits	(14)	Rose Tool & Die - low bid	$9,450
Modify Drill Chuck Shafts	(15)	Rose Tool & Die - low bid	$870
Bronze Air Collars	(15)	Rose Tool & Die - low bid	$563
Air Manifold System	(1)	ABM Cost Estimation	$3,206
Compressed Air Dryer Sys.	(1)	Compressor Engineering	$3,033
Installation of Air Dryer	(1)	ABM Cost Estimation	$4,831
Hydraulic Cylinder Mounts	(2)	Rose Tool & Die - low bid	$450
Hydraulic Drive System	(1)	ABM Cost Estimation	$6,301
Install Hydraulic System	(1)	Rose Tool & Die - low bid received	$1,075
Fabricate Bunk Braces	(4)	Rose Tool & Die - low bid ($90 ea.) received	$360
Install Bunk Braces-Set of 4	(1)	Rose Tool & Die - low bid received	$395
Total Case 3 Cost			$30,534

3.4.3.2 Cost Reductions

Manufacturing man-hour requirements were estimated in detail for both the former and the current drilling operation and the three proposed methods of improving the root stud drilling station. The results of these studies are summarized in Table 3-8.

Table 3-8 Total Man-hour Requirements for the Two Man Crew

OPERATION	MAN HOURS
Baseline (5) "self-cleaning" tapered end mills usage	3.0
Current (1) "improved" bit usage	11.5
Proposal # 1 - (3) "improved" bit usage	8.0
Proposal # 2 - (5) "improved" bit usage	4.0
Proposal # 3 - (15) "improved" bit usage	2.0

It is apparent from this analysis that only Proposal #3 offers the potential for reduced costs relative to the baseline condition.

3.4.3.3 Simple Economic Analysis

The change from the former to the present method of drilling the root stud cavity dramatically increased the costs of this operation. The baseline blade costs were developed from data gathered when the former method was in use. Therefore the baseline costs do not reflect the actual current method of drilling the root studs. The following return on investment (ROI) analysis is relative to the current method and the production cost impacts are calculated relative to baseline cost. As result, in several cases the cost of the blade increases relative to the baseline while there is a positive return on investment. This is because the

former method of making the holes, which was used to develop the baseline costs, can no longer be used and the presently used method substantially increases the cost of the blades. Several of the changes evaluated in this report will reduce the costs of the presently used method, thus providing a positive return on investment, without reducing the costs to the levels used to develop baseline costs

CASE 1:

Man hour reduction projected with implementation of Case 1 = 3.5 hours per blade.

Estimated equipment purchase and installation cost to implement = $ 13,007

A. Return on Investment Calculation

Economic savings = 3.5 man-hours * ($ 10.00/Hr. + $3.50/Hr. {employee overhead}) = $ 47.25 / blade manufactured or ($ 47.25* 3 blades/day * 253 worked days per year) = $ 35,863 / year.

R.O.I. = $ 35,863 / $ 13,007* 100% = 277 %

B. Percent **Escalation** in Blade Manufacturing Cost relative to baseline cost

Projected blade cycle increases from 3 hours/blade to 8 hours/blade for the 2 man stud crew. Therefore blade manufacturing costs will increase relative to the baseline cost.

% Blade Cost **Escalation** = (5 Hr * $13.50/Hr) / ($ 6158) * 100% = 1.10 %

CASE 2 :

Man hour reduction projected with implementation of Case 2 Proposal = 7.5 hours per blade.

Estimated equipment purchase and installation cost to implement proposal = $ 23,329

A. Return on Investment Calculation

Economic savings = 7.5 man-hours * ($ 10.00/Hr. + $ 3.50/Hr. {employee overhead}) = $ 101.25 / blade manufactured or ($ 101.25* 3 blades/day * 253 worked days per year) = $ 76,849 / year

R.O.I. = $ 76,849/ $ 23,329* 100% = 329 %

B. Percent **Escalation** in Blade Manufacturing Cost relative to baseline cost

Projected blade cycle increases from 3 hours/blade to 4 hours/blade for the 2 man stud crew. Therefore blade manufacturing costs will increase relative to the baseline cost.

% Blade Cost **Escalation** = (1 Hr * $13.50/Hr) / ($ 6158 * 100% = 0.22 %

CASE 3 :

Man hour reduction projected with implementation of Case 3 Proposal = 9.5 hours per blade.

Estimated equipment purchase and installation cost to implement proposal = $ 30,534

A. Return on Investment Calculation

Economic savings = 9.5 man-hours * ($ 10.00/Hr. + $ 3.50/Hr. {employee overhead}) = $ 128.25 / blade manufactured or ($ 128.25* 3 blades/day * 253 worked days per year) = $ 97,342 / year

R.O.I. = $ 97,342/ $ 30,534* 100% = 319 %

B. Percent **Reduction** in Blade Manufacturing Cost relative to baseline cost

Actual projected blade cycle decreases from 3 hours/blade to 2 hours/blade for the 2 man stud crew. Therefore blade manufacturing costs will decrease as relative to the baseline cost.

% Blade Cost **Decrease** = (1 Hr * $13.50/Hr) / ($ 6,158) * 100% = 0.22 %

3.4.4 Conclusions

The work completed indicates that the root stud machining operation should be changed to drill 15 root stud cavities per drilling operation. While the economic analysis was completed assuming the full production rate of 3 blades per day, the estimated benefits are sufficiently large that even at one blade per day the change would be justified. In addition to the cost savings, there will be a significant improvement in the quality of the work for the stud insertion crew.

3.5 Blade Machining

Following assembly of the two blade shells and installation of the shear web, Step 6 of the blade manufacturing process is machining the ends of the assembled blades and installing end caps. The current process is time consuming and inefficient. It also results in an excessive workload for the root stud crew, often requiring the use of overtime to accomplish their scheduled tasks. The purpose of this portion of the project was to identify ways to improve the efficiency of this task, thus reducing blade costs.

3.5.1 Baseline Process

The blade machining process is currently accomplished by the Root Stud Crew and constitutes their first daily activity. The process steps are as follows:

a) Remove the previous day's assembled blade from the assembly fixtures, transferring the blade to one of the bunk systems used for stud insertion.
b) Align the blade in the bunks to assure that the blade root is perpendicular and parallel to the stud bolt insertion plate.
c) Position the stud insertion plate as required to allow machining of the blade root to the desired dimensions.

d) Machine the blade root to the desired dimensions using a hand power router,
e) Once the machining is completed, the root cap is bonded into position using epoxy resin.
f) Following the epoxy cure period, the blade is transferred from the stud insertion bunk to the bunk used to drill the root stud bolt cavities.
g) Following the drilling of the root stud bolt cavities, the blade is transferred back to the stud insertion bunks to install the root stud bolts. Alignment of the blade to the insertion plate is again required.

The current process requires aligning the blade to the stud insertion plate in the stud insertion bunks twice, which is a time consuming process. A similar process is followed for machining and capping the tip end of the blade.

3.5.2 Research Completed

The initial idea for improving the process was to machine both ends of the blade while the blade was still in the blade assembly fixture and utilize the blade assembly crew to complete the tasks. The blade assembly crew is larger than the stud crew and currently has some slack time. This change would improve the efficiency of the root stud crew, reducing the frequent requirement of extended work days to complete their assigned fabrication duties. In addition, using the blade assembly fixtures to secure the blade while completing the root stud machining, would eliminate the extra moving and alignment of the blades into the stud insertion bunks. Overall, the crews would perform more efficiently, with one high labor repetitive task eliminated per blade manufactured.

After reviewing the current design of the blade assembly fixtures, it was determined that completing the tip machining operation in the present assembly fixtures would require very extensive modifications to the fixtures and possibly require their complete replacement. In addition, a review of the proposed crew responsibilities did not result in a significant savings of labor if the blade tip machining operation was modified. For these reasons, it was decided not to modify the blade tip machining operation.

After examining various approaches to machining the roots in the blade assembly molds it was decided that the optimal approach was to modify the molds to include an additional reference plate fixture which would allow machining of the blade root. It was also observed that this approach would "dove tail" nicely with the molded shear web changes because the blade assembly crew labor saved by that change could be utilized to machine the blade root and install the root cap.

Preliminary designs for the recommended revisions and additions to the present blade assembly fixtures were developed. There are currently 3 blade assembly stations in the factory. Therefore, it would be necessary to build three sets of new tooling. The tooling can be produced by ABM technicians utilizing the same propriety technology now employed in manufacturing other ABM assembly fixtures.

3.5.3 Cost/Benefit Analysis

3.5.3.1 Capital Equipment Costs

Detailed cost estimates for the three assembly jig modifications were developed.

A summary of the total costs is presented in Table 3-9.

Table 3-9 Blade Root Machining - Capital Cost Estimate

DESCRIPTION	QUANTITY	MATERIAL	LABOR	CONTINGENCY	TOTAL
Reference Plates	(3)	$798	$6,211	$1,402	$ 8,411

3.5.3.2 Cost Reductions

Detailed manufacturing man-hour utilization studies were completed for both the current and proposed methods of machining the blade roots and installing the root cap. These showed a reduction in the man-hours required for the blade root machining operation from 3.5 to 2.5, a savings of 1 man-hour.

In addition to the decreased man hours another desirable benefit is realized. This benefit is that the epoxy resin cure cycle associated with installing the root cap will occur "off-shift". The current cycle requires that the blades remain undisturbed in the root stud installation bunks for nearly two hours. Although this does not result in a direct labor reduction (as the technicians are employed elsewhere during this period) it does increase the flexibility of the factory operation since the restrictions on blade movement and equipment availability are removed.

3.5.3.3 Simple Economic Analysis

Man hour reduction projected with implementation of revised root machining = 1 hour per blade.

Estimated equipment purchase and installation cost to implement proposal = $ 8,411

A. Return on Investment Calculation

Economic savings = 1 man-hours * ($ 10.00/Hr. + $3.50/Hr. {employee overhead}) = $ 13.50 / blade manufactured or ($13.50 * 3 blades/day * 253 worked days per year) = $ 10,246 / year.

R.O.I. = $10,246 / $ 8,411* 100% =122 %

B. Percent Reduction in Blade Manufacturing Cost

% Blade Cost Reduction = ($13.50 / $ 6158) * 100% = 0.22 %

3.5.4 Conclusions

The proposed changes in the manufacturing process to machine the blade root and install the root cap in the blade assembly fixture results in a modest cost savings per blade. However the capital costs to realize this improvement are also relatively small and at full plant production capacity results in an acceptable economic return. In addition, the change will increase the flexibility in factory operations and better spread the workload among the available crews. These changes would be expected to improve blade quality by improving working conditions in the plant.

4. Blade Materials and Design Elements

4.1 Alternative Materials Evaluation

The present ABM blade manufacturing process uses only the highest quality grades of Douglas fir veneer, manufactured from mature timber stands in Oregon . The continued long term usage of this material is unacceptable due to the increasingly high economic cost of the veneer, the rapidly decreasing available supply, and environmental concerns associated with harvesting mature timber. It was the objective of this portion of the BMP to identify lower cost replacement material that does not compromise blade quality or operating characteristics and for which there are fewer environmental concerns.

4.1.1 Approach

ABM's approach to finding an alternative veneer material can be summarized as follows:

1. Research lumber sources to identify potential alternatives. Contact current sources on the west coast and also identify and contact sources in or near Michigan to reduce incoming freight charges.

2. Evaluate alternative materials such as new growth Douglas fir, bamboo, poplar, yellow pine and veneers produced from composite strips of more readily available grades of Douglas fir to determine how well they meet the following initial criteria:

    a) Provides a substantial cost improvement
    b) Is readily available
    c) Is similar in material characteristics to the current baseline wood
    d) Resin absorption rate is acceptable

    The potential exists for direct replacement of the current material or a replacement in combination with other blade construction revisions such as increased fiber reinforcements or a change in the number of layers used in the present blade manufacturing process.

    This work was done in consultation with experts in the forest products industry.

3. Once alternative materials and/or construction revisions were identified the necessary raw materials to manufacture samples were procured.

4. A test plan was developed which clearly defined the types of samples to be fabricated and the testing they were to undergo. This test plan is summarized below.

    - Sample blocks were prepared under closely controlled conditions, recording moisture level, veneer weight, epoxy spread rate, vacuum pressure, etc. to maximize process integrity and repeatability. During production the following additional wood characteristics were visually noted and recorded by laminate for each sample block:

        a) Any inconsistency in the distribution of knots and or other surface irregularities
        b) Handling/bending characteristics of the veneer and laminate

- All sample blocks were then laboratory tested in a low-cycle R=.4 compression test to determine the bulk modulus of the material. Samples exhibiting the best combined results of the visual and laboratory tests were further tested in static and fatigue tests to establish material properties for design purposes.

5. The combined results of all of the tests and analysis were to be used to draw conclusions. Measured material properties were compared to the material properties assumed for the baseline blade design. The baseline properties had been developed based on earlier tests on the baseline material.

4.1.2 Candidate Materials Selection

The process of identifying and obtaining alternative wood species suitable for replacement of the baseline blade veneer was divided into three portions:

1. Contact existing veneer suppliers to obtain samples of new growth Douglas fir veneer that would meet all present raw material purchase specifications, except for those relating to appearance (quantity and size of knots).

2. Employ a consultant knowledgeable of the wood veneer industry to evaluate the current U. S. wood veneer manufacturers and recommend alternative wood veneers for evaluation.

3. Contact "Bamboo Hardwoods, Inc." located in Seattle to determine applicability of bamboo to blade manufacturing.

A summary of the results of the above studies follows.

4.1.2.1 Existing Veneer Suppliers

Both the Cascade Forest Group, Freres Lumber Co. Division and the Superior Lumber Co. were previous suppliers of veneer to ABM. Each was contacted to determine availability and pricing of new growth Douglas fir veneer that would meet all previous veneer purchase specifications, except that of appearance relating to the quantity and size of knots contained in the veneer. Results of vender contact were:

(a) Superior Lumber Co. has removed the Metriguard veneer grader from their veneer manufacturing operation and were unable to supply veneer meeting ABM's Metriguard requirement. They did indicate a willingness to supply ABM production requirements for the new growth Douglas fir, but could not currently supply sample quantities due to the cost of reinstalling the Metriguard grader.
(b) Freres Lumber Co. continues to grade all production with a Metriguard veneer grader and produces a high grade new growth Douglas fir veneer, that they recommended for ABM's consideration. This veneer was readily available and sold for $3.20/sheet versus $6.00 to $7.00/sheet for the baseline material.

A purchase order for 210 sheets (one pallet) of new growth Douglas fir was placed to the Freres Lumber Co.

4.1.2.2 Veneer Consultant

Robert Kunesh, R. K. Consulting Co., was retained to survey the current North American commercial veneer manufacturers and identify the best possible replacement(s) for the baseline material. His recommendation was that two types of yellow pine, Loblolly and Slash Southern pine, were suitable for further consideration and testing. His recommendation included specific potential suppliers that had indicated the ability to meet ABM's requirements. The largest potential supplier identified was the Trus Joist Co. in Cobert, Georgia which manufactures high volumes of Loblolly Southern pine veneer. Their mill produces a grade of Loblolly Southern pine veneer which is routinely processed through a Metriguard grader and is available in the quantities which could be required by ABM. The Loblolly veneer was estimated to cost $3.00 to $ 3.30 per sheet in truckload quantities. An alternate supplier that produces a much smaller quantity of Slash Southern pine veneer was also recommended by Robert Kunesh, especially if the Loblolly pine veneer should prove unacceptable in subsequent analysis. This alternative supplier was not contacted due to their limited supply potential.

The Loblolly Southern pine has very similar physical properties (density, modulus of rupture, working modulus, compressive strength, etc.) to the baseline material and the new growth Douglas fir. The close match in physical properties, significantly lower cost than the baseline material, and readily available production supplies of acceptable veneer resulted in Loblolly Southern Pine being selected as a potential alternative species.

4.1.2.3 Bamboo Wood Products

Contact was made with Andy Royer, Bamboo Hardwoods, Inc., of Seattle, WA. to determine the current availability of commercial quantities of bamboo veneer. Bamboo Hardwoods, Inc. was first contacted by ABM in late 1995 to determine the potential for future use of their bamboo wood veneer products. At that time Bamboo Hardwoods was a start-up company whose business was primarily related to the home and business wall decoration market. However, they expressed interest in pursuing the ABM veneer application in the near future as they planned to produce commercial quantities of bamboo veneer that they felt would meet ABM's purchase requirements. At the most recent contact, it was learned that Bamboo Hardwoods is still unable to offer full 4'x 8' veneer sheet materials to the industrial market. Subsequent efforts to determine other alternative suppliers of bamboo veneer stock were unsuccessful.

While it was found that Bamboo was not an alternative material at this time due to the unavailability of commercial quantities of veneer, the potential of long term usage of bamboo veneer to produce blades remains attractive due to the potential wide availability of source stock in countries with potentially significant wind energy markets.

4.1.3 Analysis Results

4.1.3.1 Evaluation Summary for Loblolly Southern Pine

Appearance & Physical Properties

Appearance of the Loblolly veneer sheets was excellent and of high quality with regard to knot count and size of knots. Existing ABM manufacturing processes utilize a visual grading standard of Grades A through D. Visual grading criteria include quantity and quality of knots, discontinuities in grain, and flatness of the sheets. Typical ABM production veneers are generally grade A or B. The Loblolly Southern pine veneer easily met the requirements for grades A and B. The Loblolly sheets did contain knots, which were very similar to those of typical baseline veneer sheets. The knots were usually less than 10 per sheet and typically of an open or loose type, averaging less than 1 inch in width. Overall appearance of the Loblolly sheets was judged as excellent, with no concern that sheet imperfections would result in an unacceptable exterior blade appearance. The Loblolly veneer sheets were receipt checked at ABM using a Metriguard Model 2600 ultrasonic veneer grader. Nearly all the sheets fell within the purchase specifications.

Handling & Processing Characteristics

In preparation for materials properties testing the Loblolly veneers were used to fabricate a laminated billet from which the test coupons would be cut. During this process the handling and processing characteristics of the material were evaluated.

The Loblolly veneer was noticeably less warped than the new growth Douglas fir and very similar to the baseline fir veneer. The sheets were also slightly thicker than the baseline material. The flatter, slightly thicker sheets contributed to a decreased splitting of the sheets (parallel with the grain) during handling as compared with the new growth Douglas fir and was similar to the baseline veneer. The Loblolly average density was 4.81 grams/cubic inch, which is about 18% higher than the Douglas fir. The higher density is a detriment as it would increase the overall weight of the finished blade. Average moisture content of the Loblolly was measured to be 8.8%, which is within normal specifications and very similar to the baseline material. Overall, the handling properties of the Loblolly were judged excellent and were similar to the baseline material.

The Loblolly pine sample billet was produced using an average epoxy resin spread rate of 29.6 grams/ft^2. This application rate is at the upper end of the normal application rate used for the baseline materiel and was also used for the new growth Douglas fir test billet. Examination of the billet after manufacturing indicated that little or no "squeeze out" of epoxy resin from between the veneers had occurred during the vacuum forming step. This appeared to indicate that the Loblolly Pine had a significantly higher resin absorption rate than the baseline material. The amount of "squeeze out" present in the test billet was judged marginal (as compared to typical baseline laminate) for development of the desired veneer sheet to veneer sheet bond strengths. However, it was decided to proceed with the fatigue testing of the billet samples since increasing the amount of epoxy used will increase cost and weight and exceed the capability of ABM's equipment.

When the billet was cut into test coupons it was possible to make additional visual observations relating to the resin adsorption of the wood veneer. Observation of the "exposed" surfaces of the Loblolly billet

revealed that the internal butt joints of the samples were also only "marginally" filled with epoxy resin. An "appropriately" filled butt joint contains sufficient epoxy resin to yield an oval shaped void. This has been determined in prior research to yield a strong butt joint in the cross grain. Too large or too small a void in the butt joint yields a reduction in the fatigue capability of the joint. The Loblolly pine laminate butt joints appeared dryer or less filled than a typical acceptable baseline Douglas fir joint. This was another indication that the resin adsorption of the Loblolly pine was higher than the Baseline Douglas fir.

Overall, the handling properties of the Loblolly veneer was judged excellent and fully comparable to that of the baseline Douglas fir. The processing equipment used for the baseline material was fully satisfactory for the Loblolly Pine.

Composite Laminate Properties

The test specimens prepared from the Loblolly Pine test billet were analyzed by Mr. Bill Bertelsen, of Gougeon Brothers, Inc. to determine the composite laminate fatigue strength. The objective was to establish values in compression, tension, and reverse axial fatigue loading. The original plan for the testing was to perform an initial series of progressive loading tests to determine the appropriate loads for classical fatigue testing. The series of classical fatigue tests were never performed because the progressive fatigue tests yielded very poor results for the Loblolly Pine laminate. In all cases, the Loblolly Pine failed at loading levels far under that originally obtained for the baseline Douglas fir. Failures of the laminate were judged to occur both by delamination of the laminate between veneer layers and by fracture through the butt joint area. In both cases, the cause of the failure was believed to be excessive absorption of epoxy resulting in poor bonding between veneer layers and inadequate filling of the butt joint cavities. The compressive fatigue values for the Loblolly Pine were comparatively closer to the values achieved for the baseline Douglas fir. Since the preliminary data showed that the Loblolly billets which had been tested would not meet the requirements for blade manufacturing, additional testing of the Loblolly Pine billet under classical fatigue loading was not completed. A complete copy of Mr. Bertelsen's report documenting the Loblolly test results is Appendix A.

An overall summary of measured and observed properties of the Loblolly Southern pine compared with typical baseline Douglas fir is presented in Table 4-1 below:

Table 4-1 Loblolly Southern Pine Comparison with Baseline Douglas Fir

Property	Observation - Baseline Comparison
Dimensional Thickness	0.113" avg. - Slightly Thicker
Dimensional Regularity	0.006 to 0.023" - Similar
Veneer Appearance	
Knots	<10/sheet - Similar
Knot Type	Open or Loose - Similar
Surface	Smooth - Similar
Other Defects	No Major - Similar
Overall Grade	A/B - Similar
Warp	Low - Similar to Improved
Splitting	Low - Improved
Veneer Density	4.81 gm/in3 - Higher
Epoxy Adsorption	Higher, Dryer Appearance
Overall Process-ability Judgment	Very Good - Similar
Final Laminate Appearance	Acceptable - Similar

Butt Joint Appearance - Laminate	50% filled - Less Filled, May be Weaker
Epoxy Spread Rate	Comparable, High End Normal Usage
Progressive Tension Fatigue	Considerably Lower
Progressive Compression Fatigue	Lower
Progressive Reverse Axial Fatigue	Considerably Lower

4.1.3.2 Evaluation Summary for New Growth Douglas Fir

Appearance & Physical Properties

Visual examination of the new growth Douglas fir veneer sheets received revealed no sheet defects exceeding the former baseline Douglas fir specification limits with the exception of the size and number of "quarter sized" knots contained in the sheets. Baseline Douglas fir veneer can be easily purchased having a very few (typically less than 10 to 20) knots per sheet, while the new growth veneer received contained 100 or more small knots per sheet. All the individual veneer sheets of the trial veneer were graded using the Metriguard Model 2600 ultrasonic veneer grader. This device measure the time required for ultrasonic waves to traverse the veneer sheet. Only approximately 25% of the veneer sheets met the standard ABM 450 micro second (u-sec) limit. Subsequently, the supplier assured ABM that the problem of out of specification veneer is not normal and that there should be no long-term problem assuring a supply of new growth Douglas fir veneer meeting ABM's specifications.

Handling & Processing Characteristics

In preparation for materials properties testing the new growth veneers were used to fabricate a laminated billet from which the test coupons would be cut. During this process the handling and processing characteristics of the material were evaluated.

An important factor that contributes to the handling of veneer and the quality of the final laminate is the flatness of the veneer received from the mill. Veneer that is heavily warped results in handling problems due to difficulty cutting it to desired dimensions and the potential for increased void formation in the final billet. The new growth Douglas fir veneer was noticeably more warped than the Southern pine and slightly more warped than the typical baseline Douglas fir veneer. Highly warped veneer sheets also contribute to increased splitting of the sheets (parallel with the grain) during handling. Experience has shown that split sheets do not result in a significant reduction in physical properties for the final laminate as long as the splits are not allowed to spread widely apart and adequate thickened epoxy resin is used to fill in the gap between the split edge wood fibers. Some splitting of the new growth Douglas fir had occurred by the time the test billet was manufactured. The new growth Douglas fir average density of 4.08 grams/cubic inch and average moisture content of 7.5 were near the mid-point of the typical range of baseline Douglas fir.

Manufacture of the test billet was carried out following the normal production sequence with no changes in processing due to the wood veneer. The average epoxy resin spread rate used for the new growth laminate billet was 29.3 grams/ft^2 which is at the upper end of the normal manufacturing range. This was also the range of epoxy resin application utilized for the Loblolly Pine billet, allowing data from the two billets to be directly comparable. During preparation of the test specimens visual observation of the internal butt joint of the samples indicated each was "appropriately" filled with epoxy resin. The new growth Douglas fir laminate butt joint appeared excellent, indicating that the resin adsorption of the new growth Douglas fir was acceptable.

Overall, the handling properties of the new growth Douglas fir were judged acceptable and comparable to that of baseline Douglas fir. No processing variations due to the wood species were observed.

Composite Laminate Properties

As with the Loblolly Pine evaluation, test coupons were cut and prepared from the new growth Douglas fir test billet and analyzed by Mr. Bill Bertelsen of Gougeon Brothers to determine the composite laminate fatigue strengths. The initial series of progressive loading tests indicated that the new growth Douglas fir laminate out-performed the Loblolly Pine laminate, with both tension and compression fatigue values closer to those developed by the baseline Douglas fir. Early in the classical fatigue test program, it was observed that the new growth Douglas fir samples were yielding a wide range of results under tension fatigue loading. Three sets of samples from selected areas of the original billet were tested in classical tension fatigue, with only one performing at the historical baseline Douglas fir levels. The other sets demonstrated laminate failure at significantly reduced levels. The wide range of values caused the test results to have a large standard deviation. When this large standard deviation is used to calculate the representative material strength for design purposes, the resulting strength is lower than would be obtained if the standard deviation was lower. As a result the blade that would either be unable to meet current design requirements or would be substantially heavier and more expensive as additional laminates would have to be added to the design. Based on this data, the classical fatigue testing of the new growth Douglas fir was stopped. Examination of the failed new growth Douglas fir test specimens revealed that the high incidence of knots contained in the veneer were only rarely involved in the initiation of the failures. Often, the fracturing of the sample specimen was occurring through the wood laminate in a region not containing a knot or the butt joint contained in the specimen. The specimens are designed so that failure is expected to be at the butt joint location in the center of the specimen. Closer inspection of the failure sites provided no complete explanation for the cause except that microscopic wood fiber compression fractures may have been pre-existing in some veneers prior to usage. Fracture zones are known to be created if timber is mishandled or shocked in some way prior to entering the veneer mill. Mr. Bertelsen's complete test report on this material is in Appendix A.

Following the fatigue testing, samples of the new growth Douglas fir were submitted for examination to the ABM veneer consultant, Robert Kunesh. This examination indicated that the veneer had been manufactured from quite small Douglas fir tree boles (6 to 10 inch in diameter) and that the veneer did appear to be much weaker across grain than standard Baseline Douglas fir. Further microscopic examination could not determine if the veneer had been damaged by improper handling or processing. However, the use of juvenile wood for production of the large veneer sheets could be a source of the veneer weakness, since heart wood is weaker than sap wood. Juvenile wood would also be more susceptible to damage during handling since the smaller logs can be more easily bent or excessively shocked by harvesting procedures. Discussions with the wood veneer supplier did not reveal any processing irregularities during the manufacture of the veneer provided to ABM. Therefore, it is believed that the weakness of the new growth Douglas fir tested was representative of the juvenile wood used to produce the veneer.

An overall summary of measured and observed properties of the new growth Douglas fir usage compared with typical Baseline Douglas fir is presented in Table 4-2.

Table 4-2 New Growth Douglas Fir Comparison with Baseline Douglas Fir

Property	Baseline Comparison
Dimensional Thickness	0.098" avg. - Typical
Dimensional Regularity	0.006 to 0.023" - Typical
Veneer Appearance	
Knots	Numerous (100+) vs. <10/sheet
Knot Type	Closed & Tight vs. Open or Loose
Surface	Smooth - Typical
Other Defects	No Major - Typical
Overall Grade	C/D versus A/B
Warp	Medium - Typical
Splitting	Medium/High - Above Average
Veneer Density	4.08 gm/in^3 - Typical
Epoxy Adsorption	Typical Appearance, Very Good
Overall Process-ability Judgment	Acceptable
Final Laminate Appearance	Acceptable
Butt Joint Appearance – Laminate	Comparable, Very Good
Epoxy Spread Rate	Comparable, Very Good, High End Normal Usage
Stress Wave Test Results - Laminate	No Voids, High Avg., Bond Strength - Comparable
Progressive Tension Fatigue	Similar to much lower
Progressive Compression Fatigue	Similar
Progressive Reverse Axial Fatigue	Similar to much lower
Laminate Failure Mechanism	Wood Failure (brittle)

4.1.4 Conclusions

Neither the new growth Douglas fir nor the Loblolly Southern Pine satisfied the requirements for wind turbine blade manufacture. Use of either species would unacceptably increase blade cost and weight either due to lower material properties or increased resin usage.

It is possible that a more strongly bonded Loblolly Pine laminate could be produced using a higher epoxy resin application rate. However, the epoxy spread rates used for the tests were approaching the limit of the equipment used to apply epoxy to the veneers.

Although this task did not identify an acceptable substitute for the currently used baseline Douglas fir, the data generated may eventually contribute to that replacement. The Loblolly Southern Pine veneer may be a viable replacement if the epoxy resin adsorption property can be reduced. Later in this report the results of tests of epoxy using fumed silica as a filler are discussed. This additive appears to significantly reduce the adsorption of epoxy resin into wood veneer. If this or another additive can be identified that would significantly decrease the adsorption of the resin into the Loblolly Pine, it is possible that Loblolly Pine could be an acceptable alternative wood species.

Douglas fir veneer also may still be a viable replacement species. After observing the properties of the new growth Douglas fir, veneer manufacturers were consulted to identify possible alternatives. In this process several mills were identified that are currently producing veneer from larger "second growth" Douglas fir groves (boles 16 to 30+ inch diameter). It is very probable that veneer produced from these larger boles will not evidence the same failures as the juvenile wood did in fatigue testing.

4.2 Lower Cost Resins

The present blade manufacturing process employs approximately 250 pounds of 105-E Resin and 9 pounds of 205-F Hardener to bond the Douglas fir veneers together. These materials account for roughly 8% of the costs in a blade. The purpose of this portion of the BMP was to determine if these costs could be reduced either though extending the resin or using lower cost vinyl ester resin.

4.2.1 Research Conducted

The current epoxy spread-rate is 24.5 to 30 grams/square foot of veneer sheet processed. All of the epoxy used does not contribute to bonding of the individual veneer sheets. A significant quantity of the epoxy is absorbed into the wood veneer and or fills veneer surface irregularities. Neither of these functions, contribute to the bond strength between veneers. The original project plan was to evaluate potential reductions in epoxy cost by utilizing a lower cost vinyl ester resins/hardeners or by using a low cost resin extender (such as fumed silica, micro-spheres, or other fillers) to reduce the absorption of resin into the veneer and/or amount required to fill veneer irregularities in the lamination process.

Gougeon Brothers, Inc., was contracted to provide assistance in evaluating alternatives to the present epoxy used by ABM. Gougeon was very supportive of the program objectives and agreed to assist in the program both by evaluating the feasibility of utilizing an alternative lower cost resin system and by recommending potential epoxy resin fillers or extenders for evaluation.

4.2.1.1 Alternative Resin System Recommendation

Gougeon's review of historical alternative adhesive testing, and a literature search, resulted in a strong recommendation that vinyl ester not be considered for ABM applications. The primary concerns identified were:

1. Vinyl esters are not usually used as adhesives. They are usually combined with fiberglass and post cured to achieve the strengths attributed to them by their manufacturers. This would not be compatible with the ABM process.

2. Vinyl esters require 30-40 mils of resin thickness to cure properly. This would not be present in a wood laminate similar to that made by ABM.

3. Carbon fiber used in the ABM blades is not compatible with vinyl esters

4. Vinyl esters are environmentally more hazardous than epoxies and substantially more explosive. Their use presents significant environmental and safety hazards.

These conclusions were reviewed and adapted by the project team and it was agreed that no further evaluation of vinyl ester resin systems would be warranted.

4.2.1.2 Use of Epoxy Resin Filler or Extenders

Extender/Filler Selection

Gougeon's evaluation identified several potential fillers and extenders which appeared to warrant further study. These included:

- Z-Light G-3500
- Scotchlite 3M K1-40622134354
- Dualite M6050 - AE04
- Recyclospheres LVO1-SG
- Extendospheres SG
- Q-Cel 2116
- Sil-Cell 43-23
- Aerosil 200
- Cab-o-Sil TS-720

The first seven of these items are micro-spheres which can be used as extenders. The last two are fumed silica additives which could reduce resin absorption and thereby permit less resin to be applied during the manufacturing process.

To be suitable for comprehensive testing any additive would have to meet the following requirements:

- The current resin spread rate specification of 24.5 to 30 grams per square foot of veneer surface for the lamination process is adequate to A) allow for epoxy resin absorption into the wood veneer, B) provide adequate bulk to fill in minor surface irregularities of the veneer sheet surfaces and butt joints between sheets, and C) allow a sufficient remainder to yield the necessary bond strength between veneer layers. Any thickened or extended resin system must reduce required epoxy usage by reducing the absorption into the veneer or reducing the amount required to fill the minor surface irregularities. The bond strength between veneer layers must be maintained at present levels.

- The ABM machine used to spread the epoxy mixture onto the veneer is a double roll coater. The thickened or extended resin mixture must be compatible with this unit.

- Initial testing would be conducted with a resin mix which would yield an overall cost saving of 20% relative to the present "neat" resin usage. This value was selected somewhat arbitrarily as a value which was sufficient to warrant the anticipated changes in processes and tooling but small enough to have a reasonable probability of being achievable without sacrificing bond strength.

Testing Completed

Initial testing of the micro-sphere extenders was done by making up samples of the epoxy extender mixture, completing test runs on the roll coater and test bonding pieces of laminate. Through this process it rapidly became apparent that the use of microspheres was not going to meet the requirements which had been established. The roll coater had difficulty in applying the microsphere extended epoxy in a uniform manner. In addition, the microspheres seemed to interfere with the bond strengths in the relatively thin bond lines used for wood-epoxy laminate production. As a result of these findings, no further work was completed with microsphere extenders.

The preliminary testing of fumed silica as an additive showed far more promising results. No problems with materials handling or apparent bond strength were observed when 2% by weight was added to the epoxy mixture. Based on these results a test billet was manufactured using an epoxy spread rate of 22 gm/ft2 (a 20% reduction) and epoxy extended with 2% fumed silica.

The billet was subsequently cut into test specimens which were provided to Gougeon for testing. The program scope and budget precluded extensive testing; however, preliminary progressive fatigue testing was completed. The test results were reviewed by the ABM blade consultant, Mr. Mike Zuteck. His conclusion was that the properties of the test specimens were very similar to the properties assumed for the original blade design. The Gougeon test report is Appendix B and Mr. Zuteck's analysis is Appendix C.

4.2.2 Simple Economic Analysis

4.2.2.1 Impact on Manufacturing System

To utilize the extended resin technology in the blade manufacturing process few changes in manufacturing procedures will be required. Production of the test laminate using the extended resin resulted in the following observations and processing recommendations:

- The existing roll coating machine would not require any revisions to the equipment or the current machine operating procedures.

- An additional mixing tank system would be required to pre-mix fumed silica into the epoxy resin. Based on the present use of epoxy resin, a 200 gallon capacity mixing system would be required. Cost to construct an existing 200 gallon system in 1995 was $9,000. Allowing for inflation at 2.5% per year, a duplicate 200 gallon mix system is estimated at $9,700 in 1998 dollars.

- Addition of the fumed silica to the epoxy hardener component of the epoxy mixture will not be necessary. The extended resin component containing fumed silica at 2.0% to 2.5% is very fluid and will transfer easily via the pumping systems used in the present process. The epoxy resin will be extended to contain 2.4% weight percent fumed silica. When mixed with neat hardener at a 5:1 weight ratio the final mixture will contain 2.0% fumed silica.

- Operating technician labor used to apply epoxy resin system to the veneer will remain unaffected by addition of the fumed silica.

4.2.2.2 Cost Reductions

Current Process Economics

The present ABM blade manufacturing process uses approximately 19.25 gallons of epoxy resin, equivalent to 210 pounds, per blade shell manufactured. Standard pricing of the raw materials used for the following cost benefit calculations is:

Epoxy Resin = $1.96 / pound
Epoxy Hardener = $ 2.78 / pound
Fumed Silica = $7.34 / pound

Total cost of current blade shell raw materials = resin + hardener = (210 * $1.96) + (210/5 * $2.78) = $528.36 per blade

Proposed Process Economics

The use of the extended resin allow a 20% reduction in the amount of epoxy used.

Requirement for epoxy resin using extended resin = 0.80 * 210 = 168 pounds / blade
Requirement for fumed silica = 168 * 2.4% = 4.032 pounds / blade

Total cost using extended resin = resin + fumed silica + hardener @ 20% reduction:
Total cost = (168 * $1.96) + (4.032 * $7.34) + (168/5 * 2.78) = $452.28 per blade

Blade cost reduction achievable using the extended resin technology = $528.36 - $452.28 = $76.08 per blade.

Return on Investment Calculation

Cost savings = $ 76.08 / blade manufactured or ($76.08 * 3 blades/day * 253 worked days per year) = $57,745 / year.

R.O.I. = $57,745 / $9,700 * 100% =595 %

Percent Reduction in Blade Manufacturing Cost

% Blade Cost Reduction = ($76.08 / $ 6,158) * 100% = 1.24 %

4.2.3 Conclusions

The use of fumed silica to extend the epoxy used in blade manufacturing appears to offer significant opportunities for blade cost reduction. It may also offer the opportunity to use other wood species with higher resin absorption characteristics. This was not evaluated as a part of this study due to time and resource limitations. A full set of classical fatigue tests should be completed to compliment the progressive fatigue test results completed in this study prior to using extended resin test data for detailed design.

4.3 Pre-sealed Scarfed Joints

4.3.1 Background

The present ABM blade shell is manufactured using approximately 150 separate pieces of veneer, each cut to an individual pattern to fit a specific position in the buildup of the blade shell laminate. In a blade with overall length of 43', many of the veneer pieces are necessarily joined end to end. Scarfed joints are used in the highly stressed outer layers of the blade shell while butt joints are used in locations of lower loading. In the AWT-26/27 blade design, scarfed joints are used in the outermost layer of both the high and low pressure blade shells and in laminate layers 2 through 6 of the high pressure shell. Scarfed veneer joints are used only where necessary, since the scarf cutting and the installation of the scarfed sheets into the blade shell molds are both more labor intensive than butt joints.

Previous research completed by Gougeon Brothers, Inc. (GBI), demonstrated that the presence of joints consistently resulted in a significant reduction of the fatigue life of laminate. It was found that the scarfed joint provided superior performance to the butt joint; however, the scarfed joint did not perform as well as

would be expected. It has been theorized that the lower than expected performance of the scarfed joint is caused by very small air bubbles forming in the epoxy resin in the joint areas when subjected to a vacuum. The air bubbles form as air contained in the natural wood fiber conduits is "sucked out" by the vacuum forming operation. These bubbles are trapped when the epoxy resin solidifies, weakening the joints.

The objective of this task was to identify a sealer which could plug the pores in the natural wood fibers, preventing the "bleed out" of small air bubbles into the epoxy resin in the joint region. If successful, the improved laminate strength would allow a reduction in the number of laminates in the blade design or potentially a reduction it the amount of carbon reinforcing required.

It has been noted that the standard 105 resin mixed with either 205 (fast) or 206 (slow) hardener should perform as a good pre-sealer. This would be true except for the amine "blush" which typically occurs on its surface during curing. The blush results in a poor bond formation if subsequent coatings of epoxy resin are attempted without the removal of the "blush" by mechanical sanding prior to bonding. Due to the highly irregular scarfed edges of the veneer pieces, any need for sanding to thoroughly remove an amine "blush" between coatings would be unacceptable. Therefore, there is currently no known effective sealer for this application. An effective sealer must be easy to apply to the roughened scarf surface, result in a cured surface that will bond excellently with the standard 105/206 resin system and effectively seal the natural wood fibers exposed on the veneer panel end grain.

4.3.2 Research Completed

4.3.2.1 Joint Sealer Research

The project team, in consultation with Gougeon, evaluated many different materials to be used as a sealer for the scarfed joints. A preliminary screening resulted in four potential sealant materials for evaluation testing. These materials were:

1. Duratec Epoxy Bond-Cote manufactured by Hawkeye Industries, Inc.. This material is currently used in the manufacturing process to aid bond development between the outer blade exterior gel coat and the inner epoxy resin substrate.
2. GBI standard 105 Resin at 3:1 ratio of 207 Special Coating Hardener. The 207 Hardener is a new product by GBI and upon curing, typically results in a much reduced formation of amine "blush".
3. A commercially available End Grain Sealer manufactured by Boatlife Co.. It is a two component epoxy and polysulfide based coating recommended to seal the end grain on all woods.
4. Shellac, commonly used for wood sealant purposes. This sealer is readily available and low cost.

These sealers were each subsequently subjected to a two step testing process to identify the most promising candidate sealer. The tests completed were:

1. Test to determine sealing capability - the candidate sealer was applied to one end grain surface of a piece of 1" thickness Douglas fir Board Stock which had been pre-sealed with standard GBI 105/206 resin mix on the side surfaces and the other end grain surface. Following cure of the candidate sealer the sample was placed into a vacuum jar with the sample submersed under water. Vacuum was then applied and the sample monitored for the formation of air bubbles escaping through the end treated with the sealer candidate. Observance of air bubbles indicated the sealant failed the test. Two samples using each sealer candidate were run.

2. Test to determine the bondability of the sealer candidate to the GBI 105/206 epoxy resin system used in blade manufacture. This was determined using a Patti-meter test. The Patti-meter instrument has been used by Gougeon to determine the adhesion of the Gougeon epoxy system to various surfaces. In this test a standard Patti-meter "pull-stud" is bonded onto a surface and, following full bond formation, is subjected to an axial pull until the stud is pulled free. The force required to pull the stud free is then converted into a yield strength.

   There were two series of Patti-meter tests performed, differing on the length of cure time allowed for the sealer to cure prior to the application of the 105/206 GBI adhesive. Both one and three day cure times were tested to model the current weekday only factory operation. A sealer which passed both these tests would allow the sealer to be applied on the scarfed veneer panels on the day of veneer panel fabrication, which is typically the working day prior to actual blade shell lamination.

These tests showed that the Gougeon 105 resin with the 207 special coating hardener was the most suitable candidate for further testing.

4.3.2.2 Fatigue Testing

To determine the fatigue capability of a pre-sealed scarfed joint, a test billet was fabricated whose joints were pre-sealed with the Gougeon 105 resin/207 hardener. Test specimens from this test billet were tested by Gougeon to obtain preliminary material properties. The Gougeon test report is Appendix D. Note that resource and time constraints limited the testing to progressive fatigue tests only. Prior to using pre-sealed scarfed joints for detailed design a full set of classical fatigue test data should be obtained.

An analysis of the test data was completed by Mr. Mike Zuteck . This analysis indicated that the pre-sealed scarf joint is significantly stronger than an unsealed scarfed joint. Analysis of the reverse axial fatigue data indicated that the blade allowable design stress would be 32% higher than the original design basis, which at equal stress would yield about 24 times as many allowable fatigue cycles. Analysis of the tension fatigue data indicated that the blade allowable design stress would be 11% higher than the original design basis, which at equal stress would yield approximately 4 times as many fatigue cycles. Mr. Zuteck's complete report is included as Appendix E.

4.3.2.3 Impact on Manufacturing

Manufacturing Procedures

Manufacturing procedures to incorporate the pre-sealed scarf technology into the blade manufacturing process were developed by ABM. The current design uses scarf joints in the first 6 layers of laminate on the high pressure blade shell. The six layers contain a total of 15 panels of veneer 97 inches in length that are scarfed on each end and 9 lengths of veneer of varying shorter lengths that are scarfed on one end only. The current procedure is to fabricate scarfed veneer panels in a batch lot which subsequently are stacked for use in blade construction at a later time. Typically, a batch lot of veneer panels provides three days of factory production. Toward the end of each manufacturing day the veneer panels for the next day are assembled into blade lifts. In the blade lift the individual sheets are removed from storage and stacked on one another in the order they are to be processed through the epoxy applying roll coater prior to placement into the blade molds. Each stack is on a lift cart that is used to transport the veneer lift to the roll coater and blade molding operation.

Using pre-sealed scarf joints in the blade production process is not expected to cause major changes to the current manufacturing cycle. The epoxy sealant will be rolled onto the scarfed edge of the panels generating a uniform application. It will be important to apply the sealant uniformly since drops or beads of sealant may interfere with creating a tightly seated joint when the panels are placed into the blade mold. ABM would seal the scarfed edges during stacking of the panels onto the lift cart. As one technician loads the panels onto the cart a second would apply the coating to the scarf edges. It will be necessary to use small scrap veneer slats to maintain spaces between coated edges and adjacent sheets to prevent bonding between sheets. The technician applying the sealer will also place these slats between panels. Stacking of a lift currently requires about 15 minutes using one technician. It is estimated that the addition of the scarf sealing operation will cause the stacking time to approximately double to 30 minutes. It will also be necessary to add a second technician for this period to apply the sealant. The application of the scarfed joint sealant will therefore require an additional ¾ man-hour per blade relative to current procedures. Since the pot life of the sealant is 25 to 35 minutes at the conditions present in the factory completing the lift while sealing the scarfed edges will be feasible.

Pre-sealed Scarf Joint Equipment Requirements

Equipment required to incorporate pre-sealed scarf technology into the ABM factory is minimal. A small resin and hardener mixing and dispensing system available from Gougeon Brothers will be required. This dispensing system currently lists at $400.00 per unit.

4.3.2.4 Impact on Blade Design

Mr. Zuteck's assessment of the data for pre-sealed scarfed joints concluded that the increase in strength indicated by the available data was sufficient to eliminate the carbon from the blade design. This is a significant advantage because the carbon is relatively expensive material and it is difficult and time consuming to handle in the blade manufacturing process. Mr. Zuteck's report on this subject is Appendix F.

4.3.3 Simple Economic Analysis

The projected elimination of carbon in the blade results in both a significant manufacturing cost reduction and a reduction in final blade weight. An ABM analysis of these factors resulted in the following determinations:

Blade Manufacturing Cost Reduction:

Raw Materials

Carbon re-enforcement used per blade = 120 Ft^2 per blade @ $1.92 / Ft^2 = $230.40 per blade
NOTE: No additional raw material cost is incurred due to usage of 105/207 epoxy resin system to seal scarf veneer edges, since edges are currently sealed with 105/206 epoxy resin at similar usage and cost during present manufacturing operations.

Installation Labor

Fabricate carbon re-enforcement strips = 1.5 hr. per blade (reduction)
Install carbon re-enforcement = ¼ hr per 15 technicians per blade = 7.5 hr. per blade (reduction)
Additional Labor to pre-seal scarf edges = ¾ hr. per blade (increase)
Total labor impact per blade = 8.25 Hr. reduction

Labor Cost Reduction @ $13.50 per hour = $111.38 per blade

Total Blade Impact

Total Blade Cost Reduction = $230.40 + $111.38 = $341.78 per blade
Percentage Blade Cost Reduction = $341.78/$6,158.44 * 100% = 5.55 %

Total Weight Reduction = 0.375 Lb. / Ft^2 * 120 Ft^2 = 45.0 Lb.

4.3.4 Conclusions

The results of the preliminary performance testing for the pre-sealed scarfed joints indicates that their performance is superior to unsealed scarfed joints. The performance improvement appears to be sufficient to remove the carbon reinforcement from the blade. The costs of achieving these improvements are minimal and the savings significant. A full spectrum of classical fatigue tests should be conducted to confirm the properties indicated by the progressive testing completed in these study; however, it is expected that future wood blade designs should use pre-sealed scarfed joints in their design.

5. Preliminary Blade Design

5.1 Design and Manufacturing Improvements

Based on the work documented in the preceding sections of this report, ABM, working in conjunction with AWT and Mr. Mike Zuteck, developed a preliminary design of a blade which would incorporate the improvements identified in this project.

Mr. Zuteck estimated the impact removal of the carbon from the blade shell would have on the stiffness of the blade. Using this data, AWT evaluated the overall turbine dynamics and concluded the change would not have a significant impact.

With these results, ABM concluded that the preliminary blade design would be very similar to the baseline blade with the following changes:

1. Elimination of the carbon fiber reinforcement
2. Pre-seal all scarfed joints
3. Use of a molded shear web
4. Use of extended resins

The blade manufacturing operations would be changed to incorporate the preceding design changes as well as the following process changes:

1. Improved vacuum monitoring
2. Improved resin application rate monitoring
3. Improved blade shell NDT
4. Machining the root end in the blade assembly jig
5. Drilling all 15 root stud holes simultaneously
6. Reduction in blade cure cycle time

The impact of these changes on blade cost was then assessed.

5.2 Cost Benefit Analysis

5.2.1 Capital Costs

The capital costs required to achieve the improvements outlined above for single and dual production shifts are summarized in Table 5-1.

Table 5-1 Capital Costs for Preliminary Blade Design

Item	Capital Cost Single Shift	Capital Cost Dual Shift
Pre-seal all scarfed joints	$400	$400
Use of a molded shear web	$17,508	$17,508
Use of Extended Resins	$9,700	$9,700
Improved vacuum monitoring	$27,871	$27,871
Improved Resin Application Rate Monitoring	$1,520	$1,520
Improved blade shell NDT	$5,197	$5,197
Machining the root end in the blade assembly jig	$8,411	$8,411
Drilling all 15 root stud holes simultaneously	$32,831	$32,831
Reduction in blade cure cycle time	$0	$403,685
Total	**$103,438**	**$507,123**

5.2.2 Blade Cost Reductions

The blade cost reductions realized by incorporating the design changes outlined above for single and dual production shifts are summarized in Table 5-2.

Table 5-2 Blade Cost Reductions

Item	Cost Reduction Single Shift	Cost Reduction Dual Shift
Pre-seal all scarfed joints	$342	$342
Use of a molded shear web	$54	$54
Use of Extended Resins	$76	$76
Improved vacuum monitoring	$0	$0
Improved Resin Application Rate Monitoring	$0	$0
Improved blade shell NDT	$0	$0
Machining the root end in the blade assembly jig	$13.5	$13.5
Drilling all 15 root stud holes simultaneously	$13.5	$13.5
Reduction in blade cure cycle time	$0	$373
Total Cost Reduction per Blade	$499	$872

5.2.3 Simple Economic Analysis

For single shift operation the improvements identified would reduce blade cost approximately 8% ($499/$6,158) and provide a first year return on investment of approximately 366% ($499/blade*759 blades per year/$103,438) if the plant was operated at full capacity. Even if the plant were operating at one third capacity there would be a positive return on investment in the first year.

For higher blade capacities and dual shift operation, the improvements identified would reduce blade cost approximately 14% ($872/6158) and provide a first year return on investment of approximately 260% ($872/blade*759 blades per shift*2 shifts/$507,123) if the plant were operated at full capacity. Full capacity would not be required to warrant the initial investment to move to two shift operation.

6. Summary and Conclusions

This project identified several significant improvements in the technology for manufacturing wood epoxy wind turbine blades. These improvements result in substantial reductions in the cost of the blades and are expected to improve blade quality. However, the project was not successful in identifying an alternative material to replace the mature Douglas fir presently used in the design. Continued use of this material remains commercially and environmentally unacceptable due to its limited supply and the environmental problems associated with using mature forest products. A subsequent ABM review of additional alternatives to the baseline material resulted in the identification of a limited number of veneer suppliers of mid-grade Douglas fir veneer, peeled from older "second growth" trees. These trees are substantially larger in diameter than the trees used for the "new growth" veneers tested in this program and would be expected to exhibit material properties much more consistent with the baseline timber properties. In addition, other alternative wood species such as the Loblolly pine, used with an extended resin, Slash pine, or Russian Larch may be viable selections, but additional testing is required.

The wind turbine market has changed substantially since this project was originally proposed. The market for utility scale wind turbines has shifted from turbines with 24-27 meter diameters and roughly 300 kW ratings to turbines with diameters of 40-50 meters and ratings of 600-750 kW. These larger units have diminished the competitiveness of the AWT-26 and AWT-27 models on which the ABM blades are used. As a result, the market for AWT products has decreased. This, together with the problems associated with FloWind's bankruptcy, have resulted in AWT and ABM being shut down.

Despite the failures of ABM and AWT, the technical potential for wood epoxy technology in wind turbine blade manufacture is significant. The wood epoxy material, when properly manufactured, offers a combination of light weight, relatively low cost and high strength not available in other known materials. As wind turbines continue to develop into larger diameters, these properties are expected to become even more desirable.

However, the technology continues to have serious commercial limitations. Due to the inherent variability of the wood raw material the variability in the manufacturing process is likely to be greater than for man-made materials such as fiberglass. This variability, if not well controlled, can result in low quality blades being produced. In addition, this variability must be considered when establishing the material properties to be used in design. If there is a high degree of variability in the test data, the allowable strength of the material for design purposes will be reduced relative to what it would otherwise be.

The technology currently uses a wood species which is no longer commercially or environmentally feasible. The effort to find an alternative species revealed the sensitivity of the laminate properties to the wood species. While Loblolly pine appeared to have the required material properties, its high absorption of epoxy resulted in a poorly performing laminate. The new growth Douglas fir exhibited poor performance, not due to the large number of knots it contained, but due to immature trees having different properties than more mature trees. While none of these problems are insurmountable, they illustrate the difficulty of working with natural material for engineered applications.

The sensitivity of the blade properties to the wood species used presents a commercial problem for wind turbine suppliers as well. The wind turbine market is a worldwide market, with many countries participating. At this time the costs of shipping blades and other components long distances gives a

competitive advantage to companies with production facilities in the county where the projects are being built. Many companies are establishing assembly facilities and blade manufacturing facilities in the home country of the projects they are building. While it is always possible to import raw material for operations such as this, it is preferable to use domestic supplies whenever possible. This is believed to present a competitive disadvantage for wood epoxy blades due to the costs associated with re-engineering the blade design and manufacturing processes for a new wood species.

Another barrier to wood epoxy technology in the wind turbine market is its cost sensitivity to production rates. While this is a common problem for blade manufacturing technologies, the lack of a significant market for wood epoxy blades aggravates the problem and presents a barrier to entry. Without an order of sufficient size to benefit from economies of volume production, it will be difficult for a wooden blade manufacturer to have a competitive product. As wind turbine sizes increase to the megawatt scale, this may be less of a barrier due to the relatively low production volumes for turbines of this size.

In addition, wood epoxy technology does not lend itself to forming the cylindrical root shapes used in most commercial wind turbine designs. Wood epoxy roots tend to be modified oval shapes and have a continuous taper from the airfoil section to the root. As a result, it is not practical to consider manufacturing wood-epoxy blades for the existing wind turbine market. The adapters which would be required would significantly offset any weight and cost advantage wood epoxy could offer. In addition it is more difficult and less cost effective to design and build a single set of molds which can be used to produce different length blades by varying the length of the root as is done by fiberglass blade manufacturers.

Based on the above, it is suggested that a careful assessment of the barriers to wood-epoxy in the wind turbine market place should be completed prior to any further research on the technology. The technical advantages are very attractive, however the commercial limitations of the technology should be understood and additional technical research directed toward addressing these limitations. Areas which may warrant further research include:

- Identification of a suitable wood species which is available in many parts of the world
- Examination of approaches to making blades with easily varied lengths
- Examination of techniques for making blades with round roots and would thereby be more readily accepted by existing turbine manufacturers
- Further examination of the benefits available from wood epoxy as turbines increase in size.

If these limitations can be addressed, or the benefits of wood epoxy can be shown to be large enough, market acceptance will follow.

Appendix A

Preliminary Fatigue Tests of New-Growth Douglas Fir Laminate and Southern (Loblolly) Pine w.r.t Suitability for Wood/Epoxy Wind Turbine Blade Construction

Preliminary Fatigue Tests of New-Growth Douglas Fir Laminate and Southern (Loblolly) Pine Laminate w.r.t. Suitability for Wood/Epoxy Wind Turbine Blade Construction

William D. Bertelsen
GOUGEON BROTHERS, INC.
October, 1997

1.0 Background and Overview: A successful wood/epoxy wind turbine technology was developed and implemented in the 1980's based on WEST SYSTEM™ epoxy and rotary-peeled Douglas fir veneer from the continental U.S. Northwest. The veneer supply was maintained for a decade by the harvesting and peeling of large-diameter (old-growth) tree trunks. Unfortunately, as the 1990's wear on, the large-diameter fir logs may no longer be available in sufficient numbers to sustain volume blade production. Manufacturers must prepare to accept veneers from younger (new-growth) fir trees or switch to an entirely different wood species.

This report documents the preliminary investigation of new-growth Douglas fir and Southern (loblolly) pine as to suitability for wind turbine blade construction in terms of laminate fatigue strength. Three fatigue loading situations were used: tension fatigue @ R = 0.1, compression fatigue @ R = 0.1, and reverse-axial, tension-compression fatigue @ R = -1.

2.0 Specimen Design and Preparation: Two billets of parent material were fabricated by Advanced Blade Manufacturing, Pinconning, MI. Each billet consisted of 19 layers of rotary-peeled veneer, treated and vacuum-formed with clear WEST SYSTEM™ 105/206 epoxy. However, one billet was made using 0.100"-thick new-growth Douglas fir veneer, and the other billet made with 0.115"-thick Loblolly pine veneer. Grain direction was the same in every layer. Specimen designs were patterned after tension and compression samples used in the 1990 DOE blade laminate fatigue test program, Contract DE-AC02-86ER80385, as documented in the Phase 2 Final Report, December 1990 (Reference 1). All test specimens were to have 0.5"-wide butt joints in the middle three veneer layers, staggered 3" apart in the grain direction.

The compression specimens were identical in configuration to the DOE "wide-butt" specimens, being approximately 2" x 2" x 8", grain aligned with the long dimension. The ends of the blocks were specially prepared to mate with the platen faces of the test machine using a procedure described in detail in Reference 2.

The design of the tensile/reverse-axial style specimens was modified in three ways: (1) Overall specimen length was increased from 16" to 24", (2) Specimen width was increased from 0.4" to 0.5", and (3) specimen grip regions were reinforced with unidirectional carbon fiber (ANCAREF C-150) rather than bidirectional E-glass. Note: DOE tension fatigue strength data had been somewhat below expectations. Since the shortfall could not be explained any other way, specimen geometry was indicted. The ABM/Sandia specimens were lengthened in hopes of creating a more uniform stress distribution in the test section.

The two parent billets were each divided into seven sectors from which could be cut four tensile-style specimens and two compression-style specimens. Specimens were to be numbered consecutively across sector boundaries and marked either "NG" for new-growth Douglas fir or "SP" for Southern (loblolly) pine. The compression blocks were cut in pairs from the far edge of each sector. It happened that both parent billets were too short after finishing, so that the last (compression) specimen of Sector 7 (#042) was eliminated from each billet. It had the effect of creating an isolated compression sample with no near-neighbor twin. These #041 "orphans" were later used for progressive fatigue testing. (See Section 5.2.)

3.0 Test Matrix: Table 1 is a diagram illustrating both specimen spatial relation within the respective parent billets and each sample's specific utilization in the test program. The shaded half of the table delineates the loblolly (SP) population. The column labelled "Compr. E Test?" identifies which compression specimens were subjected to non-destructive bulk compression modulus testing. (See Section 4.0 below.) The general plan was to conduct modulus and progressive fatigue tests on a few specimens from both populations, and then to choose just one species for classical fatigue tests. As indicated in Table 1, the new-growth Douglas fir was eventually selected for classical fatigue tests.

4.0 Compression Modulus Tests: Since wind-turbine blade engineering is weight and stiffness-driven, it was important to measure the density and compression modulus of both wood species' laminates. The modulus tests were done using a non-destructive, low-load/low-cycle compression fatigue method developed for the DOE veneer joint research of Reference 1.

4.1 Equipment and Setup: The testing was carried out in the Gougeon Materials Testing Laboratory using an MTS Model 312.41 110-kip servo-hydraulic load frame, load cell, and actuator with Model 442 Controller, Model 421 Amplitude Controller. All fatigue testing, including compression modulus testing, was conducted in load-control mode (i.e., with the test machine hydraulic actuator responding to actual load cell measurements throughout each cycle). The loading function was sinusoidal with the use of an amplitude controller in the feedback loop. Amplitude control provides additional boost to the hydraulic servo-valves which operate the actuator. This boost is necessary to overcome slight losses in peak load values due to the change in specimen compliance as it accumulates damage. The primary control system on its own is often unable to handle the compliance change, particularly at the end of a test when the test sample is near breaking. Amplitude control insured that a specimen was subjected to its full peak load on every cycle no matter how much internal damage had accumulated.

4.2 Compression Modulus Test Method: The compression modulus testing was accomplished without an extensometer by attaching Model 643.41C-01 self-aligning compression platens to the 110-kip MTS and running a low-cycle, low-load fatigue program. The built-in actuator L.V.D.T. (linear variable differential transformer) and digital indicator were then used to monitor specimen displacement. Each compression specimen was carefully installed between the platens of the test machine while making certain the specially squared and prepared block ends were seated properly on each facing steel surface. After start-up @ 4 Hz, the peak load was set at 10,000 lbs. with a stress ratio (R value) of 0.4. This meant that each specimen experienced a sinusoidal compression load pattern which oscillated between 4,000 and 10,000 lbs. The large specimen cross sections (about four square inches) translated the resulting peak psi loads to about 2,500 psi.

Specimens were allowed to cycle up to the count of 1,000 before reading the "delta stroke", the indicated linear distance between the actuator position at minimum load and at maximum load. Because some of the indicated displacement was actually due to slight bending and flexing of the test machine itself, the test was repeated without the test specimen installed. Using the same load settings, the test machine was restarted with the compression platens simply pushing against each other. Reading the delta stroke in this configuration told just how much to subtract from the indicated specimen displacement as measured during the previous run in order to arrive at the true specimen displacement. Given knowledge of the load changes and actuator motions during the cycling, a bulk compression modulus number could be calculated.

4.3 Compression Modulus and Density Data: The results of the compression modulus testing are presented in Table 2. Specimens with the "NG" designation are from the new-growth Douglas fir population. The "SP" specimens are all Southern (loblolly) pine. Note that the average pine modulus (2.34 million psi) is some 10% higher than for the fir (2.12 million psi). The conventional/historical modulus value for wood/epoxy blade laminate used in design work is 2.25 million psi. The new-growth fir modulus is disappointing with respect to the established database. It might seem that the loblolly is the clear winner, however the laminate density also needs to be considered. Density values were calculated for each specimen by multiplying the cross-sectional area by the length and then dividing by the weight, as measured on a gram scale accurate to the nearest 0.1 g. Cross-section measurements were made in the middle of each specimen with a dial calipers accurate to the nearest 0.001". It can be seen in the 7th column of Table 2 that the average density of the fir and pine are 37.21 lbs./ft.^{3} and 42.71 lbs./ft.^{3}, respectively. In other words, the pine was 15% heavier per unit volume than the fir, offsetting its modulus advantage.

It follows that it would be instructive to calculate an average modulus/density ratio (i.e., specific modulus) for each species to see which had the best stiffness per unit weight. These averages appear in the last column of Table 2. If the historical value for blade grade laminate is taken to be 0.0584, then both fir and pine species are found wanting to the extent of 2.6% and 6.2%, respectively.

As a "reality check", several unjointed 2" x 2" x 8" compression specimens were cut from existing old-growth Douglas fir/epoxy laminate and tested at room temperature on August 4, 1997. One group came from a billet fabricated by Advance Blade Manufacturing, Pinconning, MI. These were designated "AOG" for ABM old-growth fir. The other group was made from leftover laminate used in the construction of stud test specimens by GOUGEON BROTHERS, INC. for R. Lynette & Associates, Redmond, WA, in 1992-93 (Reference 3). These were designated "GOG" for GBI old-growth fir. Note that the test results for both of these old-growth sub groups are included at the bottom of Table 2. It can be seen that they meet or exceed the historical, old-growth blade laminate values, thereby validating the NG and SP modulus test results.

5.0 Progressive Fatigue Tests: The test plan (Reference 2) called for conducting block-cycle progressive fatigue testing on both laminate species in all three loading modes prior to attempting classical fatigue tests. "Block cycle" progressive fatigue meant that, if a specimen remained unfailed after an arbitrary number of constant-mean stress/constant-amplitude cycles, the peak load would be increased by a set

amount, and the test allowed to continue for the same number of cycles (or until failure, whichever came first). The block cycle testing was to have the following format: (1) The stress ratio (R value) was to be held constant throughout, (2) The cycle block length was to be 10,000 cycles, and (3) The increment of peak stress increase was to be 10% of the start value. It would be up to the principle investigator to choose the initial peak stress level, with the aim of generating a failure within a 5-block period. In the initial study, only one representative of each species was to take part in each loading situation.

5.1 Progressive Tension Fatigue Tests: .

5.1.1 Tension Fatigue Equipment and Setup: All tension fatigue tests were conducted with the GBI MTS 22-kip load frame, a servo-hydraulic test machine equipped with a 20,000 lb. load cell and 7.57 $in.^2$ actuator as part of the MTS "810" series Material Test System. The tests were controlled with the 459.10 TestLink™ Automated Control System with manual inputs from a Compaq 286 desk-top computer.
The TestLink™/Compaq combination generated the sinusoidal R = 0.1 fatigue loading with amplitude control. Built-in data-acquisition functions were utilized to monitor and document each test. TestLink™ recorded setup parameters for each test, including test number, peak load, stress ratio, and frequency.

Critical to the execution of the tension fatigue series was the implementation of the MTS 647.10A-01 hydraulically-operated, wedge-action grips. These grips provided regulated clamping pressure through a manifold valve set by the operator. Since the wedge shape of the grips causes clamping pressure to increase as the axial tensile load is applied, the first tests were run with the use of crush limiters, i.e., steel "bite blocks" to restrict the squeezing of the specimen ends and prevent grip-induced, premature failures.

Experience with glass-reinforced DOE tensile specimens showed that the grip/specimen interface worked best when crush-limiters were made 0.050-0.055 inches less than the specimen thickness. For the ABM/Sandia carbon-reinforced specimens, that margin was reduced to .034-.044 inches. Figure 1 shows sample NG-039 installed in the grips and ready for test. Depth of grip engagement at each end was 2.375 inches. That left an effective test section length of 19.25 inches since all tensile-style specimens were 24.0 inches in length overall. The set-up procedure was to hold Hydraulic grip line pressure to the minimum (200 psi) while first engaging the clamps. Then a proof tensile load of 500 lbs. was applied, at which time the grip line

pressure was increased to 350 psi. The proof load was removed before startup. This method resulted in a virtually trouble-free fatigue test series with no grip-induced failures.

Progressive tension fatigue testing began with specimen NG-039 on July 22, 1997. Starting load for all tensile tests was 6,000 psi at 6 Hz. Stress ratio was held constant at R = 0.1.

5.1.2 Progressive Tension Fatigue Data

The results of all the progressive fatigue tests are presented in Table 3. Table 3 lists tested specimens by number in a horizontal row. Beneath each specimen number is the number of cycles run at the load specified in the first column. The first cycle block length for the NG-039 and SP-039 was 11,020 cycles instead of 10,000 because of a software problem which prevented the automatic 10% incrementing of the peak load at the 10,000-cycle count. Subsequent tests had to be stopped at the end of each cycle block with the tripping of a count limit and then manually restarted. NG-039 eventually failed after 8,911 cycles at the 7,800 psi peak load, the fourth block of cycles.

Note in Table 3 the listing of laminate moisture content (Laminate M.C.) for selected specimens just below their respective cycle totals. Immediately after test, the carbon-augmented grip regions were cut off with a band saw. The remains (test section) of each specimen were weighed and placed in a VWR 1630 circulating oven at 103 °C. The initial test-section weight was recorded in a card file. Specimens were removed from the oven periodically and re-weighed. When a sample showed no further weight decrease, it was assumed that all moisture had been removed.

The laminate moisture content was calculated using the following expression:

$$\text{L.M.C.} = \frac{(\text{Post-test weight}) - (\text{Dry weight})}{(\text{Dry weight})} * 100$$

L.M.C. for NG-039 was calculated to be 7.04% after 14 days in the circulating oven.

Since strength is a function of wood moisture content (W.M.C.), direct comparisons of strength between two or more test specimens are only possible when their moisture content is equal. The wood industry uses 12% as the standard W.M.C. value for performance comparison. Since it is not possible to condition all specimens to 12%, the USDA Forest Products Research Lab in Madison, Wisconsin has studied the effect

of moisture content on the static strength of Douglas fir. The results are published in the USDA Wood Handbook, p. 4-32 (Reference 4). Their function for tensile strength variation with moisture content can be used to estimate the failure strength of fir at 12% W.M.C. when the strength at some other W.M.C. value is known. One needs only to adjust measured laminate moisture content (L.M.C.) values to compensate for the presence of some epoxy. The multiplication factor of 1.22 was derived for DOE data analysis and was used again in this report. So, W.M.C. = 1.22 * L.M.C. Applying the Wood Handbook relations to NG-039 converts the 7,800 psi failure stress at 7.04% L.M.C. to 7,389 psi at 12% W.M.C.

5.1.3 Progressive Tension Fatigue Failures: Figures 2 and 3 are photographs of the failed specimens NG-039 and its counterpart SP-039. Both failures were solidly in the test sections with heavy butt-joint involvement, however the rather early failure in the pine sample initiated away from the butt joints, in the outer 3 veneer layers, apparently due to local grain-dive. The single fir specimen performed up to the standards of its old-growth predecessors in the DOE tension fatigue study of Reference 1. A typical wide-butt DOE specimen with the same laminate moisture content would have run 13,500 classical fatigue cycles at the final NG-039 stress level.

The performance of the pine specimen was disappointing, succumbing to grain dive in the outer layers at only the 6,600 psi stress level. Two more progressive fatigue tests of the wide-butt, loblolly pine specimens were subsequently conducted on September 5 and 8, 1997. These were tests of SP-001 and SP-019 that were authorized after most of the new-growth Douglas fir specimens performed poorly in the classical tension fatigue series (Section 6.2) Unfortunately, this second look at the loblolly laminate only served to reinforce the conclusion that the pine laminate could not be considered a viable successor to old-growth Douglas fir laminate. The cycle and load specifics are reported in Table 3.

The test of SP-001 at only 6,000 psi was characterized by very early middle butt-joint failure (200 cycles). By 2,060 cycles both the outer veneer and the lower butt joint had failed. Complete separation occurred at 3,300 cycles. Examination revealed that there was an absence of epoxy in the butt-joint cavities. This implied that during construction, the neat epoxy might have been absorbed into the wood to the point where pine veneers simply could not be adequately bonded.

Sample SP-019 also had the dry-butt-joint look, but the failure initiated 6,870 cycles into the first cycle block in an area of grain dive in the outer veneer layers.

The specimen eventually failed after 4,367 cycles at the 6,600 psi level. Because of the need for further visual examination of these failures, neither specimen was baked-out to determine its moisture content. Analysis of other pine specimens suggest that both SP-001 and SP-019 were in the 7.75-8.00% laminate moisture range. A typical wide-butt Douglas fir DOE specimen with 8.00% laminate moisture content would have run 102,000 classical fatigue cycles at the 6,600 psi stress level.

5.2 Progressive Compression Fatigue: Testing got underway July 23, 1997 with NG-041 (the "orphan" specimen from sector 7) at 7,000 psi peak stress, R = 0.1, and 8 Hz in the 110-kip MTS machine. The frequency was chosen to match that used in the DOE tests of Reference 1. The hardware setup was basically the same as for the compression modulus testing with the use of the self-aligning compression platens. Figure 4 is an after-test photo which shows the failure of NG-041, which occurred 8,430 cycles into the second cycle block at 7,700 psi peak stress. The actuator stroke limit was set at 0.1" so that the machine turned itself off when the specimen was compressed 0.1" less than its original 8.0" length. Note that the failure initiated away from the specially prepared ends and featured a classic, nearly 45° slip line.
The failed sample was weighed and placed in the circulating oven for 29 days to determine its laminate moisture content, which turned out to be 7.21%. Results of all the progressive compression fatigue tests appear in the middle portion of Table 3.
A typical wide-butt Douglas fir DOE compression specimen with 7.21% laminate moisture content would have run 30,000 classical fatigue cycles at the 7,700 psi stress level.

The test of corresponding pine sample SP-041 was conducted in exactly the same manner. It demonstrated greater strength, failing 4,790 cycles into the third (8,400 psi) cycle block. One specimen each (unjointed) from the Gougeon and ABM old-growth fir laminate group (designated GOG and AOG, respectively) were also tested August 5, 1997, and those results are included in Table 3 as well. The two unjointed specimens proved to be substantially stronger, as expected. Data from Reference 1 show that, when results are normalized for moisture content, unjointed specimens can handle compression fatigue loads which are about 16% greater than wide-butt specimens, for test lifetimes in the 20,000 cycle range. That is reasonably close to the strength advantage demonstrated by GOG-1B-3 in this series, failing at the 9,100 psi level vs. NG-041 at 7,700 psi. The conclusion was, that in this single, isolated instance, the new-growth fir performed just about as well as had average samples from the historical/traditional old-growth fir database.

5.3 Reverse-Axial Progressive Fatigue Tests: Reverse-axial testing began July 28, 1997 with NG-040. Once again, the 22-kip MTS with wedge-action grips was used to introduce test loads into the specimens. The mechanics of the setup and specimen installation were virtually the same as for the progressive tension fatigue series of Section 5.1. The same grip pressures and crush limiters were used. The main difference was the addition of column supports to prevent buckling during the compression half of each R = -1 stress cycle. Figure 5 is a photograph of NG-040 installed with column supports and ready for test at the initial ±4,000 psi stress level.

At startup, another software problem was encountered which prevented the tests from being run with automatic amplitude control. Fortunately, the 22-kip MTS could be manually operated in sinusoidal load control mode with the model 458.11 DC Controller and 458.90 Function Generator. However, the operator was compelled to constantly monitor (and frequently adjust) the peak load to maintain the prescribed stress during each cycle block.

5.3.1 Reverse-Axial Progressive Fatigue Data: The reverse-axial test results are also presented in Table 3 along with respective laminate moisture content values. In this series, the 8.00% L.M.C. pine specimen was the clear winner, surviving to the ±5,600 psi level, while the fir specimen failed at ±4,800 psi. It was the loblolly which came closest to the typical wide-butt reverse-axial test of the DOE series, since one of those old-growth fir specimens at 8.00% L.M.C. could have been expected to do about 11,750 classical fatigue cycles at the ±5,200 psi stress level.

5.3.2 Reverse-Axial Progressive Fatigue Failures: Figures 6 and 7 show the failures of NG-040 and SP-040, respectively. NG-040 developed a crack in its outermost veneer at 3,660 cycles at the ±4,400 psi stress level. SP-040 had a butt joint fail at about 3,500 cycles into the ±5,200 psi cycle block, but it wasn't until three outer layers split off that failure became imminent. The split occurred at about 9,000 cycles into the same block. SP-040 survived the asymmetric load until the end of the count limit, but it failed on startup at the ±5,600 psi stress level.

6.0 Classical Fatigue Tests: The mixed results of the progressive fatigue series made it difficult to choose which species to evaluate in the classical fatigue format. Although the Southern (loblolly) pine had a modest performance edge in compression and reverse-axial testing, new-growth Douglas fir was selected for constant-amplitude classical fatigue testing because of its initial performance near the historical level for Douglas fir in tension fatigue. Classical fatigue testing was to include tension,

compression, and reverse-axial testing. There were to be (within each loading mode) four low-cycle, four high-cycle, and two moderate cycle tests, so that an S-N curve might be obtained with a reasonably well-defined slope. These tests began with compression fatigue on August 8, 1997

6.1 Classical Compression Fatigue: The equipment and set up were the same as for the progressive fatigue tests of Section 5.2. Once again the 110-kip MTS load frame and self-aligning compression platens were used in load control mode with amplitude control. Stress ratio (R value) was maintained at 0.1 throughout, with a test frequency of 8 Hz. The first test was NG-017 at 8,200 psi. It failed at 3,350 cycles, providing an excellent low-cycle data point. L.M.C. turned out to be 7.11%. Its near-neighbor, NG-018 was started at 6,500 psi in hopes of obtaining a corresponding high-cycle data point, but it remained unfailed and quite stable after over 3 million cycles. It had to be retired as a runout.

6.1.1 Classical Compression Fatigue Data: Two additional compression fatigue tests were conducted before the project was terminated. All the compression results are presented in Table 4, which includes modulus and laminate moisture content for all failed specimens. Note that the failure strengths converted to 12% W.M.C. (Reference 4) values are also listed in the last column.

Figure 8 is a graph of the compression S-N curve in log-log form using the 12% W.M.C. values. In this form it is possible to compare performance with the typical wide-butt DOE fir trend established for 12% W.M.C. in Reference 1. Note that the ABM/Sandia new-growth fir compression specimens performed at effectively the same level. The "runout" with the right-pointing arrow was never baked out to determine L.M.C. It was plotted by assuming it had an L.M.C. value which was the same as the average of the other three.

6.2 Classical Tension Fatigue: These tests required the 22-kip MTS machine and wedge-action grips described in detail in Section 5.1.1. However, crush limiters were not regularly used, since there were indications in the progressive series that they were not needed.

6.2.1 Classical Tension Fatigue Data: Classical R = 0.1 tension fatigue began with NG-008 running at 6 Hz on August 14, 1997. The peak load was 7,200 psi. The load was chosen based on aiming for a moderate-cycle failure, but the test lasted 569,696 cycles. Unexpected results were the rule rather than the exception in this series.

All the tension fatigue results are presented in Table 5. Note the lack of high-cycle data. There is a column for L.M.C. but the listed values have to be regarded as lower bounds only. Bake-outs were never completed because the excessive variability within the new-growth fir population mandated thorough inspection of the failed specimens.

The data were plotted in log-log form in Figure 9. Only in Figure 9 do the results make any kind of sense, since it can be seen which specimens were near-neighbor pairs. The specimen pairs from billet sectors 2, 3, and 1 seemed to perform at successively lower levels. Only NG-007 and NG-008 performed at the historical old-growth fir level. It is interesting that the respective S-N slopes seemed to be the only thing the three specimen pairs had in common. Since tension strength is a relatively weak function of wood moisture content, it was not expected that the sector 3 and 1 results would be significantly improved by normalizing them to 12% W.M.C.

6.2.2 Classical Tension Fatigue Failures: Figures 10-12 are photographs of the failures of members of each of the three billet sectors, 2, 3, and 1. They are NG-008 (Figure 10), NG-014 (Figure 11) and NG-001 (Figure 12), in descending order of performance. In spite of the wide performance differences, no obvious differences in failure appearance were noted. In all but one case there was no warning of failure. Only in the long-running test of NG-008 was a crack detected prior to failure. At 545,900 cycles, a crack could be felt between layers 4 and 5 extending from the middle upwards beyond the upper butt-joint level.

The testing of the new-growth fir was called to a halt after the test of NG-002 on August 21, 1997, after which it was decided to conduct two more progressive fatigue tests of the Southern (loblolly) pine. Those tests have already been recounted in Section 5.1.3. Since the results offered no improvement over the new-growth fir, the project was terminated without proceeding to reverse-axial testing.

7.0 Conclusions and Recommendations: Neither the fir nor pine performed with the strength and the consistency required for responsible wind-turbine-blade engineering. Gross examination of the failed fir classical tension fatigue specimens showed many more small knots in new-growth veneers than were typically present historically in old-growth veneers. But knots were only rarely implicated in the initiation of failures. Closer inspection provided no complete explanation for the extreme variability of the parent billet. However, there were hints of microscopic wood fiber compression fractures in some veneers which may have existed prior to test. If so, it might mean

that the existing veneer quality control process must be improved to prevent microscopically damaged veneers from being used in construction.

With regard to the Southern (loblolly) pine, the tension fatigue failure of SP-001 was the most alarming. As mentioned in Section 5.1.3, the early failure of butt joints indicated that bonds between veneers were poor, probably due to lack of sufficient epoxy. The pine part of the research should be repeated with epoxy spread rate and consistency adjusted for a wood species with greater absorption capacity.

8.0 References:

1.0 Bertelsen, W.D., and Zuteck, M. D., "Investigation of Fatigue Failure Initiation and Propagation in Wind-Turbine-Grade Wood/Epoxy Laminate Containing Several Veneer Joint Styles", Phase 2 Report, U.S. Departement of Energy Contract No. DE-AC02-86ER80385, December, 1990.

2.0 Detailed Test Plan, Blade Manufacturing Project AN-0166, Section 2.2.2 - Replace Old-Growth Veneer, Section 3.1.7 Specimen Edge Sealing Procedure, Advance Wind Turbines, Inc., Seattle, WA, June, 1997.

3.0 Bertelsen, W.D., and Zuteck, M. D., "Static and Fatigue Tension Tests of Small-Blade Load-Transfer Studs Optimized for Cost Effectiveness", GOUGEON BROTHERS, INC., October, 1994.

4.0 U. S. Forest Products Laboratory, Forest Service, 1974. *Wood Handbook, Wood as an Engineering Material*, USDA Agricultural Handbook No. 72.

Table 1
Location and Disposition of Test Specimens Within Parent Billets

Billet Sector	New-Growth Fir	Compr. E Test?	Type of Fatigue Test Performed	Lob-lolly Pine	Compr. E Test?	Type of Fatigue Test Performed
	001		Classical Tension Fatigue	001		Progressive Tension Fatigue
	002		Classical Tension Fatigue	002		
1	003			003		
	004			004		
	005	Yes		005	Yes	
	006			006		
	007		Classical Tension Fatigue	007		
	008		Classical Tension Fatigue	008		
2	009			009		
	010			010		
	011	Yes	Classical Compression Fatigue	011		
	012	Yes	Classical Compression Fatigue	012		
	013		Classical Tension Fatigue	013		
	014		Classical Tension Fatigue	014		
3	015			015		
	016			016		
	017	Yes	Classical Compression Fatigue	017	Yes	
	018	Yes	Classical Compression Fatigue	018		
	019			019		Progressive Tension Fatigue
	020			020		
4	021			021		
	022			022		
	023	Yes		023	Yes	
	024			024		
	025			025		
	026			026		
5	027			027		
	028			028		
	029			029		
	030			030		
	031			031		
	032			032		
6	033			033		
	034			034		
	035	Yes		035	Yes	
	036			036		
	037			037		
	038			038		
7	039		Progressive Tension Fatigue	039		Progressive Tension Fatigue
	040		Progressive Reverse-Axial Fatigue	040		Progressive Reverse-Axial Fatigue
	041	Yes	Progressive Compression Fatigue	041	Yes	Progressive Compression Fatigue

Table 2
Compression Modulus and Density
New-Growth Doug. Fir vs. Old-Growth Doug. Fir and Southern (Loblolly) Pine

Specimen	Compression Modulus (psi)	Density (Lbs./Ft.3)	Modulus Density Ratio	Peak Stress (psi)	Average Modulus (psi)	Average Density (Lbs./Ft.3)	Average Modulus Density Ratio
NG-017	2.122 E+06	37.48	0.0566	2,564			
NG-041	2.119 E+06	36.97	0.0573	2,604			
NG-005	2.018 E+06	36.87	0.0547	2,576			
NG-035	2.161 E+06	37.66	0.0574	2,578	2.116 E+06	37.21	0.0569
NG-023	2.162 E+06	37.12	0.0582	2,568			
NG-018	2.098 E+06	38.22	0.0549	2,556			
NG-011	2.143 E+06	36.96	0.0580	2,589			
NG-012	2.102 E+06	36.41	0.0577	2,540			
SP-005	2.333 E+06	43.34	0.0538	2,284			
SP-023	2.385 E+06	42.63	0.0560	2,286			
SP-017	2.355 E+06	42.48	0.0554	2,232	2.340 E+06	42.71	0.0548
SP-035	2.316 E+06	43.17	0.0536	2,235			
SP-041	2.312 E+06	41.91	0.0552	2,240			
AOG-3A-1	2.348 E+06	40.79	0.0576	2,578	2.382 E+06	41.07	0.0580
AOG-3A-2	2.415 E+06	41.34	0.0584	2,566			
GOG-1B-1	2.387 E+06	39.54	0.0604	2,561			
GOG-1B-2	2.341 E+06	39.49	0.0593	2,570	2.345 E+06	39.22	0.0598
GOG-1B-3	2.307 E+06	38.61	0.0598	2,572			

Table 3
ABM/Sandia Progressive Fatigue Data
10-17-97

Progressive Tension Fatigue, R = 0.1

Peak Load (psi)	Hz	Wide-Butt NG-039 Cycles	Wide-Butt SP-039 Cycles	Wide-Butt SP-001 Cycles	Wide-Butt SP-019 Cycles
6,000	6	11,020	11,020	3,300	10,005
6,600	6	10,000	6,860		4,367
7,200	6	10,000			
7,800	5	8,911			
Laminate M.C.:		7.04%	7.79%	N.A.	N.A.
Drying Days:		14	13	0	0

Progressive Compression Fatigue, R = 0.1

Peak Load (psi)	Hz	Wide-Butt NG-041 Cycles	Wide-Butt SP-041 Cycles	Unjointed GOG-1B-3 Cycles	Unjointed AOG-3A-1 Cycles
7,000	8	10,000	10,000	10,000	10,000
7,700	8	8,430	10,000	10,000	10,000
8,400	8		4,790	10,000	10,000
9,100	8			4,770	10,000
9,800	8				1,870
Laminate M.C.:		7.21%	7.81%	7.64%	6.33%
Drying Days:		29	28	71	71

Progressive Rev. Ax. Fatigue, R = -1.0

Peak Load (psi)	Hz	Wide-Butt NG-040 Cycles	Wide-Butt SP-040 Cycles
4,000	4	10,005	10,005
4,400	4	10,005	10,005
4,800	4	6,137	10,005
5,200	4		10,165
5,600	3		21
Laminate M.C.:		7.15%	8.00%
Drying Days:		24	23

Table 4
Classical Compression Fatigue Data, R = 0.1
New-Growth Douglas Fir Laminate

Test Date	Specimen	Compression Modulus (psi)	Peak Load (psi)	Cycles to Failure	Hz	Laminate Moisture Content	Drying Days	Peak Load 12% W.M.C. (psi)
8/8/97	NG-017	2.122 E+06	8,200	3,350	8	7.11%	68	6,844
8/11/97	NG-018	2.098 E+06	6,500	3,410,000*	8	N.A.	0	N.A.
8/15/97	NG-011	2.143 E+06	7,600	40,090	8	6.95%	61	6,276
8/15/97	NG-012	2.102 E+06	7,300	26,370	8	7.05%	61	6,068

*Specimen NG-018 remained unfailed at the cycle total listed.

Table 5
Classical Tension Fatigue Data, R = 0.1
New-Growth Douglas Fir Laminate

Test Date	Specimen	Peak Load (psi)	Cycles to Failure	Hz	Log 10 Peak Load	Log 10 Total Cycles	Laminate Moisture Content*	Drying Days
8/14/97	NG-008	7,200	569,696	6	3.8573	5.7556	6.63%	6
8/19/97	NG-007	8,500	3,068	4	3.9294	3.4869	6.61%	2
8/19/97	NG-001	8,300	40	4	3.9191	1.6021	N.A.	0
8/20/97	NG-013	7,800	1,400	4	3.8921	3.1461	6.50%	2
8/21/97	NG-014	6,600	12,680	6	3.8195	4.1031	6.00%	1
8/21/97	NG-002	5,200	22,853	6	3.7160	4.3589	N.A.	0

*Moisture values should be regarded as lower bounds only, due to inadequate drying time.

GOUGEON BROTHERS, INC.

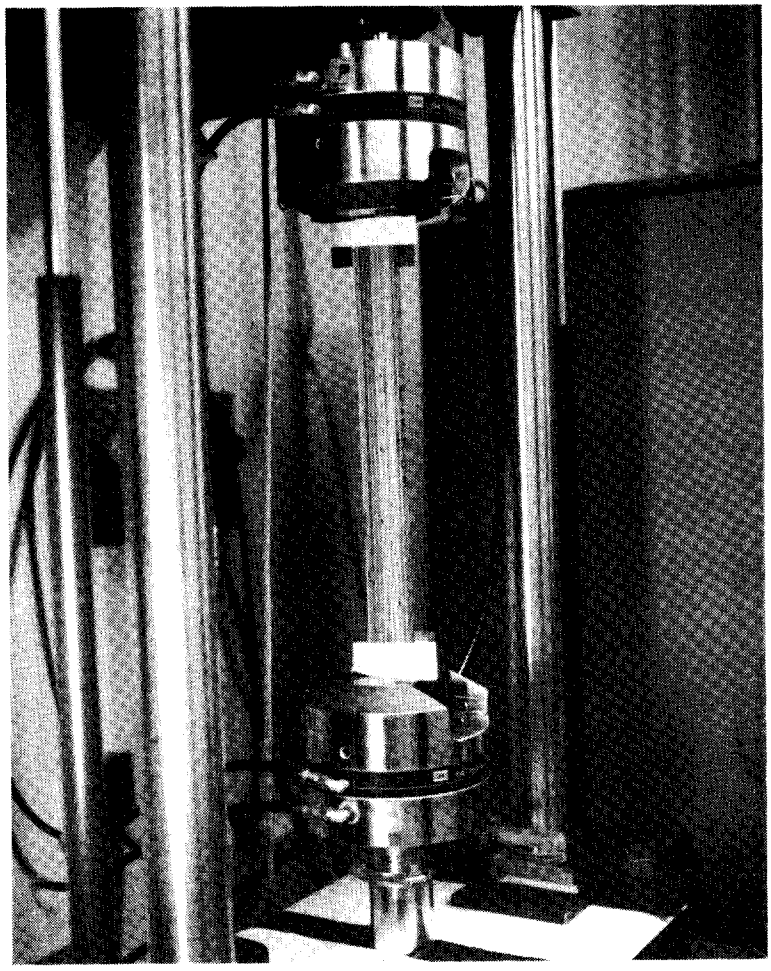

Figure 1

Setup for progressive tension fatigue tests showing specimen NG-039 installed in 22-kip MTS with wedge-action grips.

GOUGEON BROTHERS, INC.

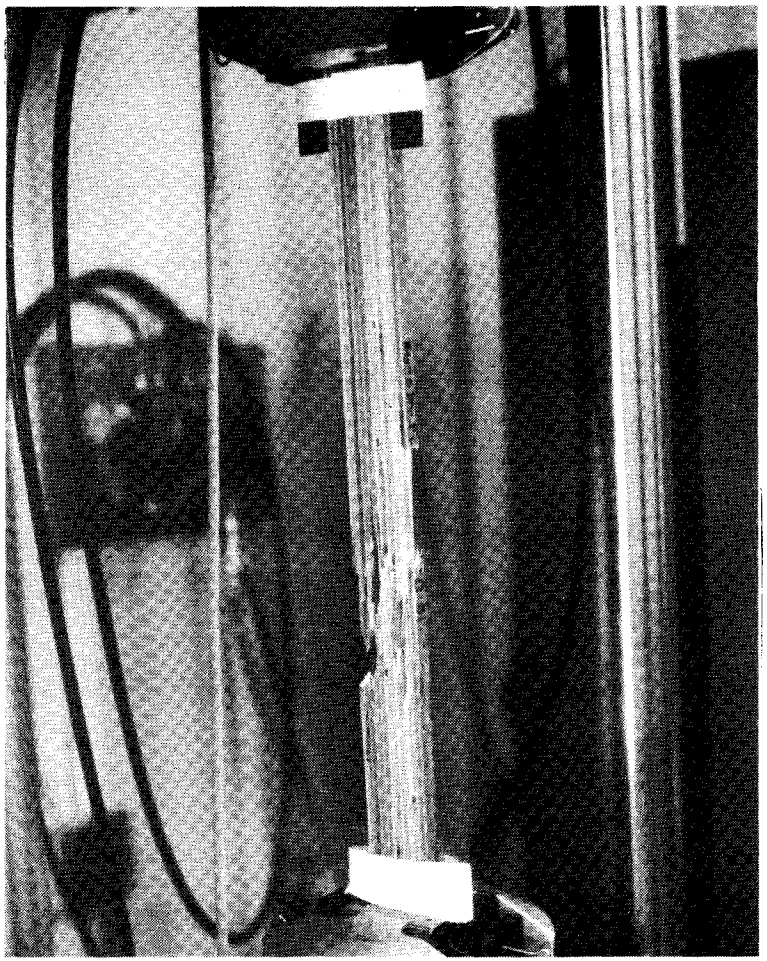

Figure 2

Failure of progressive tension fatigue specimen NG-039, new-growth fir.

GOUGEON BROTHERS, INC.

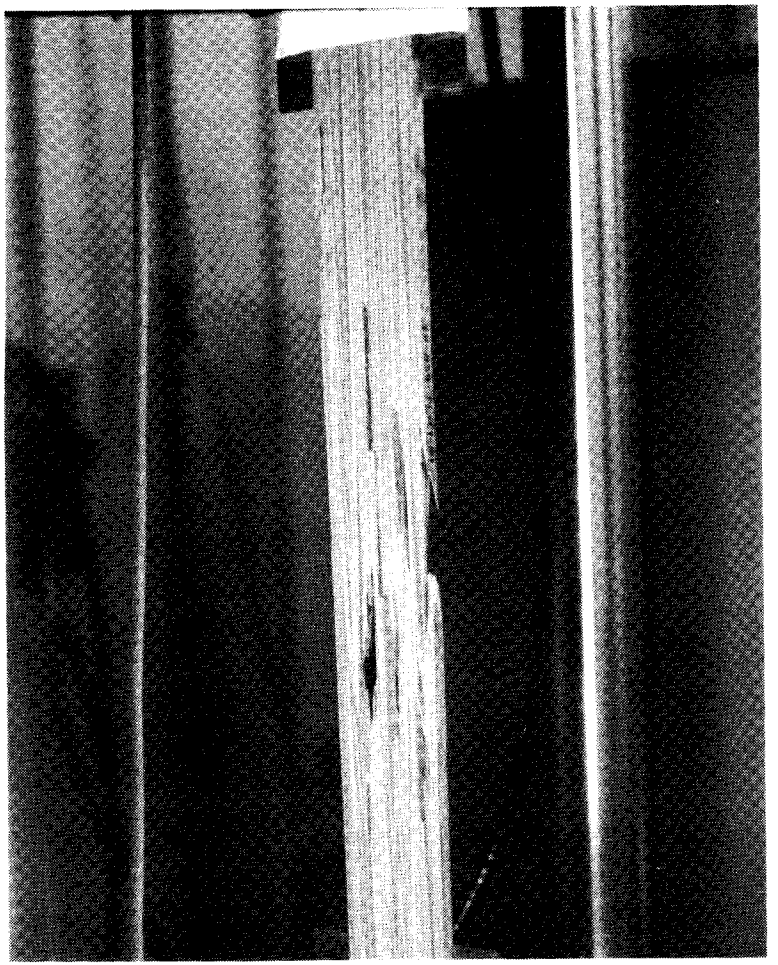

Figure 3

Failure of progressive tension fatigue specimen SP-039, loblolly pine.

GOUGEON BROTHERS, INC.

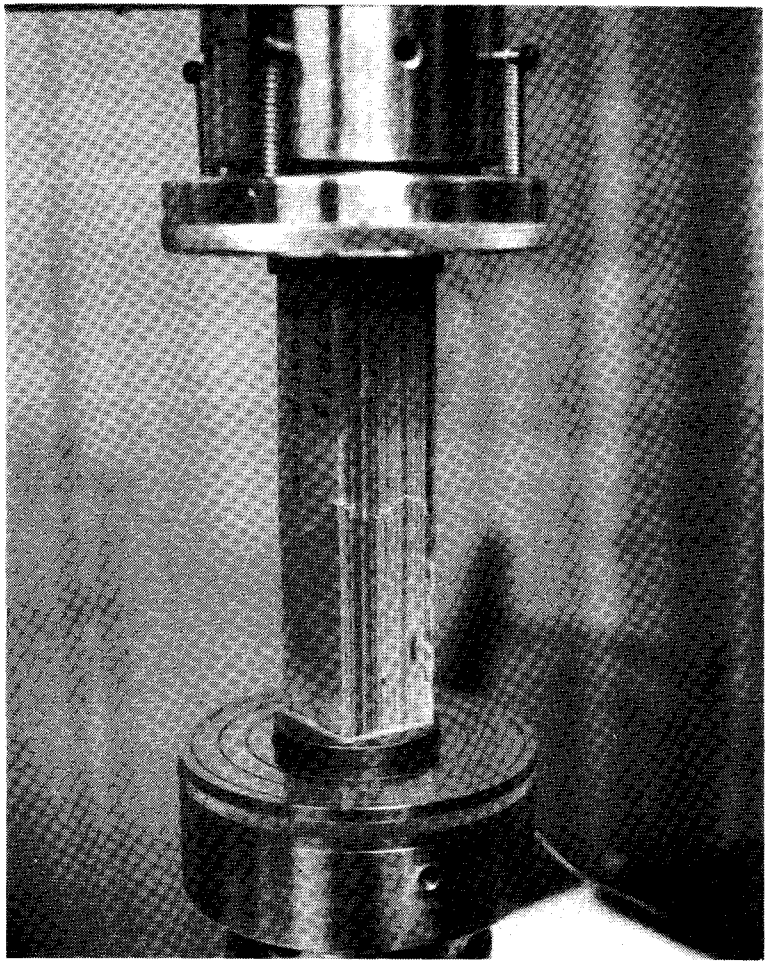

Figure 4

Failure of progressive compression fatigue test specimen NG-041 in 110-kip MTS with self-aligning platens.

GOUGEON BROTHERS, INC.

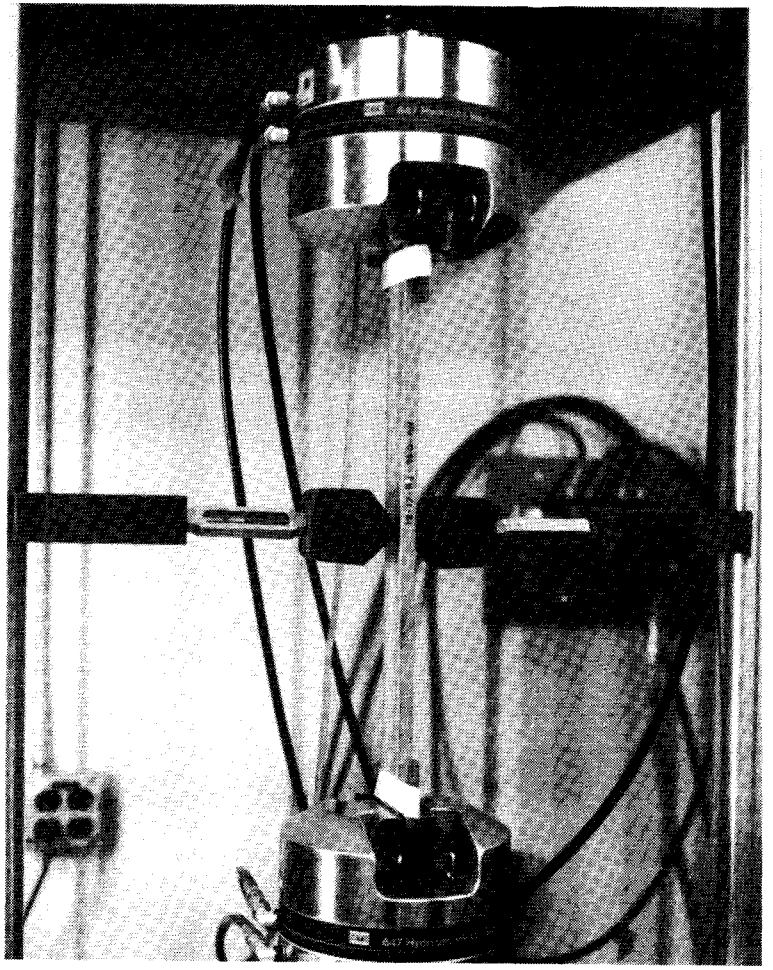

Figure 5

Setup for progressive reverse-axial fatigue tests showing specimen NG-040 installed in 22-kip MTS with wedge-action grips and column supports.

GOUGEON BROTHERS, INC.

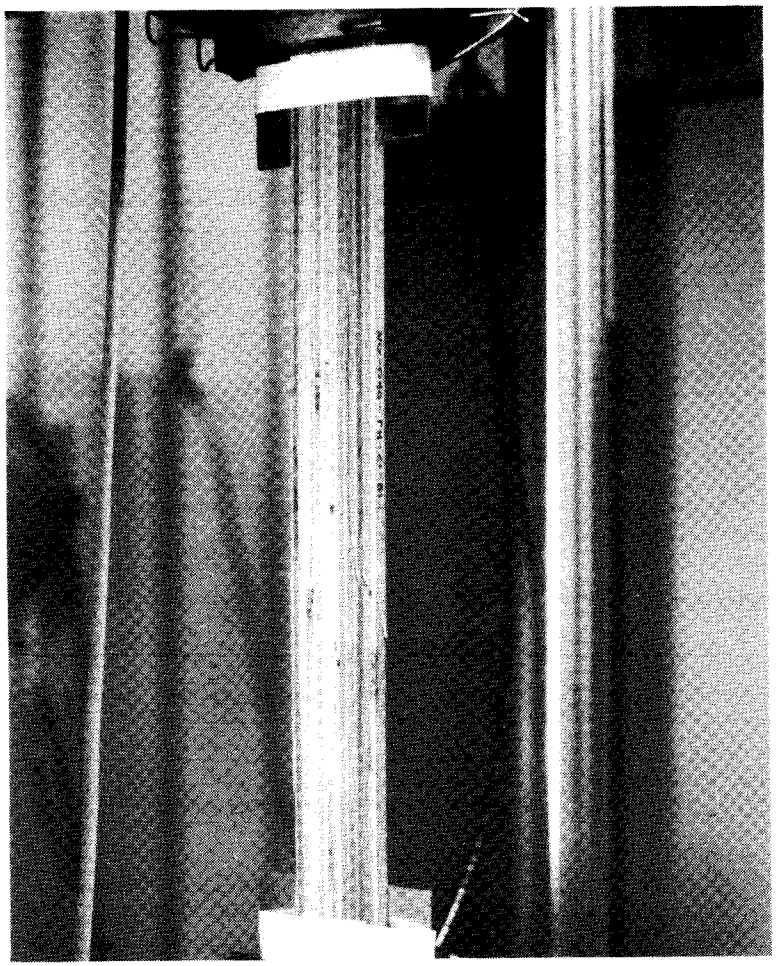

Figure 6

Failure of reverse-axial progressive fatigue specimen NG-040, new-growth fir.

GOUGEON BROTHERS, INC.

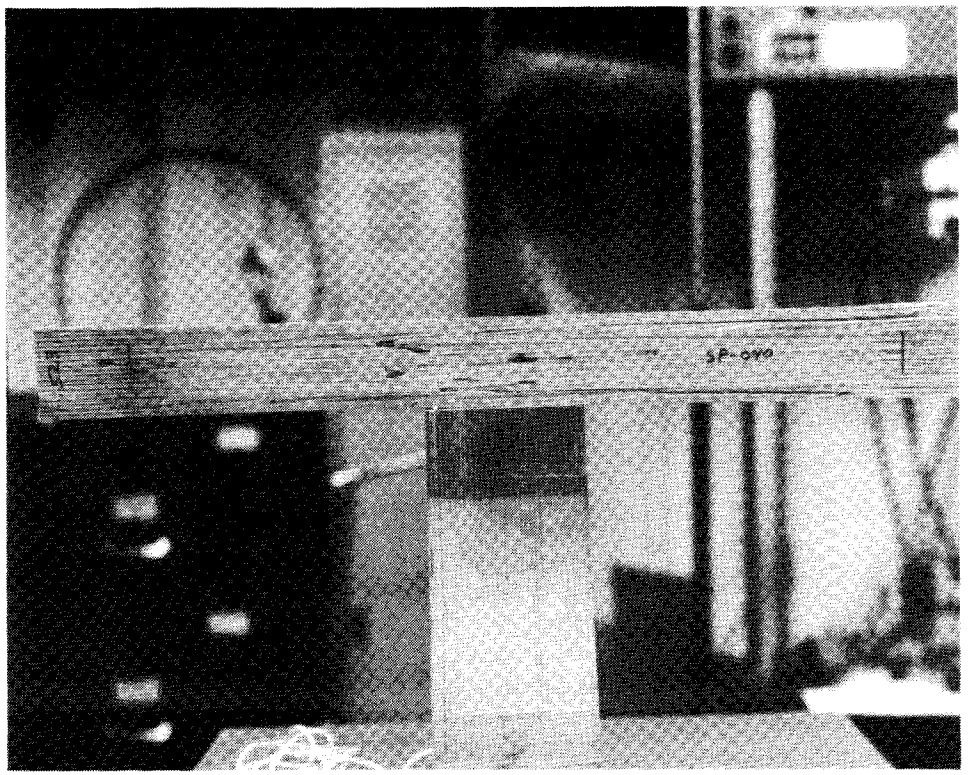

Figure 7

Failure of reverse-axial progressive fatigue specimen SP-040, loblolly pine.

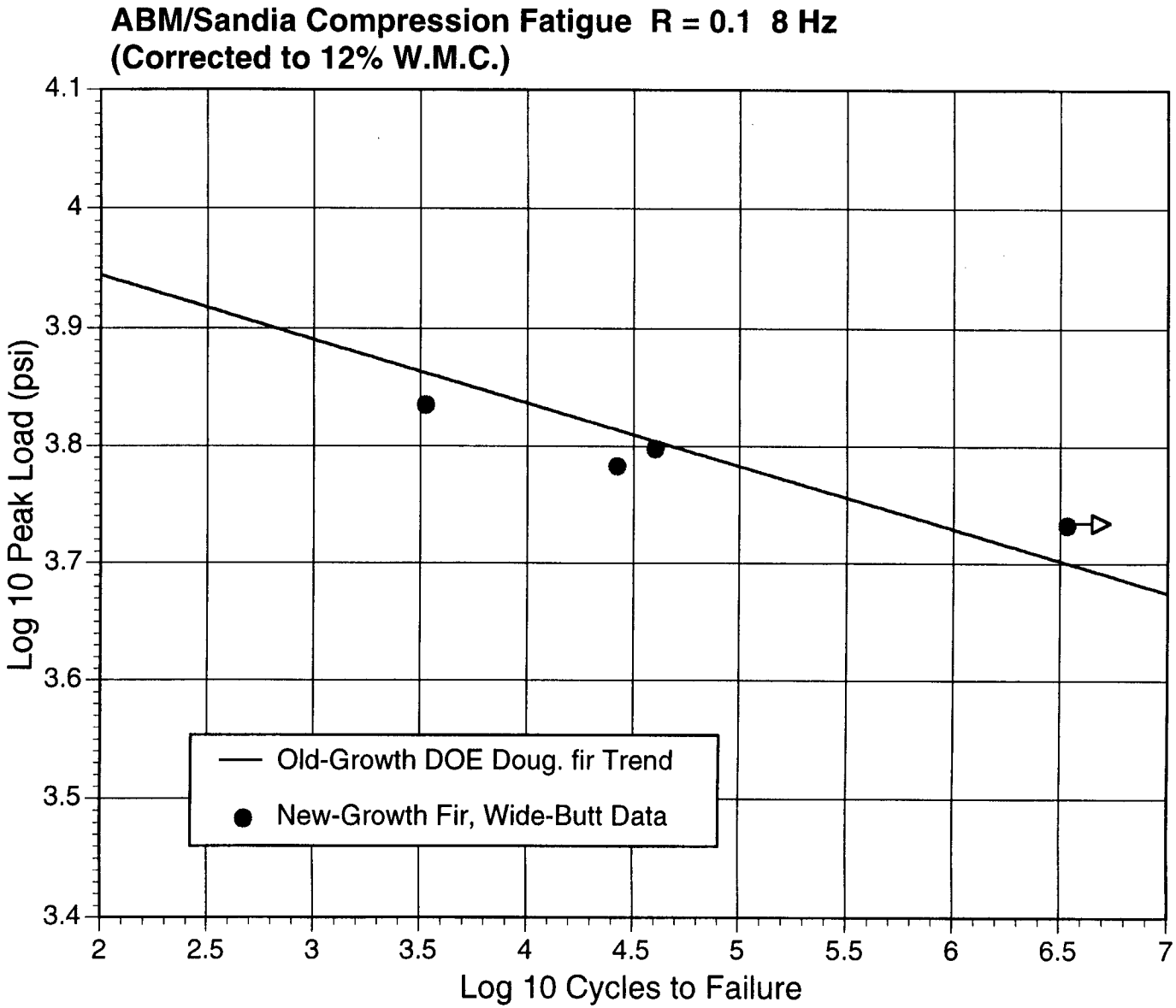
ABM/Sandia Compression Fatigue R = 0.1 8 Hz
(Corrected to 12% W.M.C.)
Log 10 Peak Load (psi)
4.1
4
3.9
3.8
3.7
3.6
3.5
3.4
2
2.5
3
3.5
4
4.5
5
5.5
6
6.5
7
Log 10 Cycles to Failure
Old-Growth DOE Doug. fir Trend
New-Growth Fir, Wide-Butt Data

Figure 8

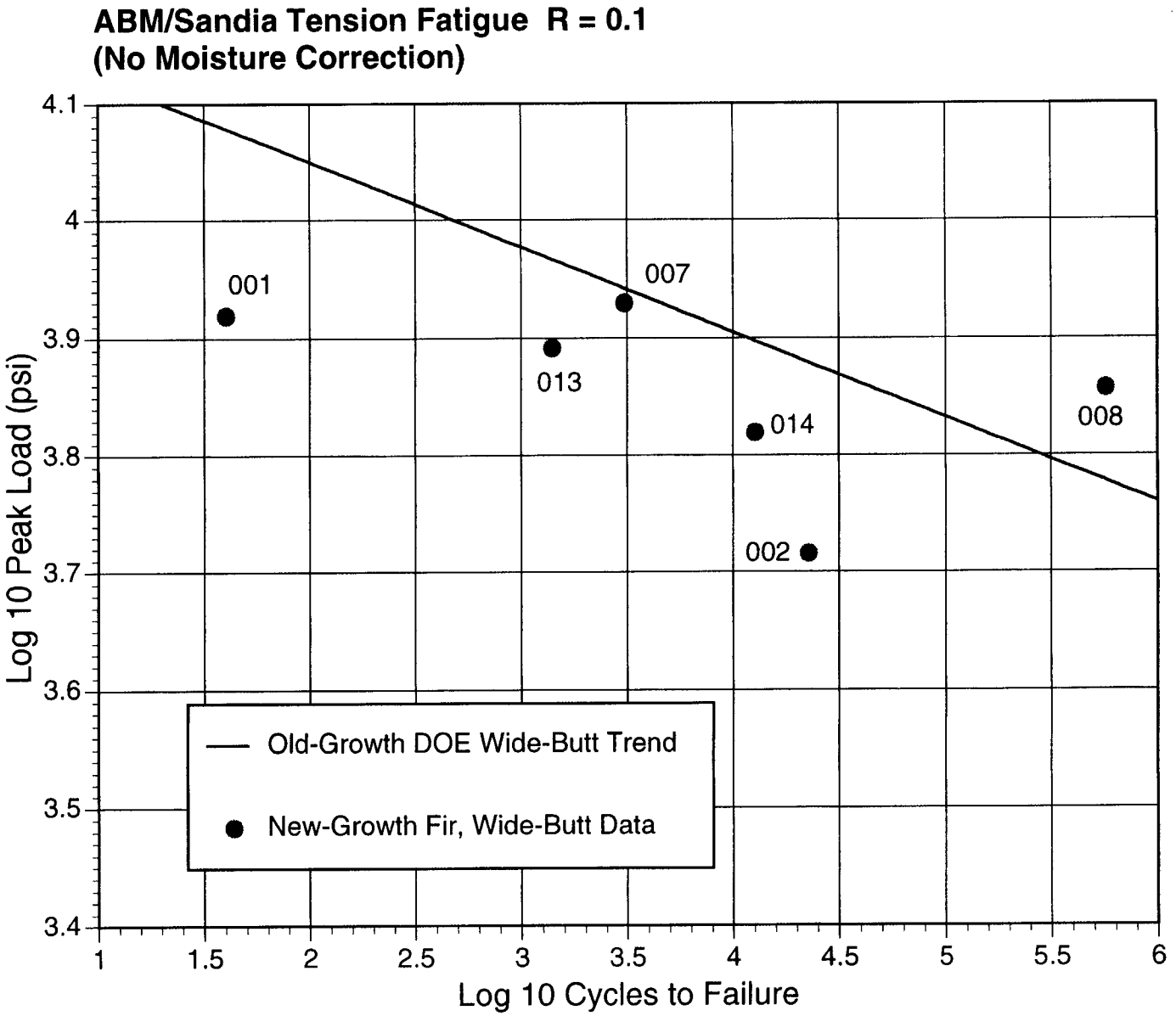
ABM/Sandia Tension Fatigue R = 0.1
(No Moisture Correction)
Log 10 Peak Load (psi)
4.1
4
3.9
3.8
3.7
3.6
3.5
3.4
1
1.5
2
2.5
3
3.5
4
4.5
5
5.5
6
Log 10 Cycles to Failure
001
007
013
014
008
002
Old-Growth DOE Wide-Butt Trend
New-Growth Fir, Wide-Butt Data

Figure 9

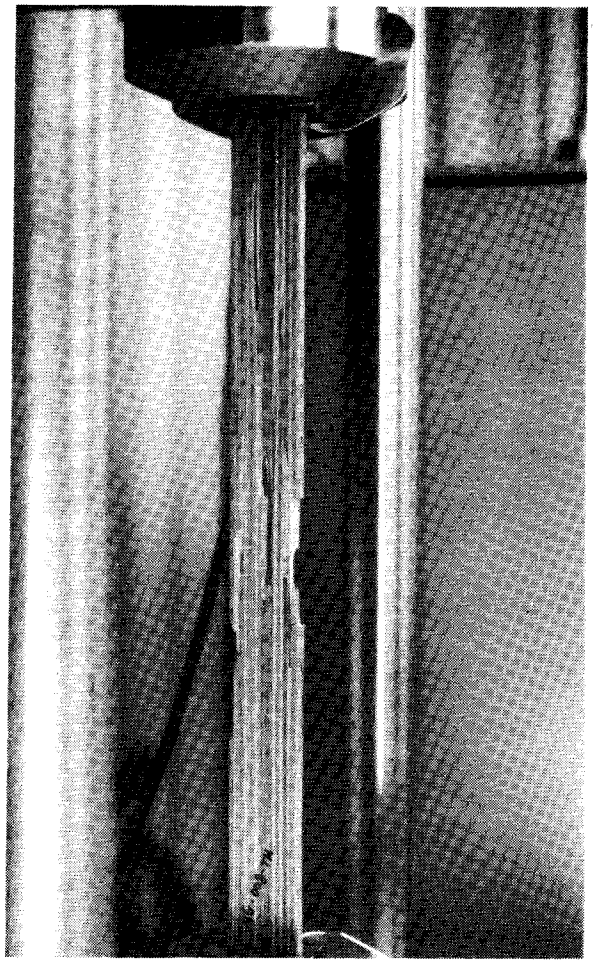

Figure 10

Failure of classical tension fatigue test specimen NG-008.

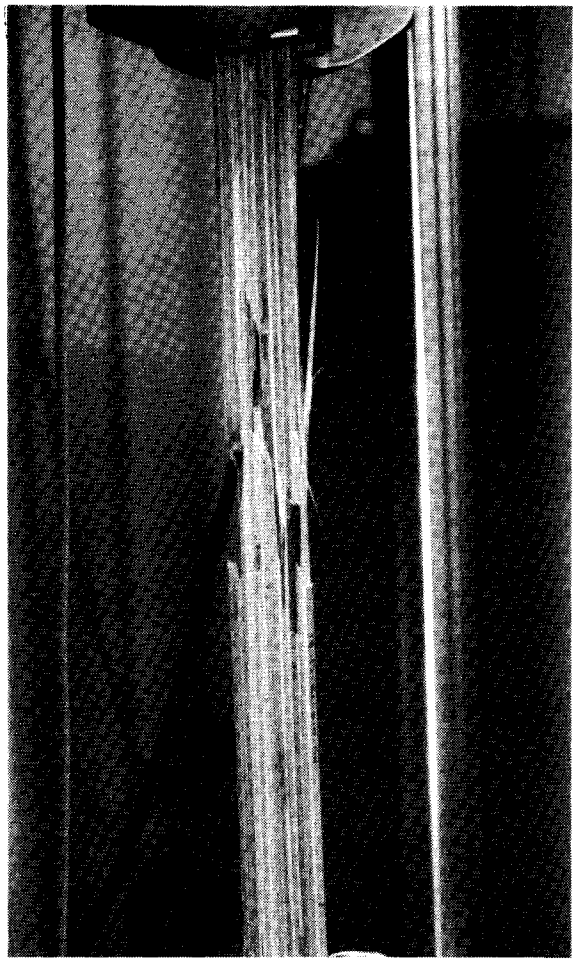

Figure 11

Failure of classical tension fatigue test specimen NG-014.

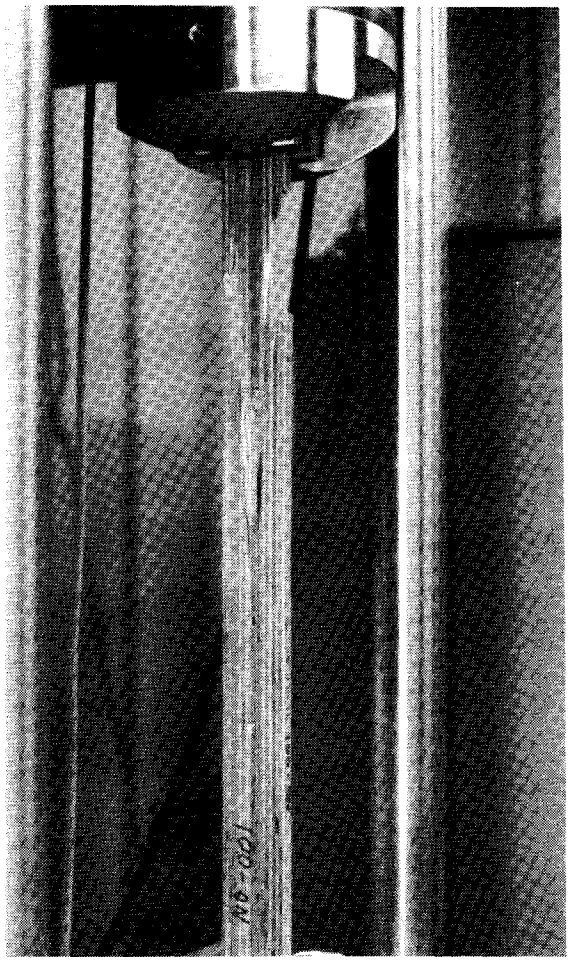

Figure 12

Failure of classical tension fatigue test specimen NG-001.

Appendix B

Progressive Fatigue Tests of Blade-Grade Old-Growth Douglas Fir Laminate with Extended Epoxy

Progressive Fatigue Tests of Blade-Grade Old-Growth Douglas Fir Laminate with Extended Epoxy

William D. Bertelsen
GOUGEON BROTHERS, INC.
December, 1997

1.0 Background and Overview: A successful wood/epoxy wind turbine technology was developed and implemented in the 1980's based on WEST SYSTEM™ epoxy and rotary-peeled Douglas fir veneer from the continental U.S. Northwest. With the capability of wood/epoxy blades now well established, the quest to reduce the cost of wind-generated electricity has intensified. Pound for pound, epoxy is the most expensive of the essential materials utilized in blade construction. If the manufacturing process could be modified to use epoxy more judiciously (without sacrificing laminate fatigue life), system costs could be reduced directly. Indirect savings might also be realized due to the resulting reductions in the all-up weight.

Static short-block-shear testing by R. H. Kunesh, as reported in Reference 1, led to the requirement of a specific, uniform quantity of the WEST SYSTEM 105/206 epoxy to be applied to each of the rotary-peeled Douglas fir veneer pieces used blade manufacture. This quantity was specified by weight, and became generally referred to as the standard "spread rate". Since the roll-coating machine applies epoxy to both sides of veneer sheets as they pass through, it is the total weight added that really counts. Based on the Kunesh work, the historical spread rate value for blade production over the last fifteen years has been 60 pounds of epoxy per 1,000 $ft.^2$ of 0.1"-thick veneer stock. Equally important, the significant body of blade laminate fatigue data which has been assembled over the years all relates to specimens from billets built with the intent of achieving this target value.

On the production floor, the spread rate has been monitored by weighing individual one-foot-square veneer pieces on a gram scale and then passing them through the roll-coating machine. The wet pieces are immediately weighed again to make sure they fall into an acceptable range, which has been established as dry weight plus 24.5-30.0 grams of epoxy. The arithmetic average of the two extremes (27.25 $g/ft.^2$) corresponds almost exactly to the 60 lbs./1000 $ft.^2$ standard.

This report documents the preliminary investigation of the fatigue strength of butt-jointed, old-growth Douglas fir laminate made with extended epoxy, i.e., mixed with filler and applied at a reduced spread rate. All test specimens originated from a 19-layer billet which was made with WEST SYSTEM 105/206 epoxy mixed with 2% fumed silica (by weight) and then applied to constituent veneer pieces at the target rate of 22.0 grams of epoxy per square foot, the acceptable range being 18.0-26.0 $g/ft.^2$. The epoxy weight reduction to be realized by achieving the lower target spread rate was therefore on the order of 20%.

2.0 Specimen Design and Preparation: A billet of old-growth Douglas fir parent material was fabricated by Advanced Blade Manufacturing, Pinconning, MI. Each billet consisted of 19 layers of 0.1"-thick, rotary-peeled, old-growth Douglas fir veneer, treated and vacuum-formed with extended WEST SYSTEM™ 105/206 epoxy as reported above. Grain direction was the same in every layer. Specimen designs were patterned after tension and compression samples used in the 1990 DOE blade laminate fatigue test program, Contract DE-AC02-86ER80385, as documented in the Phase 2 Final Report, December 1990 (Reference 2). All test specimens were to have wide butt joints joints in the middle three veneer layers, joint centers staggered 3" apart in the grain direction. Typical butt joint gaps in the finished laminate were 5/16-3/8" in length.

The compression specimens were identical in configuration to the DOE/SBIR specimens, being approximately 2" x 2" x 8", grain aligned with the long dimension. The ends of the blocks were specially prepared to mate with the platen faces of the test machine using a procedure described in detail in Reference 3.

The design of the tensile/reverse-axial style specimens was modified in three ways: (1) Overall specimen length was increased from 16" to 24", (2) Specimen width was increased from 0.4" to 0.5", and (3) specimen grip regions were reinforced with unidirectional carbon fiber (ANCAREF C-150) rather than bidirectional E-glass. Note: DOE tension fatigue strength data had been somewhat below expectations. Since the shortfall could not be explained any other way, specimen geometry was indicted. The ABM/Sandia specimens were lengthened in hopes of creating a more uniform stress distribution in the test section.

The parent billet was divided into seven sectors from which could be cut four tensile-style specimens and two compression-style specimens. Specimens were to be numbered consecutively across sector boundaries and marked "OGS" for old-growth

Douglas fir extended with silica. The compression blocks were cut in pairs from the far edge of each sector.

3.0 Test Matrix: Table 1 is a diagram illustrating both specimen spatial relation within the respective parent billets and each sample's specific utilization in the test program. The column labelled "Compr. E Test?" identifies which compression specimens were subjected to non-destructive bulk compression modulus testing. (See Section 4.0 below.) The general plan was to conduct modulus tests on one compression specimen from each sector, and then to perform progressive fatigue tests on three specimens each from Sectors 2, 4, and 6. The lowest-numbered specimen within a sector was to be for R = 0.1 tension fatigue. The third sample in a sector was to be for R = -1, reverse-axial tension-compression testing. The fifth sample in a sector was for R = 0.1 compression fatigue.

4.0 Compression Modulus Tests: Since wind-turbine blade engineering is weight and stiffness-driven, it was important to measure the density and compression modulus of the laminate. The modulus tests were done using a non-destructive, low-load/low-cycle compression fatigue method developed for the DOE veneer joint research of Reference 2.

4.1 Equipment and Setup: The testing was carried out in the Gougeon Materials Testing Laboratory using an MTS Model 312.41 110-kip servo-hydraulic load frame, load cell, and actuator with Model 442 Controller, Model 421 Amplitude Controller. All fatigue testing, including compression modulus testing, was conducted in load-control mode (i.e., with the test machine hydraulic actuator responding to actual load cell measurements throughout each cycle). The loading function was sinusoidal with the use of an amplitude controller in the feedback loop. Amplitude control provides additional boost to the hydraulic servo-valves which operate the actuator. This boost is necessary to overcome slight losses in peak load values due to the change in specimen compliance as it accumulates damage. The primary control system on its own is often unable to handle the compliance change, particularly at the end of a test when the test sample is near breaking. Amplitude control insured that a specimen was subjected to its full peak load on every cycle no matter how much internal damage had accumulated.

4.2 Compression Modulus Test Method: The compression modulus testing was accomplished without an extensometer by attaching Model 643.41C-01 self-aligning compression platens to the 110-kip MTS and running a low-cycle, low-load fatigue program. The built-in actuator L.V.D.T. (linear variable differential transformer) and

digital indicator were then used to monitor specimen displacement.
Each compression specimen was carefully installed between the platens of the test machine while making certain the specially squared and prepared block ends were seated properly on each facing steel surface. After start-up @ 4 Hz, the peak load was set at 10,000 lbs. with a stress ratio (R value) of 0.4. This meant that each specimen experienced a sinusoidal compression load pattern which oscillated between 4,000 and 10,000 lbs. The large specimen cross sections (about four square inches) translated the resulting peak psi loads to about 2,500 psi.

Specimens were allowed to cycle up to the count of 1,000 before reading the "delta stroke", the indicated linear distance between the actuator position at minimum load and at maximum load. Because some of the indicated displacement was actually due to slight bending and flexing of the test machine itself, the test was repeated without the test specimen installed. Using the same load settings, the test machine was restarted with the compression platens simply pushing against each other. Reading the delta stroke in this configuration told just how much to subtract from the indicated specimen displacement as measured during the previous run in order to arrive at the true specimen displacement. Given knowledge of the load changes and actuator motions during the cycling, a bulk compression modulus number could be calculated.

4.3 Compression Modulus and Density Data: The results of the compression modulus testing are presented in Table 2. The conventional/historical modulus value for wood/epoxy blade laminate used in design work is 2.25 million psi, and the ABM OGS-series specimens slightly exceed that value on average. Density values were calculated for each specimen by multiplying the cross-sectional area by the length and then dividing by the weight, as measured on a gram scale accurate to the nearest 0.1 g. Cross-section measurements were made in the middle of each specimen with a dial calipers accurate to the nearest 0.001". It can be seen in the 7th column of Table 2 that the average density of the experimental laminate is 39.51 lbs./ft.^{3}. This is slightly above the norm for old-growth Douglas fir laminate with the standard spread rate.

It is useful to calculate an average modulus/density ratio (i.e., specific modulus) to assess stiffness per unit weight. This average appears in the last column of Table 2. If the historical value for blade-grade laminate is taken to be 0.0584, then ABM old-growth fir with extended epoxy is within 2% of the norm.

5.0 Progressive Fatigue Tests: The test plan called for conducting block-cycle progressive fatigue testing in all three loading modes. "Block cycle" progressive fatigue meant that, if a specimen remained unfailed after an arbitrary number of constant-mean stress/constant-amplitude cycles, the peak load would be increased by a set amount, and the test allowed to continue for the same number of cycles (or until failure, whichever came first). The block cycle testing was to have the following format: (1) The stress ratio (R value) was to be held constant throughout, (2) The cycle block length was to be 10,000 cycles, and (3) The increment of peak stress increase was to be 10% of the start value. It would be up to the principle investigator to choose the initial peak stress level, with the aim of generating a failure within a 5-block period. In the initial study, only nine specimens were to take part in all, three in each loading situation. Cyclic frequencies were to be adjusted at each load increase to maintain a nearly-constant strain rate.

5.1 Progressive Tension Fatigue Tests: .

5.1.1 Tension Fatigue Equipment and Setup: All tension fatigue tests were conducted with the GBI MTS 22-kip load frame, a servo-hydraulic test machine equipped with a 20,000 lb. load cell and 7.57 $in.^2$ actuator as part of the MTS "810" series Material Test System. The tests were controlled with the 459.10 TestLink™ Automated Control System with manual inputs from a Compaq 286 desk-top computer.
The TestLink™/Compaq combination generated the sinusoidal R = 0.1 fatigue loading with amplitude control. Built-in data-acquisition functions were utilized to monitor and document each test. TestLink™ recorded setup parameters for each test, including test number, peak load, stress ratio, and frequency.

Critical to the execution of the tension fatigue series was the implementation of the MTS 647.10A-01 hydraulically-operated, wedge-action grips. These grips provided regulated clamping pressure through a manifold valve set by the operator.

Depth of grip engagement at each end was 2.375 inches. That left an effective test section length of 19.25 inches since all tensile-style specimens were 24.0 inches in length overall. The set-up procedure was to hold Hydraulic grip line pressure to the minimum (200 psi) while first engaging the clamps. Then a proof tensile load of 500 lbs. was applied, at which time the grip line pressure was increased to 350 psi. The proof load was removed before startup. This method resulted in a virtually trouble-free fatigue test series with no grip-induced failures.

Progressive tension fatigue testing began with specimen OGS-007 on November 17, 1997. Starting peak load was 8,000 psi at 5.0 Hz. Stress ratio was held constant at R = 0.1. Since the standard strain rate for the series was to be held at that for an 8,000 psi peak load and 5 Hz, the appropriate frequency for a 8,800 psi peak load was calculated by dividing 8,800 psi into the product of 5 Hz and 8,000 psi and rounding off to the nearest 0.1 Hz. The same method was used to determine Hz frequencies for peak loads in excess of 8,800 psi as well.

5.1.2 Progressive Tension Fatigue Data

The results of all the progressive fatigue tests are presented in Table 3. Table 3 lists tested specimens by number in a horizontal row. Beneath each specimen number is the number of cycles run at the load specified in the first column. OGS-007 eventually failed after 914 cycles at the 9,600 psi peak load, the third block of cycles.

Because of the strength exhibited by OGS-007, the next test (OGS-019) was also started at the 8,000 psi peak load. It proved to be somewhat stronger, failing 7,393 cycles into the 9,600 psi load level. The third test (OGS-031) was also good, failing after 1,471 cycles at the 9,600 psi level.

Note in Table 3 the listing of laminate moisture content (Laminate M.C.) for specimens just below their respective cycle totals. Immediately after test, the carbon-augmented grip regions were cut off with a band saw. The remains (test section) of each specimen were weighed and placed in a VWR 1630 circulating oven at 103 °C. The initial test-section weight was recorded in a card file. Specimens were removed from the oven periodically and re-weighed. When a sample showed no further weight decrease, it was assumed that all moisture had been removed.

The laminate moisture content was calculated using the following expression:

$$\text{L.M.C.} = \frac{\text{(Post-test weight)-(Dry weight)}}{\text{(Dry weight)}} * 100$$

L.M.C. for OGS-007 was calculated to be 8.40% after 27 days in the circulating oven. The values for the other two specimens were also high, at 8.09% and 8.25% L.M.C.

To obtain values for actual wood moisture content, one needs only to adjust L.M.C. values to compensate for the presence of some epoxy. The multiplication factor of 1.22 was derived for DOE/SBIR data analysis, i.e., W.M.C. = 1.22 * L.M.C. For the

extended-epoxy laminate with its 20% epoxy weight reduction, the correction factor is reduced to 1.18. Applying that relation to the OGS tension group, the range for actual wood moisture content was 9.55-9.91%.

5.1.3 Progressive Tension Fatigue Failures: All three tests failures initiated at one of the butt-joint sites. On 009, there was an outer layer fracture at 4,400 cycles in the 8,800 psi level, but the specimen survived to finish the cycle block.
The comprehensive failures generally included one or more butt-joint sites, but there was no obvious visual evidence of delamination due to incomplete veneer bonding. Photographs of all three failures were taken for future review.

5.2 Progressive Compression Fatigue: Testing got underway November 19, 1997 with OGS-011 from Sector 2 at 8,000 psi peak stress, R = 0.1, and 8.0 Hz in the 110-kip MTS machine. The starting frequency was chosen to match that used in the DOE/SBIR tests of Reference 2. Since the standard strain rate for the series was to be held at that for an 8,000 psi peak load and 8.0 Hz, the appropriate frequency for an 8,800 psi peak load was calculated by dividing 8,800 psi into the product of 8 Hz and 8,000 psi and rounding off to the nearest 0.1 Hz.

The hardware setup was basically the same as for the compression modulus testing with the use of the self-aligning compression platens. The 011 specimen failed after 7,390 cycles at the 8,000 psi start-up peak stress. The actuator stroke limit was set at 0.1" so that the machine turned itself off when the specimen was compressed 0.1" less than its original 8.0" length. The failure initiated away from the specially prepared ends and was manifest as a slplit down the middle. The failed sample was weighed and placed in the circulating oven for 26 days to determine its laminate moisture content, which turned out to be 8.09%. Results of all three progressive compression fatigue tests appear in the middle portion of Table 3. Moisture levels were on a par with the tension group.

As with the tension fatigue group, there appeared to be no failure initiation due to incomplete veneer bonding, and only minimal butt-joint involvement in the comprehensive failures themselves. The overall variability of the compression group was only slightly more than that seen in the tension fatigue series. Photographs were taken of all three compression fatigue failures. They were remarkably similar in appearance with splits in the middle and centrally-located crush ridges.

5.3 Reverse-Axial Progressive Fatigue Tests: Reverse-axial testing began December 9, 1997 with OGS-009 running at ±6,000 psi and 3.0 Hz. Once again, the 22-kip MTS with wedge-action grips was used to introduce test loads into the specimens. The mechanics of the setup and specimen installation were virtually the same as for the progressive tension fatigue series of Section 5.1. The same grip pressures were used. The main difference was the addition of column supports to prevent buckling during the compression half of each R = -1 stress cycle. The second R = -1 test specimen (OGS-021) exhibited a lower-half, column instability problem shortly after start-up at ±6,000 psi. An additional pair of column supports was installed "on the fly" at about 1,500 cycles. After that, the test continued smoothly with only brief interruptions to increase peak loads.

For R = -1 testing, the 22-kip MTS was manually operated in sinusoidal load control mode with the model 458.11 DC Controller and 458.90 Function Generator. The operator was compelled to constantly monitor the peak load to maintain the prescribed stress during each cycle block. However, very little adjustment was required.

Since the standard strain rate for the series was to be held at that for an ±6,000 psi peak load and 3 Hz, the appropriate frequency for a ±6,600 psi peak load was calculated by dividing 6,600 psi into the product of 3 Hz and 6,000 psi and rounding off to the nearest 0.1 Hz. The 18,000 Hz-psi "magic number" was used to calculate Hz rates for all the successive load increases.

5.3.1 Reverse-Axial Progressive Fatigue Data: The reverse-axial test results are also presented in Table 3 along with respective lower-bound laminate moisture content values. (Bake-outs were incomplete for the R = -1 group at the time of this writing.) In this series, two of the three samples survived the ±6,000 psi level. Only OGS-009 from Sector 2 failed at the start-up load ±6,000 psi after only 4,224 cycles. In this case the failure was on the tension half of the last cycle. The lower butt joint had cracked loose at about 1,850 cycles. The middle and upper butt joints were not involved in the failure.

Specimen OGS-021 developed a cracked upper butt joint at 3,230 cycles into the ±6,600 psi peak load run, but it successfully completed the 10,000 cycle block. At the final ±7,200 psi load level, the specimen carried full load until failing in tension at 1,481 cycles. Only the middle butt joint was involved in the comprehensive failure. Butt joint gaps on OGS-021 ranged in length from 7/32-1/4" in length.

OGS-033 was the only specimen in the R = -1 series to fail in the compression half of the cycle. The upper butt joint cracked loose at about 7,360 cycles at the start-up load. Noise indicated that the failure was imminent just as the 10,020 end of count limit was reached. It collapsed after only 83 cycles at ±6,600 psi. Only the upper butt joint was involved in the failure. As was the case in all the other fatigue tests of OGS specimens, no failures were seen to initiate by delamination.

6.0 Conclusions and Recommendations: These preliminary tests indicate that it might indeed be possible to build long-lasting wood blades with lesser amounts of epoxy. Classical fatigue testing needs to be done to confirm acceptable working stress allowables for blade laminate with the reduced-spread-rate, extended epoxy.

7.0 References:

1. Kunesh, R.H., "Strength Properties of Rotary Peeled Douglas Fir Veneer Composite Material for Use in Large Wind Turbine Blades", K Consulting Company, Phase A-2 Report for Project MOD 5-A, GOUGEON BROTHERS, INC., October, 1982.

2. Bertelsen, W.D., and Zuteck, M. D., "Investigation of Fatigue Failure Initiation and Propagation in Wind-Turbine-Grade Wood/Epoxy Laminate Containing Several Veneer Joint Styles", Phase 2 Report, U.S. Department of Energy Contract No. DE-AC02-86ER80385, December, 1990.

3. Detailed Test Plan, Blade Manufacturing Project AN-0166, Section 2.2.2 - Replace Old-Growth Veneer, Section 3.1.7 Specimen Edge Sealing Procedure, Advance Wind Turbines, Inc., Seattle, WA, June, 1997.

Table 1: Extended Epoxy, Old-Growth Fir, Wide Butt Joints
Location and Disposition of Test Specimens Within Parent Billet

Billet Sector	Old-Growth Fir	Compr. E Test?	Type of Fatigue Test Performed
	001		
	002		
1	003		
	004		
	005	Yes	
	006		
	007		Progressive Tension Fatigue
	008		
2	009		Progressive Reverse-Axial Fatigue
	010		
	011	Yes	Progressive Compression Fatigue
	012		
	013		
	014		
3	015		
	016		
	017	Yes	
	018		
	019		Progressive Tension Fatigue
	020		
4	021		Progressive Reverse-Axial Fatigue
	022		
	023	Yes	Progressive Compression Fatigue
	024		
	025		
	026		
5	027		
	028		
	029	Yes	
	030		
	031		Progressive Tension Fatigue
	032		
6	033		Progressive Reverse-Axial Fatigue
	034		
	035	Yes	Progressive Compression Fatigue
	036		
	037		
	038		
7	039		
	040		
	041	Yes	
	042		

Table 2
Compression Modulus and Density
Old-Growth Doug. Fir, Extended Epoxy, Wide Butts

Specimen	Compression Modulus (psi)	Density (Lbs./Ft.3)	Modulus Density Ratio	Peak Stress (psi)	Average Modulus (psi)	Average Density (Lbs./Ft.3)	Average Modulus Density Ratio
OGS-005	2.258 E+06	39.26	0.0575	2,624			
OGS-011	2.361 E+06	39.65	0.0596	2,622			
OGS-017	2.357 E+06	40.46	0.0583	2,642			
OGS-023	2.262 E+06	39.63	0.0571	2,640	2.270 E+06	39.51	0.0574
OGS-029	2.291 E+06	39.48	0.0580	2,615			
OGS-035	2.224 E+06	39.28	0.0566	2,631			
OGS-041	2.137 E+06	38.79	0.0551	2,595			

Table 3
Old-Growth Fir/Extended Epoxy/Wide-Butt Joints
Progressive Fatigue Data 12-15-97

Progressive Tension Fatigue, R = 0.1

Peak Load (psi)	Hz	OGS 007 Cycles	OGS 019 Cycles	OGS 031 Cycles
8,000	5.0	10,020	10,020	10,020
8,800	4.5	10,020	10,020	10,020
9,600	4.2	914	7,393	1,471
Laminate M.C.:		8.40%	8.09%	8.25%
Drying Days:		27	27	27

Progressive Compression Fatigue, R = 0.1

Peak Load (psi)	Hz	OGS 011 Cycles	OGS 023 Cycles	OGS 035 Cycles
8,000	8.0	7,390	10,000	2,980
8,800	7.3		1,070	
Laminate M.C.:		8.09%	7.86%	8.26%
Drying Days:		26	26	26

Progressive Rev. Ax. Fatigue, R = -1.0

Peak Load (psi)	Hz	OGS 009 Cycles	OGS 021 Cycles	OGS 033 Cycles
6,000	3.0	4,224	10,020	10,020
6,600	2.7		10,020	83
7,200	2.5		1,481	
Laminate M.C.:		7.04%	7.13%	7.07%
Drying Days:		7	6	6

Appendix C

Extended Resin Butt-Jointed Fir Design Impact Preliminary Assessment

Extended Resin Butt-Jointed Fir Design Impact Preliminary Assessment

Introduction

The recent fatigue tests conducted at the Gougeon Bros. Inc. lab in Bay City, Michigan, on laminated Douglas Fir with reduced resin spread rate demonstrated high mechanical performance. This reduced resin spread rate was made possible by the addition of a filler which limited resin absorption into the veneer, thereby keeping more of the resin on the surface, where it was able to provide bonding. This approach might have lead to inadequate penetration, and reduced strength. However, as will be seen, the fatigue results were excellent. The filler selection, loading amount, and spread rate studies that lead up to the current extended resin formulation appear not only to have side-stepped low performance, but may in fact be conferring a subtle benefit. It is too early in the testing to have the complete story, but the initial results are encouraging.

At this time, nine filled resin butt jointed specimens have been fatigue tested; three each in tension (R=.1), compression (R=.1), and reverse-axial (R= -1). These tests were performed using progressively increasing loads, with 10% load steps, and 10,000 cycle blocks. The details of those tests are reported in: "Progressive Fatigue Tests of Blade-Grade Old-Growth Douglas Fir Laminate with Extended Epoxy", by William D. Bertelsen, Gougeon Bros, Inc., December, 1997. The purpose of this document is to take a preliminary look at the possible impact of extended resin on blade fatigue performance and design. Since the data sets are quite limited, it isn't appropriate to go into great detail regarding possible future design and manufacturing improvements. However, the results are encouraging enough that an initial indication of potential impact is warranted.

Since the primary motivation of the Sandia/ABM manufacturing development program is to provide an equal or better strength and quality blade at lower cost, and since the use of pre-sealed scarf jointed material on the tension side of the blade may afford considerable cost savings by allowing removal of the carbon reinforcing, this preliminary look at design impact of the extended resin butt jointed fir laminate will focus on how the filled resin laminate might fit into that promising design evolution. For further details on the results of the pre-sealed scarf testing and the possible impact on the AWT blade design, see the Advanced Blade Manufacturing

Deliverable #6c Pre-sealed Scarfed Laminate report and the Deliverable #4e Preliminary Design Review Package.

Filled Resin Butt Joint vs Pre-Sealed Scarf Comparison

To explore how extended resin butt jointed laminate might be combined with pre-sealed scarf jointed laminate in the AWT 26/27 blade design, the comparative fatigue performance of the two joint styles is examined. The table below gives the mean value of peak stress for each joint style that would be expected for 10,000 cycles, based on the three progressive fatigue results for each loading type that have currently been obtained. These are corrected to a 12% wood moisture content condition to eliminate differences due to moisture variations between specimen groups. Since comparative performance is sought, other corrections used to develop the design allowable equations (ref 2) are not needed.

10,000 Cycle Progressive Fatigue Capability Comparison

	Extended Resin Butt Joints	Pre-Sealed Scarfs	Percentage Increase
Tension	8,982 psi.	8,964 psi	0%
Reverse Axial	5,640 psi.	5,864 psi	4%
Compression	6,866 psi.	7,429 psi	8%

These results require some discussion. In previous work done under an SBIR research program, it was found that the elimination of joints in the laminate had the greatest benefit in tension, but in the above table tension shows the least effect. In fact, the tension comparison shows no benefit of pre-sealed scarf joints relative to the extended resin butt joints at all. This is inconsistent with the body of pre-existing research, which has shown even marginally bonded scarfs to perform considerably better than butt joints. It stands to reason that a better bonded joint with intrinsically lower stress raisers should perform even better. While it might be true that the filler used to extend the resin may be conferring a tension strength increase in fatigue, it is not reasonable to believe the effect would be so large as to outperform scarf joints. The more probable interpretation is that these results are subject to random variation due to the fact that only three specimens were tested in each group. Given that the strength variability of individual specimens will typically range between 5% - 10%, this is certainly the more plausible hypothesis. Given the preceding, the best way to provide an initial assessment of how pre-sealed scarfs

and extended resin butt joints might work together in a blade design appears to be to take the average improvement of all three loading cases, which triples the number of specimens in the comparison. That leads to a 4% average improvement for the pre-sealed scarfs vs the extended resin butt joints. This 4% value will be used in the following discussion, since no better value is available at present.

Impact on Design

The current blade design uses six scarfed veneer layers on the upwind side of the blade. These are needed to provide continuous, straight surfaces at the joints for the five layers of carbon which are used to reinforce the upwind blade shell. If butt joints were used, the carbon would not be kept in alignment at the joints, and the overall fatigue strength benefit of the carbon would have been substantially compromised.

One of the promising avenues for reducing blade cost is to remove the carbon from the upwind blade shell. The fatigue strength improvement achieved with pre-sealed scarfs seems to bring this option within reach. If further research confirms that extended resin butt jointed laminate has fatigue performance that is within a few percent of that of the pre-sealed scarfs, that would open up the possibility that the upwind blade shell need not be entirely composed of pre-sealed scarf laminate. Instead, only a number of the outer layers, where the stresses are higher, would need to be composed of pre-sealed scarfs. Inner layers, where the stresses have dropped, could be composed of reduced resin butt jointed laminate, thereby saving the cost of the scarfing and pre-sealing operations. The result would be an upwind blade shell composed partly of scarfs, and partly of butts, just as is done now, except that the carbon would be gone.

The analysis performed at station 35% r/R to assess the potential impact of pre-sealed scarfs on the blade design (ref 2), gave a value of 6.810" for the critical fiber distance on the upwind side of the blade for a construction modified to contain no carbon reinforcing. An inset of 4% of that distance is about 0.27", less than the thickness of three of the tenth inch thick veneers. If butt jointed laminate were used from that location inward, in theory an equal probability would exist of fatigue failure initiating in either the scarfed laminate, or the butt jointed laminate. Blade life optimization would imply using a few more scarfed layers, so the higher strength scarfed laminate would dominate the failure probability and life calculations. If the 4% strength differential were to be substantiated by further data accumulation, the upwind blade shell might well end up with about the same number of scarfed layers

as it has now, except that they would be pre-sealed scarfs, and the carbon would be gone. Since this constitutes an easily understood variation of the current design, it appears to make sense at this juncture to evaluate possible manufacturing cost savings on that basis.

Summary and Conclusions

Recent progressive loading fatigue tests performed at the Gougeon Bros. Inc. lab in Bay City, Michigan have demonstrated a high level of performance for Douglas Fir laminate constructed with extended resin wide butt joints. The purpose of the resin extension is to reduce the amount (and cost) of resin used in the blade laminate. It is possible that an increase in fatigue performance has also been obtained, although there is little theoretical reason to expect that, and much more data will be needed to support such a conclusion.

In order to get a feel for the possible impact of extended resin wide butt joints on the AWT 26/27 blade design, the fatigue performance of the extended resin butt joints was compared to the pre-sealed scarf test results reported previously. It was found that no performance improvement was demonstrated in tension fatigue, an entirely improbable state of affairs. This was most likely the result of having only three specimens in each progressive loading fatigue test group. The best way to use the preliminary data was thus judged to be to combine all of the loading cases, and the result was a 4% fatigue strength advantage for the pre-sealed scarf laminate.

Given a 4% strength increase, only three pre-sealed scarf veneer layers would be needed at station 35% r/R to give an equal probability of failure initiation in either the pre-sealed scarfs, or the extended resin wide butt material. Blade life optimization implies using enough pre-sealed scarf layers that the higher strength outer laminate would dominate the fatigue life calculations. If the 4% strength differential were to be substantiated by further data accumulation, the upwind blade shell might well end up with about the same number of scarfed layers as it has now, except that they would be pre-sealed scarfs, and the carbon would be gone. This variation on the current blade design appears to constitute as good a basis for cost saving evaluation as can be derived from the existing preliminary fatigue data.

It is my judgement, based on results from previous tests of different joint styles, that the tension fatigue differential between pre-sealed scarfs and extended resin wide butt joints will ultimately be larger than has been indicated by the preliminary data discussed herein. However, this may have a rather minor effect on blade cost, since

removal of the carbon reinforcing is likely to have the greatest impact on final cost. An entirely scarfed upwind blade shell can be regarded as an upper bound cost case. The real cost impact should lie between it, and the case discussed here. Either way, the downwind blade shell can use the extended resin laminate, and thereby save both weight and cost. Reducing weight is just what's needed to compensate the reduced blade stiffness from removing the carbon, and still maintain similar blade frequencies and dynamics. This makes use of pre-sealed scarfs and extended resin synergistic. While the full, constant load fatigue testing program will be required to support a detailed blade re-design, the current data appears to provide a good initial look at the possibilities, which are encouraging.

Appendix D

Progressive Fatigue Tests of Blade-Grade Old Growth Douglas Fir Laminate with Pre-Coated Scarf Joints

Progressive Fatigue Tests of Blade-Grade Old-Growth Douglas Fir Laminate with Pre-Coated Scarf Joints

William D. Bertelsen
GOUGEON BROTHERS, INC.
December, 1997

1.0 Background and Overview: A successful wood/epoxy wind turbine technology was developed and implemented in the 1980's based on WEST SYSTEM™ epoxy and rotary-peeled Douglas fir veneer from the continental U.S. Northwest. With the capability of wood/epoxy blades now well established, the quest to reduce the cost of wind-generated electricity has intensified. Since wind turbines are fatigue-driven structures, one approach is to look for ways to increase the fatigue strength of the parent laminate. Cost reductions could then be realized by engineering lighter, longer-lasting blades.

Research reported in References 1 and 2 verified that the way veneer sheets are joined at the ends has a significant effect on the fatigue life of the bulk laminate. Section 4.2.1 of Reference 2 presents R = 0.1 tension fatigue data from tests of blade-grade laminate with several veneer splice joint styles, including ordinary butt joints and 12:1 scarf joints. Curiously, some scarf-jointed specimens approached the strength of unjointed laminate while others performed only at the level of 0.1" butt joints (See Figure 1). The unpredictability of scarf-joint performance in tension fatigue has forced acceptance of a lower allowable working tension stress for outer-shell blade laminate. The real and meaningful consequence has been a weight and cost penalty for any complete turbine structure engineered with wood/epoxy blades.

One possible explanation for the bimodal "Jekyl/Hyde" scarf behavior in SBIR tension fatigue was that some mating scarf joint surfaces failed to bond when brought into contact during vacuum lay-up of the billet. This theory remains plausible, because although the joints may be liberally treated with epoxy when set in place, activation of the vacuum force draws air from the interior that can escape at the joint surfaces. The resulting air bubbles would create random voids and permit only spotty scarf bonding.

Obviously, the goal of increasing the fatigue strength of the parent laminate could be realized if the scarf joints were completely and consistently bonded. This report documents the preliminary investigation of the effectiveness of one particular scarf-

joint preparation technique designed to improve the scarf bonds. Three fatigue loading situations were used in the study: tension fatigue @ R = 0.1, compression fatigue @ R = 0.1, and reverse-axial, tension-compression fatigue @ R = -1. Because of time and budget constraints, it was advantageous to implement a total progressive fatigue loading regimen in the preliminary study. (See Section 5.0.)

2.0 Specimen Design and Preparation: A billet of old-growth Douglas fir parent material was fabricated by Advanced Blade Manufacturing, Pinconning, MI. Each billet consisted of 19 layers of 0.1"-thick, rotary-peeled, old-growth Douglas fir veneer, treated and vacuum-formed with clear WEST SYSTEM™ 105/206 epoxy. Grain direction was the same in every layer. Specimen designs were patterned after tension and compression samples used in the 1990 DOE blade laminate fatigue test program, Contract DE-AC02-86ER80385, as documented in the Phase 2 Final Report, December 1990 (Reference 2). All test specimens were to have 12:1-slope scarf joints in the middle three veneer layers, joint centers staggered 3" apart in the grain direction.

The key departure from the SBIR scarf-joint fabrication was that in this case, freshly-cut scarf-joint surfaces were treated with clear WEST SYSTEM™ 105/207 epoxy three days prior to the actual vacuum layup of the billet. Thus, the mating joint surfaces were already sealed with cured epoxy when subjected to vacuum in the subsequent layup, reducing the risk of vacuum-engendered air bubbles. The scarfed surfaces were not sanded after sealing, but fresh 105/206 epoxy was applied to all the joints during layup.

The compression specimens were identical in configuration to the DOE/SBIR specimens, being approximately 2" x 2" x 8", grain aligned with the long dimension. The ends of the blocks were specially prepared to mate with the platen faces of the test machine using a procedure described in detail in Reference 3.

The design of the tensile/reverse-axial style specimens was modified in three ways: (1) Overall specimen length was increased from 16" to 24", (2) Specimen width was increased from 0.4" to 0.5", and (3) specimen grip regions were reinforced with unidirectional carbon fiber (ANCAREF C-150) rather than bidirectional E-glass. Note: DOE tension fatigue strength data had been somewhat below expectations. Since the shortfall could not be explained any other way, specimen geometry was indicted. The ABM/Sandia specimens were lengthened in hopes of creating a more uniform stress distribution in the test section.

The parent billet was divided into seven sectors from which could be cut four tensile-style specimens and two compression-style specimens. Specimens were to be numbered consecutively across sector boundaries and marked "OG-SJ" for old-growth Douglas fir with scarf joints. The compression blocks were cut in pairs from the far edge of each sector.

3.0 Test Matrix: Table 1 is a diagram illustrating both specimen spatial relation within the respective parent billets and each sample's specific utilization in the test program. The column labelled "Compr. E Test?" identifies which compression specimens were subjected to non-destructive bulk compression modulus testing. (See Section 4.0 below.) The general plan was to conduct modulus tests on all compression specimens, and then to perform progressive fatigue tests on three specimens each from Sectors 2, 4, and 6. The lowest-numbered specimen within a sector was to be for R = 0.1 tension fatigue. The third sample in a sector was to be for R = -1, reverse-axial tension-compression testing. The fifth sample in a sector was for R = 0.1 compression fatigue.

4.0 Compression Modulus Tests: Since wind-turbine blade engineering is weight and stiffness-driven, it was important to measure the density and compression modulus of the laminate. The modulus tests were done using a non-destructive, low-load/low-cycle compression fatigue method developed for the DOE veneer joint research of Reference 2.

4.1 Equipment and Setup: The testing was carried out in the Gougeon Materials Testing Laboratory using an MTS Model 312.41 110-kip servo-hydraulic load frame, load cell, and actuator with Model 442 Controller, Model 421 Amplitude Controller. All fatigue testing, including compression modulus testing, was conducted in load-control mode (i.e., with the test machine hydraulic actuator responding to actual load cell measurements throughout each cycle). The loading function was sinusoidal with the use of an amplitude controller in the feedback loop. Amplitude control provides additional boost to the hydraulic servo-valves which operate the actuator. This boost is necessary to overcome slight losses in peak load values due to the change in specimen compliance as it accumulates damage. The primary control system on its own is often unable to handle the compliance change, particularly at the end of a test when the test sample is near breaking. Amplitude control insured that a specimen was subjected to its full peak load on every cycle no matter how much internal damage had accumulated.

4.2 Compression Modulus Test Method: The compression modulus testing was accomplished without an extensometer by attaching Model 643.41C-01 self-aligning compression platens to the 110-kip MTS and running a low-cycle, low-load fatigue program. The built-in actuator L.V.D.T. (linear variable differential transformer) and digital indicator were then used to monitor specimen displacement.
Each compression specimen was carefully installed between the platens of the test machine while making certain the specially squared and prepared block ends were seated properly on each facing steel surface. After start-up @ 4 Hz, the peak load was set at 10,000 lbs. with a stress ratio (R value) of 0.4. This meant that each specimen experienced a sinusoidal compression load pattern which oscillated between 4,000 and 10,000 lbs. The large specimen cross sections (about four square inches) translated the resulting peak psi loads to about 2,500 psi.

Specimens were allowed to cycle up to the count of 1,000 before reading the "delta stroke", the indicated linear distance between the actuator position at minimum load and at maximum load. Because some of the indicated displacement was actually due to slight bending and flexing of the test machine itself, the test was repeated without the test specimen installed. Using the same load settings, the test machine was restarted with the compression platens simply pushing against each other. Reading the delta stroke in this configuration told just how much to subtract from the indicated specimen displacement as measured during the previous run in order to arrive at the true specimen displacement. Given knowledge of the load changes and actuator motions during the cycling, a bulk compression modulus number could be calculated.

4.3 Compression Modulus and Density Data: The results of the compression modulus testing are presented in Table 2. The conventional/historical modulus value for wood/epoxy blade laminate used in design work is 2.25 million psi, and the ABM pre-coated scarf specimens match that value on average. Density values were calculated for each specimen by multiplying the cross-sectional area by the length and then dividing by the weight, as measured on a gram scale accurate to the nearest 0.1 g. Cross-section measurements were made in the middle of each specimen with a dial calipers accurate to the nearest 0.001". It can be seen in the 7th column of Table 2 that the average density of the fir is 40.46 lbs./ft.^{3}. This is slightly above the norm for old-growth Douglas fir.

It is useful to calculate an average modulus/density ratio (i.e., specific modulus) to assess stiffness per unit weight. This average appears in the last column of Table 2. If the historical value for blade grade laminate is taken to be 0.0584, then ABM old-

growth scarf fir is found wanting to the extent of 4.79%, due to the heavier wood.

5.0 Progressive Fatigue Tests: The test plan called for conducting block-cycle progressive fatigue testing in all three loading modes. "Block cycle" progressive fatigue meant that, if a specimen remained unfailed after an arbitrary number of constant-mean stress/constant-amplitude cycles, the peak load would be increased by a set amount, and the test allowed to continue for the same number of cycles (or until failure, whichever came first). The block cycle testing was to have the following format: (1) The stress ratio (R value) was to be held constant throughout, (2) The cycle block length was to be 10,000 cycles, and (3) The increment of peak stress increase was to be 10% of the start value. It would be up to the principle investigator to choose the initial peak stress level, with the aim of generating a failure within a 5-block period. In the initial study, only nine specimens were to take part in all, three in each loading situation. Cyclic frequencies were to be adjusted at each load increase to maintain a nearly-constant strain rate.

5.1 Progressive Tension Fatigue Tests: .

5.1.1 Tension Fatigue Equipment and Setup: All tension fatigue tests were conducted with the GBI MTS 22-kip load frame, a servo-hydraulic test machine equipped with a 20,000 lb. load cell and 7.57 $in.^2$ actuator as part of the MTS "810" series Material Test System. The tests were controlled with the 459.10 TestLink™ Automated Control System with manual inputs from a Compaq 286 desk-top computer.
The TestLink™/Compaq combination generated the sinusoidal R = 0.1 fatigue loading with amplitude control. Built-in data-acquisition functions were utilized to monitor and document each test. TestLink™ recorded setup parameters for each test, including test number, peak load, stress ratio, and frequency.

Critical to the execution of the tension fatigue series was the implementation of the MTS 647.10A-01 hydraulically-operated, wedge-action grips. These grips provided regulated clamping pressure through a manifold valve set by the operator.

Depth of grip engagement at each end was 2.375 inches. That left an effective test section length of 19.25 inches since all tensile-style specimens were 24.0 inches in length overall. The set-up procedure was to hold Hydraulic grip line pressure to the minimum (200 psi) while first engaging the clamps. Then a proof tensile load of 500 lbs. was applied, at which time the grip line pressure was increased to 350 psi. The proof load was removed before startup. This method resulted in a virtually trouble-free

fatigue test series with no grip-induced failures.

Progressive tension fatigue testing began with specimen OG-SJ-007 on November 7, 1997. Starting peak load was 6,400 psi at 6.3 Hz. Stress ratio was held constant at R = 0.1. A starting load of 8,000 psi at 5.0 Hz was considered to be theoretically safe, but caution dictated that the first test of sample material from an untried billet be at a substantially lower peak stress. So, the load was reduced by two steps, using the increment size based on 10 per cent of 8,000 psi. Since the standard strain rate for the series was to be held at that for an 8,000 psi peak load and 5 Hz, the appropriate frequency for a 6,400 psi peak load was calculated by dividing 6,400 psi into the product of 5 Hz and 8,000 psi and rounding off to the nearest 0.1 Hz. The same method was used to determine Hz frequencies for peak loads in excess of 8,000 psi as well.

5.1.2 Progressive Tension Fatigue Data

The results of all the progressive fatigue tests are presented in Table 3. Table 3 lists tested specimens by number in a horizontal row. Beneath each specimen number is the number of cycles run at the load specified in the first column. The third cycle block length for the OG-SJ-007 was 9,854 cycles instead of 10,000 because of an unprogrammed hydraulic shutdown, probably due to a line voltage fluctuation. OG-SJ-007 eventually failed after 7,977 cycles at the 9,600 psi peak load, the fifth block of cycles.

Because of the strength exhibited by OG-SJ-007, the next test (OG-SJ-019) was started at the 8,000 psi peak load. It proved to be significantly stronger, failing 2,627 cycles into the 11,200 psi load level. The third test (OG-SJ-031) was a disappointment, failing after only 4,086 cycles at the 8,000 psi start-up level.

Note in Table 3 the listing of laminate moisture content (Laminate M.C.) for specimens just below their respective cycle totals. Immediately after test, the carbon-augmented grip regions were cut off with a band saw. The remains (test section) of each specimen were weighed and placed in a VWR 1630 circulating oven at 103 °C. The initial test-section weight was recorded in a card file. Specimens were removed from the oven periodically and re-weighed. When a sample showed no further weight decrease, it was assumed that all moisture had been removed.

The laminate moisture content was calculated using the following expression:

$$L.M.C. = \frac{(\text{Post-test weight})-(\text{Dry weight})}{(\text{Dry weight})} * 100$$

L.M.C. for OG-SJ-007 was calculated to be 8.19% after 15 days in the circulating oven. The values for the other two specimens were also unexpectedly high, at 7.77% and 7.93% L.M.C.

To obtain values for actual wood moisture content, one needs only to adjust L.M.C. values to compensate for the presence of some epoxy. The multiplication factor of 1.22 was derived for DOE data analysis, i.e., W.M.C. = 1.22 * L.M.C. Applying that relation to the pre-coated scarf tension group, the range for actual wood moisture content was 9.48-9.99%.

5.1.3 Progressive Tension Fatigue Failures: All three tests ended with little or no warning. On 019, the failure began as a vertical split 3-4 inches above the lower grip about 4-5 veneer layers in from the edge. It worked its way up over the course of only 350 cycles until complete separation occurred.

None of the failures initiated at scarf joint sites. In fact, post-test examination of the failed specimens revealed only incidental scarf involvement in any of the fractures. That included 031 which performed so poorly in comparison to the other two.

The disappointing performance of 031 raised the question of whether the test should be considered a valid representation of the local laminate strength. The initial delta stroke value (net recurring actuator displacement) for the 8,000 psi peak load level had been 0.0823 inches, as compared to 0.0715 inches and 0.0771 inches for samples 007 and 019, respectively. It was decided to set up OG-SJ-032, the near-neighbor specimen to 031, in the test machine for a non-destructive, R = 0.1 tension fatigue test run at 4,000 psi to determine if it, too, exhibited a disproportionately large delta stroke. The test was allowed to continue for 3,009 cycles. The delta stroke value stabilized early at 0.0413 inches, almost exactly half of what its near-neighbor had exhibited at the 8,000 psi level. The delta stroke value of sample 032 was thus consistent with that of 031, and supported the suspicion that the laminate in the vicinity of Sector 6 was substandard for some reason. That premise seemed to be substantiated later when Sector 6 compression and reverse-axial samples also proved to be the weakest of the three in their respective groups. (See again Table 3.)

5.2 Progressive Compression Fatigue: Testing got underway November 14, 1997 with OG-SJ-011 from Sector 2 at 8,000 psi peak stress, R = 0.1, and 8.0 Hz in the 110-kip MTS machine. The starting frequency was chosen to match that used in the DOE/SBIR tests of Reference 2. Since the standard strain rate for the series was to be held at that for an 8,000 psi peak load and 8.0 Hz, the appropriate frequency for an 8,800 psi peak load was calculated by dividing 8,800 psi into the product of 8 Hz and 8,000 psi and rounding off to the nearest 0.1 Hz.

The hardware setup was basically the same as for the compression modulus testing with the use of the self-aligning compression platens. The 011 specimen completed the first 10,000 cycle block and failed 5,190 cycles into the second cycle block at 8,800 psi peak stress. The actuator stroke limit was set at 0.1" so that the machine turned itself off when the specimen was compressed 0.1" less than its original 8.0" length. The failure initiated away from the specially prepared ends and was confined to the middle. The failed sample was weighed and placed in the circulating oven for 21 days to determine its lower-bound laminate moisture content, which turned out to be 7.99%. Results of all three progressive compression fatigue tests appear in the middle portion of Table 3.

As with the tension fatigue group, there appeared to be no scarf-joint failure initiation and only minimal involvement in the comprehensive failure itself. The overall variability of the compression was much less than that seen in the tension fatigue series, although the specimen from Sector 6 (OG-SJ-035) was again the low performer.

5.3 Reverse-Axial Progressive Fatigue Tests: Reverse-axial testing began November 21, 1997 with OG-SJ-009 running at ±6,000 psi and 3.0 Hz. Once again, the 22-kip MTS with wedge-action grips was used to introduce test loads into the specimens. The mechanics of the setup and specimen installation were virtually the same as for the progressive tension fatigue series of Section 5.1. The same grip pressures were used. The main difference was the addition of column supports to prevent buckling during the compression half of each R = -1 stress cycle. The second R = -1 test specimen (OG-SJ-021) exhibited an upper-half, column instability problem shortly after start-up at ±6,000 psi. The test was stopped at 1,504 cycles so that an additional pair of column supports could be installed. After that, the test continued smoothly with only brief interruptions to increase peak loads.

For R = -1 testing, the 22-kip MTS was manually operated in sinusoidal load control mode with the model 458.11 DC Controller and 458.90 Function Generator. The operator was compelled to constantly monitor the peak load to maintain the prescribed stress during each cycle block. However, very little adjustment was required.

Since the standard strain rate for the series was to be held at that for an ±6,000 psi peak load and 3 Hz, the appropriate frequency for a ±6,600 psi peak load was calculated by dividing 6,600 psi into the product of 3 Hz and 6,000 psi and rounding off to the nearest 0.1 Hz. The 18,000 Hz-psi "magic number"was used to calculate Hz rates for all the successive load increases.

5.3.1 Reverse-Axial Progressive Fatigue Data: The reverse-axial test results are also presented in Table 3 along with respective laminate moisture content values. In this series, two of the three samples survived to the ±7,200 psi level, failing on the compression half of the last cycle. OG-SJ-033 from Sector 6 failed at the start-up load ±6,000 psi after only 3,188 cycles. In this case the failure was on the tension half of the last cycle.

Specimen OG-SJ-009 developed an outer layer fracture 2.5 inches above the lower grip at 4,823 cycles into the ±6,600 psi peak load run, but it successfully completed the 10,000 cycle block. A split near the middle occurred at about 340 cycles into the final ±7,200 psi load level, but the specimen continued to carry full load until collapsing at 840 cycles. With the other two samples, there was only slight cracking noise a few cycles before the end that served as any kind of a failure warning. Some "Hi-8" video photography was conducted of the last two reverse-axial tests, OG-SJ-021 and 033. While the final failure was not captured in either case, the large delta stroke motion (on the order of 0.125 inches or more) could be seen.

As was the case in all the other fatigue tests of OG-SJ specimens, no failures were seen to initiate in the scarf joints.

6.0 Conclusions and Recommendations: These preliminary tests show promise for the pre-coated scarf joining technique in terms of realizing fatigue performance which is closer to that of the ideal, i.e., unjointed laminate. The analysis of these data was handicapped to an extent by the apparent variability in wood structural properties within the test billet. More fatigue testing needs to be done to establish reliable working stress allowables for blade laminate with pre-coated scarfs.

7.0 References:

1. Spera. D. A., Esgar, J. B., Gougeon, M. A., and Zuteck, M. D., "Structural Properties of Laminated Douglas Fir/Epoxy Composite Material", NASA reference Publication 1236, DOE NASA/20320-76, 1990.

2. Bertelsen, W.D., and Zuteck, M. D., "Investigation of Fatigue Failure Initiation and Propagation in Wind-Turbine-Grade Wood/Epoxy Laminate Containing Several Veneer Joint Styles", Phase 2 Report, U.S. Department of Energy Contract No. DE-AC02-86ER80385, December, 1990.

3. Detailed Test Plan, Blade Manufacturing Project AN-0166, Section 2.2.2 - Replace Old-Growth Veneer, Section 3.1.7 Specimen Edge Sealing Procedure, Advance Wind Turbines, Inc., Seattle, WA, June, 1997.

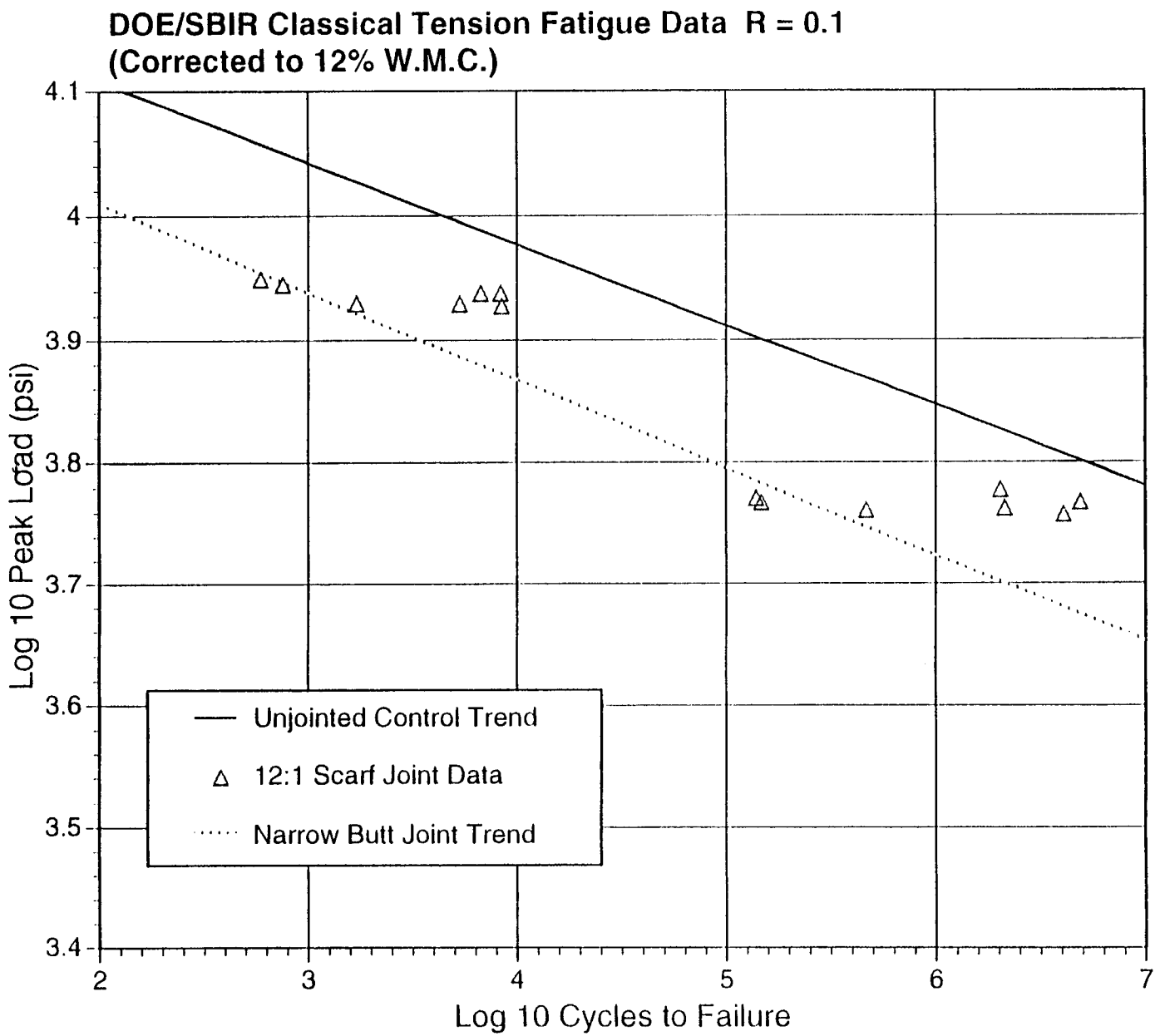
DOE/SBIR Classical Tension Fatigue Data R = 0.1
(Corrected to 12% W.M.C.)
Log 10 Peak Load (psi)
4.1
4
3.9
3.8
3.7
3.6
3.5
3.4
2
3
4
5
6
7
Log 10 Cycles to Failure
Unjointed Control Trend
12:1 Scarf Joint Data
Narrow Butt Joint Trend

Figure 1

Table 1: Pre-Coated Scarfs
Location and Disposition of Test Specimens Within Parent Billet

Billet Sector	Old-Growth Fir	Compr. E Test?	Type of Fatigue Test Performed
	001		
	002		
1	003		
	004		
	005	Yes	
	006	yes	
	007		Progressive Tension Fatigue
	008		
2	009		Progressive Reverse-Axial Fatigue
	010		
	011	Yes	Progressive Compression Fatigue
	012	Yes	
	013		
	014		
3	015		
	016		
	017	Yes	
	018	Yes	
	019		Progressive Tension Fatigue
	020		
4	021		Progressive Reverse-Axial Fatigue
	022		
	023	Yes	Progressive Compression Fatigue
	024	Yes	
	025		
	026		
5	027		
	028		
	029	Yes	
	030	Yes	
	031		Progressive Tension Fatigue
	032		
6	033		Progressive Reverse-Axial Fatigue
	034		
	035	Yes	Progressive Compression Fatigue
	036	Yes	
	037		
	038		
7	039		
	040		
	041	Yes	
	042	Yes	
	043		
	044	*	

*Incomplete veneers, sanding required which would result in sub-standard width

Table 2
Compression Modulus and Density
Old-Growth Doug. Fir with Pre-Coated Scarf Joints

Specimen	Compression Modulus (psi)	Density (Lbs./Ft.3)	Modulus Density Ratio	Peak Stress (psi)	Average Modulus (psi)	Average Density (Lbs./Ft.3)	Average Modulus Density Ratio
OG-SJ-005	2.302 E+06	40.51	0.0568	2,604			
OG-SJ-006	2.318 E+06	40.46	0.0573	2,574			
OG-SJ-011	2.418 E+06	40.92	0.0591	2,574			
OG-SJ-012	2.404 E+06	41.23	0.0583	2,569	2.251 E+06	40.46	0.0556
OG-SJ-017	2.331 E+06	41.05	0.0568	2,574			
OG-SJ-018	2.386 E+06	41.15	0.0580	2,575			
OG-SJ-023	2.237 E+06	40.35	0.0554	2,600			
OG-SJ-024	2.260 E+06	41.03	0.0551	2,579			
OG-SJ-029	2.190 E+06	40.25	0.0544	2,545			
OG-SJ-030	2.148 E+06	39.93	0.0538	2,541			
OG-SJ-035	2.186 E+06	40.67	0.0537	2,563			
OG-SJ-036	2.102 E+06	38.80	0.0542	2,455			
OG-SJ-041	2.095 E+06	39.68	0.0528	2,533			
OG-SJ-042	2.141 E+06	40.41	0.0530	2,523			

Table 3
Pre-Coated Scarf Progressive Fatigue Data
12-5-97

Progressive Tension Fatigue, R = 0.1

Peak Load (psi)	Hz	OG-SJ-007 Cycles	OG-SJ-019 Cycles	OG-SJ-031 Cycles
6,400	6.3	10,009		
7,200	5.6	10,010		
8,000	5.0	9,854	10,020	4,086
8,800	4.5	10,009	10,020	
9,600	4.2	7,977	10,020	
10,400	3.8		10,020	
11,200	3.6		2,627	
Laminate M.C.:		8.19%	7.77%	7.93%
Drying Days:		15	14	14

Progressive Compression Fatigue, R = 0.1

Peak Load (psi)	Hz	OG-SJ-011 Cycles	OG-SJ-023 Cycles	OG-SJ-035 Cycles
8,000	8.0	10,000	10,000	10,000
8,800	7.3	5,190	4,340	310
Laminate M.C.:		7.99%	7.87%	8.00%
Drying Days:		21	18	18

Progressive Rev. Ax. Fatigue, R = -1.0

Peak Load (psi)	Hz	OG-SJ-009 Cycles	OG-SJ-021 Cycles	OG-SJ-033 Cycles
6,000	3.0	10,020	10,020	3,188
6,600	2.7	10,020	10,020	
7,200	2.5	840	2,325	
Laminate M.C.:		7.41%	7.21%	7.39%
Drying Days:		11	11	10

Appendix E

Pre-Sealed Scarf Blade Design Impact Preliminary Assessment

Pre-Sealed Scarf Design Impact
Preliminary Assessment

Introduction

The recent fatigue tests conducted at the Gougeon Bros. Inc. lab in Bay City, Michigan, on laminated Douglas Fir with pre-sealed scarf joints demonstrated high mechanical performance, and that the joints were generally not involved in the failure initiation or propagation. This is in contrast to previous work done under the NASA/DOE and SBIR programs, where the joints were often involved in the failures, with a consequent substantial impact on final fatigue performance. Evidently, sealing the scarf surface to prohibit out-gassing from the end grain during vacuum formation (and consequent displacement of resin from the joint), has had the hypothesized beneficial effect that prompted the current investigation.

At this time, only nine pre-sealed scarf specimens have been tested in fatigue; three each in tension (R=.1), compression (R=.1), and reverse-axial (R= -1). These tests were performed using progressively increasing loads, with 10% load steps, and 10,000 cycle blocks. The details of those tests are reported elsewhere. The purpose of this document is to take a preliminary look at the possible impact of pre-sealed scarfs on blade fatigue performance and design. Since the data sets are quite limited, it is not appropriate to go into great detail regarding possible future design improvements or optimization. However, the initial results are encouraging enough that an indication of potential impact is warranted.

Since the current fatigue design computations show the upwind side of the inner blade to be the limit under the operating fatigue spectrum, it is the tension and reverse axial fatigue cases that have the most direct impact on performance. Indeed, computing damage weighted mean and cyclic loads for the tension side of the blade at 35% radius yields a characteristic R ratio of about -.6. Reverse-axial fatigue performance can therefore be expected to have the greater impact on the fatigue life computations, followed by the tension performance. Consequently, those two cases will be the focus of the ensuing discussion. To show the possible impact on the fatigue design, the fatigue equations which would follow from the current test results are compared to the fatigue equations which anchored the laminate fatigue performance predictions used in the existing design computations.

Reverse-Axial Performance Comparison

The laminate fatigue equation which anchored the AWT 26/27 design computations for reverse-axial fatigue loading is:

$$S = 6{,}551 * N^{-.0888}$$

where: S is stress in psi,
N is number of cycles

This equation is based on a mix of A+ and A veneer fatigue test results from the NASA/DOE program. It was conservatively anchored to an effective stress volume of 6,250 in^3, 12% wood moisture content, .5 Hz. cycle rate, and also includes a temperature spectrum adjustment to reflect field use temperatures. Since the entire fatigue model was "borrowed" from development work first done for the 142' diameter Westinghouse blade, the volume and cycle rate both conservatively reflected that larger blade design.

Progressive fatigue tests with a single block size cannot provide information about the fatigue exponent, so that exponent must be taken from previous work. The best basis currently available is from the SBIR research program, which employed near neighbor specimen pairs to determine both low and high cycle fatigue performance in classical, constant load fatigue. That's where the -.0888 exponent shown above originates, and that same value is carried forward to the present assessment.

Based on the best current estimate of moisture for the three reverse axial specimens in the current progressive tests, the reverse axial fatigue equation for 12% wood moisture content is:

$$S = 13{,}287 * N^{-.0888}$$

This equation represents the 12% wood moisture content used in design, but further corrections for volume, cycle rate, and temperature spectrum must be applied to use it for design computations or comparisons.

Volume Correction

Since the time of the initial fatigue design work, a more refined estimate of the equivalent stress volume of the AWT 26/27 blade has been made. For the tension side of the blade, that estimate is 1,404 in^3. Rather than use the older value of 6,250 in^3, this new value will be used, to better represent the design calculations as they would be made today. Using the same correction equation, with the current 19 in^3 specimen test section volume, the volume correction factor is:

$$F_{vol} = (1404 / 19) ^{-.0892} = .6813$$

Cycle Rate Correction

The SBIR program included some tests of laminate strength which suggest that the duration correction exponent for wood/epoxy laminate may lie in the vicinity of .015. Since this is the best experimental data for Douglas Fir laminate, that value is used here. The cycle rate correction factor is then:

$$F_{rate} = (3 / 1) ^{-.015} = .9836$$

Temperature Spectrum Correction

The same factor used in previous design work is applied here:

$$F_{temp} = .975$$

Fully Adjusted Reverse-Axial Equation

Applying all of the above factors, the fully adjusted reverse-axial fatigue equation based on the three progressive fatigue test results becomes:

$$\mathbf{S = 8{,}681 * N ^{-.0888}}$$

For a given number of cycles, this equation yields an allowable design stress 32% higher than the original design allowable equation. At equal stress, this implies a factor of about 24 times as many cycles. While it must be remembered that this result is based on only three experimental test results, and so must be regarded with some reservation, this is still quite encouraging. Particularly when given the additional observation that joints no longer appear to have significant involvement in the failure initiation or propagation process, there is now a real basis to believe that pre-sealed scarfs can yield a substantial improvement in blade laminate fatigue performance.

Tension Fatigue Performance Comparison

The laminate fatigue equation which anchored the AWT 26/27 design computations for R = .1 tension fatigue loading is:

$$S = 9{,}853 * N^{-.0727}$$

where: S is stress in psi,
N is number of cycles

This equation is based on large scale laminated plank fatigue test results from the Westinghouse program. It was conservatively anchored to an effective stress volume of 6,250 in^3, 12% wood moisture content, .5 Hz. cycle rate, and also includes a temperature spectrum adjustment to reflect field use temperatures. Again, the volume and cycle rate both conservatively reflected the larger Westinghouse blade design.

While the large scale plank tests set the level of performance, there were only four specimens in that data set, because of the cost and time to test each of them. The best basis for setting the exponent is again from the SBIR research program, which employed near neighbor specimen pairs to determine both low and high cycle fatigue performance in classical, constant load fatigue. Thus the -.0727 exponent shown above originates from the SBIR program, and that same value is carried forward to the present assessment. It is worth noting that the large plank exponent was -.0721, so the two data sets are really in excellent agreement.

Based on the best current estimate of moisture for the three reverse axial specimens in the current progressive tests, the tension fatigue equation for 12% wood moisture content is:

$$S = 17{,}510 * N^{-.0888}$$

This equation represents the 12% wood moisture content used in design, but again further corrections for volume, cycle rate, and temperature spectrum must be applied to use it for design computations, or fatigue performance comparison.

Volume Correction

Again, the more refined estimate of the equivalent stress volume of the AWT 26/27 blade of 1,404 in^3 will be used, to better represent the design calculations as they would be made today. Using the same correction equation, again with the current 19 in^3 specimen test section volume, but with a different exponent appropriate for tension-tension fatigue, the volume correction factor is:

$$F_{vol} = (1404 / 19) ^{-.09853} = .6545$$

Cycle Rate Correction

The cycle rate correction equation is the same as shown for the reverse-axial case, and its exponent (based on the SBIR work) is the also the same. However, due to the higher cycle rate used in the tension fatigue tests, the correction is somewhat greater, as shown below:

$$F_{rate} = (4 / 1) ^{-.015} = .9794$$

Temperature Spectrum Correction

The same factor used in previous designs is again applied here:

$$F_{temp} = .975$$

Fully Adjusted Reverse-Axial Equation

Applying all of the above factors, the fully adjusted tension fatigue equation based on the three progressive fatigue test results becomes:

$$\mathbf{S = 10{,}944 * N ^{-.0888}}$$

For a given number of cycles, this equation yields an allowable design stress 11% higher than the original design allowable equation. At equal stress, this implies a factor of about 4 times as many cycles. Again it must be remembered that this result is based on only three experimental test results, and so must be regarded with some reservation. It may be worth noting that one of the three specimens in this group exhibited much lower performance than the other two. This may be a low probability result which has unduly pulled down the overall performance of the group. That's always a risk with small data sets. Still, the fatigue performance gain is significant, and it was again the case that joints were not observed to contribute to the failure mechanism.

Summary and Conclusions

Recent progressive loading fatigue tests performed at the Gougeon Bros. Inc. lab in Bay City, Michigan have demonstrated a high level of performance for Douglas Fir laminate constructed with pre-sealed scarf joints. The purpose of the pre-sealing operation is to prevent outgassing into the joint bond lines, which was hypothesized to prevent proper bond formation, and thereby degrade joint performance. It is quite encouraging to note that no joint motion was detected during the tests, and that the joints did not appear to participate in failure initiation or propagation.

In order to get a feel for the possible impact of pre-sealed scarfs on the AWT 26/27 blade design, new allowable mean stress equations were derived for R = -1 reverse axial and R = .1 tension-tension fatigue. These two cases anchor the region of the laminate fatigue model which embraces most of the fatigue damage that currently limits the inboard blade design, which is why they were chosen.

Only three specimens were tested in each loading condition, so this assessment is necessarily of a preliminary nature, but the results are encouraging. For the reverse-axial loading condition, which has the greatest impact on the computed blade fatigue life and its acceptable loading limits, it was found that 32% higher stress than the original design equation was indicated. For the R = .1 tension case, it was found that 11% higher stress was indicated.

Work done many years ago at Gougeon Bros. under an SBIR funded research program indicated that the presence of joints was causing about a 20%-30% loss of fatigue performance compared to unjointed control specimens. The scarf joints tested during the SBIR program gave a "bi-modal" distribution of results, sometimes performing well, but sometimes performing no better than butt joints. While there were theories as to what might have caused this, until the present work there was no concrete evidence that any of the theories were correct, or that higher jointed laminate performance would ever be obtained. Now there is clear evidence that it can be done, using a practical manufacturing technique.

To gather additional data and confirm fatigue curve slopes, the classical (constant load) fatigue portion of the test program still needs to be performed. From that, a more detailed estimate of the impact on the blade design can be made. It appears likely that performance gains will converge into the 20%-30% range as

more data is accumulated. Clearly, this work could have a substantial beneficial impact on the AWT 26/27 blade design.

Appendix F

Pre-Sealed Scarf Blade Design Impact

Pre-Sealed Scarf Blade Design Impact

One of the primary motivations for the research to improve laminate fatigue performance is the potential to thereby make design changes which reduce cost, while maintaining the ability to meet the design loading conditions. Due to the limited scope of the preliminary test data currently in hand, it is now too early for a complete redesign effort. However, to get a sense of what may be possible, the blade design at 35% radius was reviewed to determine the effect of removing the carbon reinforcing from the laminate, or reducing its thickness, since either of these measures would lead to a direct cost saving.

Carbon Removal

Considerable handling is required to wet out and place the carbon reinforcing within the upwind shell of the AWT 26/27 wind turbine blade. While there is not a great deal of this material added, its placement in the region of maximum stress from flatwise bending gives it a net effect much greater than its weight or volume might suggest. However, if the laminate fatigue strength is sufficiently improved due to the use of pre-sealed scarf joints, it may be possible to remove the carbon, and save its associated material and labor costs.

To address this possibility, the mechanical properties at station 35% r/R were recomputed with the carbon reinforcing removed. This choice was made due to the blade section shape, whose dramatic concavity in the upwind afterbody limits the effective placement of tension side material much more than at other blade stations. If the carbon could be removed in this region of the blade, then it certainly should be possible to remove it elsewhere as well.

The following two pages show the computed section mechanical properties at station 35%, both with and without carbon reinforcing. The critical value is the "LOWER SURF FLATWISE MOMENT", which is the moment capability for an extreme fiber reference strain of .00375 on the upwind side of the blade. For the current design with carbon, this value is 1.481 e6 inlbs. With no carbon present, the value is 1.357 e6 inlbs. To make up this difference, a 9% increase in allowed fatigue strength is needed. Since the preliminary data indicates an 11% increase in tension fatigue strength, and a 32% increase in reverse-axial fatigue strength, the use of pre-sealed scarfs on the tension side of the blade does appear capable of providing the strength increase needed to allow removal of the carbon.

****

REPORT FOR STATION 35% int/str WITH FOIL L86 sta35%

****

Accuracy factor:0.50 Cut plane angle: 9.50 Me Axis Rotation Ang: 0.00

WEIGHT PER FOOT	FLATWISE EI	EDGEWISE EI	UPPER SURF FLATWISE MOMENT	FWD EDGE EDGEWISE MOMENT
30.089	2.639e+9	3.212e+10	1.841e+6	5.792e+6
CHORDWISE CG	**FLATWISE SHEAR CENTER**	**EDGEWISE SHEAR CENTER**	**UPPER SURF CRITICAL DISTANCE**	**FWD EDGE CRITICAL DISTANCE**
20.72	15.23	0.171	5.375	20.80
FLATWISE CG	**FLATWISE NEUTRAL AXIS**	**EDGEWISE NEUTRAL AXIS**	**LOWER SURF FLATWISE MOMENT**	**AFT EDGE EDGEWISE MOMENT**
0.138	0.067	20.80	1.481e+6	4.978e+6
ROTATIONAL MOMENT OF INERTIA	**AE PRODUCT**		**LOWER SURF CRITICAL DISTANCE**	**AFT EDGE CRITICAL DISTANCE**
5.126e+3	2.015e+8		6.682	24.20

LAYER SUMMARY DATA

X LEFT	X RIGHT	LEFT THICKNESS	RIGHT THICKNESS	WEIGHT	EDGEWISE FORCE	FLATWISE FORCE
0.00	45.00	0.020	0.020	0.541	60	661
0.00	45.00	0.020	0.020	0.556	34	-587
0.00	45.00	0.022	0.022	0.842	114	1239
0.00	45.00	0.022	0.022	0.866	66	-1098
0.00	45.00	0.912	0.912	11.308	9480	163109
0.00	5.70	0.337	0.337	0.730	-16318	-9640
5.70	7.56	0.000	0.376	0.105	-2402	-3618
7.56	17.84	0.376	0.376	1.185	-15803	-42667
17.84	17.71	0.376	0.000	0.000	0	0
5.70	7.56	0.337	0.000	0.099	-1750	-2392
17.84	19.71	0.000	0.337	0.098	-215	-2075
19.71	45.00	0.337	0.337	2.431	34105	-13268
0.00	45.00	0.575	0.575	7.376	4544	-83134
0.00	45.00	0.022	0.022	0.752	29	912
0.00	45.00	0.022	0.022	0.773	-36	-782
12.50	13.50	0.750	0.750	0.188	-1820	3308
12.50	13.50	1.000	1.000	0.254	-2452	-5626
13.50	13.80	5.000	5.000	0.219	-807	1315
13.50	13.80	6.000	6.000	1.765	-6827	-5657

TORSIONAL CELL DATA

X LEFT	X RIGHT	DS OVER T	AREA
0.00	13.65	0.000083	45.562
13.65	42.75	0.000180	98.973
0.00	13.65	0.000071	62.505
13.65	42.75	0.000177	62.595

****

****

REPORT FOR STATION 35% NoCarbon WITH FOIL L86 sta35%

****

Accuracy factor:0.50 Cut plane angle: 9.50 Me Axis Rotation Ang: 0.00

WEIGHT PER FOOT	FLATWISE EI	EDGEWISE EI	UPPER SURF FLATWISE MOMENT	FWD EDGE EDGEWISE MOMENT
29.276	2.464e+9	2.891e+10	1.761e+6	5.319e+6
CHORDWISE CG	**FLATWISE SHEAR CENTER**	**EDGEWISE SHEAR CENTER**	**UPPER SURF CRITICAL DISTANCE**	**FWD EDGE CRITICAL DISTANCE**
20.27	15.27	0.265	5.247	20.38
FLATWISE CG	**FLATWISE NEUTRAL AXIS**	**EDGEWISE NEUTRAL AXIS**	**LOWER SURF FLATWISE MOMENT**	**AFT EDGE EDGEWISE MOMENT**
0.153	0.195	20.38	1.357e+6	4.404e+6
ROTATIONAL MOMENT OF INERTIA	**AE PRODUCT**		**LOWER SURF CRITICAL DISTANCE**	**AFT EDGE CRITICAL DISTANCE**
4.765e+3	1.913e+8		6.810	24.62

LAYER SUMMARY DATA

****

X LEFT	X RIGHT	LEFT THICKNESS	RIGHT THICKNESS	WEIGHT	EDGEWISE FORCE	FLATWISE FORCE
0.00	45.00	0.020	0.020	0.541	80	626
0.00	45.00	0.020	0.020	0.556	55	-600
0.00	45.00	0.022	0.022	0.842	151	1172
0.00	45.00	0.022	0.022	0.866	106	-1123
0.00	45.00	0.912	0.912	11.308	15014	153738
0.00	45.00	0.912	0.912	11.185	-4565	-146505
0.00	45.00	0.022	0.022	0.752	63	855
0.00	45.00	0.022	0.022	0.815	101	-811
12.50	13.50	0.750	0.750	0.188	-1693	3140
12.50	13.50	1.000	1.000	0.254	-2281	-5707
13.50	13.80	5.000	5.000	0.219	-747	1239
13.50	13.80	6.000	6.000	1.750	-6284	-6024

TORSIONAL CELL DATA

****

X LEFT	X RIGHT	DS OVER T	AREA
0.00	13.65	0.000083	45.562
13.65	42.75	0.000180	98.973
0.00	13.65	0.000088	61.615
13.65	42.75	0.000201	61.446

****

Thickness Reduction

Removal of the material costs and fabrication steps associated with the carbon reinforcing is expected to provide a greater cost reduction than simply reducing the thickness of the Douglas Fir laminate, so that possibility was examined first. However, it appears likely that pre-sealed scarfs will provide a fatigue strength increase that is in the vicinity of 20%, so further cost reduction may be possible.

The next logical step was to compute the effect of removing one veneer from the tension side blade shell at 35% r/R. The following page gives the full section property output for that case. The "lower surface flatwise moment" is now found to be 1.268 e6 inlbs. To compensate that reduction in reference flatwise moment, an increase of 17% in laminate fatigue strength is needed. This is approaching the range of what the preliminary test data indicate may be achieved. At present it can't be known with certainty that this would be acceptable, but the probability is certainly high enough that it is reasonable to consider its potential impact.

Discussion

Removing the carbon from the upwind blade shell appears feasible from a pure strength standpoint, if pre-sealed scarf construction can be economically used to make up the associated reduction of fatigue strength. There are at least two other effects which would need to be considered. The first of these is that the removal of the carbon will reduce the flow of load into the most highly loaded tension side root studs, while also reducing somewhat the net stiffness of the laminate into which they shed load. These effects are to a degree offsetting. It is possible that a small loss of root fatigue capability would result, in which case a small increase in stud length may be needed for those studs. Alternatively, carbon might be retained just near the root. It is also possible that the root would be fine "as is". This will need to be analyzed if the economics of carbon removal justify serious consideration of this change in the blade design.

Another consideration that affects both carbon and veneer removal is the impact on blade stiffness and dynamics. Review of the computed results shows about a 7% reduction in flatwise stiffness (EI) from removing the carbon, and about an 11% reduction if a layer of fir veneer is removed in addition. The impact this sort of change would have on the system dynamics is unknown, and is outside the scope of this preliminary design impact discussion. More likely than not, a softer blade flatwise would reduce the loads while increasing the motions. As long as tower

clearance is acceptable, the design would work. However, dynamic analysis would be needed to assure that loads do not increase due to system resonance.

****

REPORT FOR STATION 35% NoCarb-1 lam WITH FOIL L86 sta35%

****

Accuracy factor:0.50 Cut plane angle: 9.50 Me Axis Rotation Ang: 0.00

WEIGHT PER FOOT	FLATWISE EI	EDGEWISE EI	UPPER SURF FLATWISE MOMENT	FWD EDGE EDGEWISE MOMENT
28.112	2.350e+9	2.778e+10	1.724e+6	5.090e+6
CHORDWISE CG	**FLATWISE SHEAR CENTER**	**EDGEWISE SHEAR CENTER**	**UPPER SURF CRITICAL DISTANCE**	**FWD EDGE CRITICAL DISTANCE**
20.34	15.21	0.343	5.110	20.46
FLATWISE CG	**FLATWISE NEUTRAL AXIS**	**EDGEWISE NEUTRAL AXIS**	**LOWER SURF FLATWISE MOMENT**	**AFT EDGE EDGEWISE MOMENT**
0.259	0.331	20.46	1.268e+6	4.246e+6
ROTATIONAL MOMENT OF INERTIA	**AE PRODUCT**		**LOWER SURF CRITICAL DISTANCE**	**AFT EDGE CRITICAL DISTANCE**
4.607e+3	1.822e+8		6.947	24.54

LAYER SUMMARY DATA

****

X LEFT	X RIGHT	LEFT THICKNESS	RIGHT THICKNESS	WEIGHT	EDGEWISE FORCE	FLATWISE FORCE
0.00	45.00	0.020	0.020	0.541	76	589
0.00	45.00	0.020	0.020	0.556	51	-613
0.00	45.00	0.022	0.022	0.842	144	1103
0.00	45.00	0.022	0.022	0.866	98	-1148
0.00	45.00	0.912	0.912	11.308	13936	144116
0.00	45.00	0.812	0.812	10.056	-3417	-135781
0.00	45.00	0.022	0.022	0.752	57	797
0.00	45.00	0.022	0.022	0.816	84	-868
12.50	13.50	0.750	0.750	0.188	-1718	2967
12.50	13.50	1.000	1.000	0.254	-2314	-5854
13.50	13.80	5.000	5.000	0.219	-759	1161
13.50	13.80	6.000	6.000	1.714	-6238	-6469

TORSIONAL CELL DATA

****

X LEFT	X RIGHT	DS OVER T	AREA
0.00	13.65	0.000083	45.562
13.65	42.75	0.000180	98.973
0.00	13.65	0.000096	62.430
13.65	42.75	0.000207	62.287

****

There is another (minor) issue which must be considered if a veneer is only removed from the tension side of the blade, which these computations reflect. This un-symmetric removal would then cause a nose joint which is one veneer thinner on the upwind side of the blade than on the downwind side. It is not likely that this small difference would cause a problem, but it should be reviewed. Reducing the thickness on the downwind side to match is not considered a likely option, because buckling stability would be adversely affected, and this could reduce the static strength capability of the blade.

There is a quality control implication in the above discussion, and this is that the scarf joints must be very reliably bonded in the blade manufacturing process. Unbonded pre-sealed scarfs would perform no better than the existing scarfed laminate, and removal of the carbon would then be an uncompensated loss of strength. Joint bonding can be checked by examining and testing edge trimmings, among other methods, but it should be recognized that the process won't tolerate marginal joint bonding to the degree that the current design can, and that an associated QC cost may therefore exist.

Conclusions

The fatigue strength gained by the use of pre-sealed scarf joints appears capable of readily overcoming the loss of strength due to removing the upwind shell carbon reinforcing which is present in the current design. In fact, if further testing validates the preliminary test results, it appears likely that the blade could sustain a somewhat more rigorous fatigue regime, even with the carbon removed, than is the case now.

Going further, it appears that one layer of the upwind side veneers might also be removed, if no limitation other than fatigue strength is found to exist. In fact, issues such as possible system resonance or reduction of root strength may limit what can be done. This preliminary discussion can't address structural resonance, but there do appear to be sufficient ways to address root strength and other blade design issues which would result from removing the carbon, and possibly one veneer, in order to reduce blade cost. It does not appear that blade strength issues would limit these possibilities.

Alternatively, it may be advantageous to certify the blade to a more severe use class, at much lower cost than could be done without the improved laminate fatigue performance. In either case, the pre-sealed scarfs will have opened up new options, and extended the cost/performance envelope, well beyond what is possible today.

DISTRIBUTION

T. Almeida
TPI Inc.
225 Alexander Road
Portsmouth, RI 02871

H. Ashley
Dept. of Aeronautics and
Astronautics Mechanical Engr.
Stanford University
Stanford, CA 94305

B. Bell
Zond Systems Inc.
13000 Jameson Road
P.O. Box 1910
Tehachapi, CA 93561

K. Bergey
University of Oklahoma
Aero Engineering Department
Norman, OK 73069

C. P. Butterfield
NREL
1617 Cole Boulevard
Golden, CO 80401

G. Bywaters
Northern Power Technology Co.
Box 999
Waitsfield,VT 05673

J. Cadogan
U.S. Department of Energy
Office of Photovoltaic & Wind
Technology
Energy Efficiency & Renewable Energy
EE-11
1000 Independence Avenue SW
Washington, DC 20585

D. Cairns
Montana State University
Mechanical & Industrial Engineering Dept.
Bozeman, MT 59717

S. Calvert
U.S. Department of Energy
Office of Photovoltaic & Wind
Technology
Energy Efficiency & Renewable Energy
EE-11
1000 Independence Avenue SW
Washington, DC 20585

J. Chapman
OEM Development Corp.
840 Summer St.
Boston, MA 02127-1533

R. N. Clark
USDA
Agricultural Research Service
P.O. Drawer 10
Bushland, TX 79012

J. Cohen
Princeton Economic Research, Inc.
1700 Rockville Pike
Suite 550
Rockville, MD 20852

C. Coleman
Northern Power Co.
Box 999
Waitsfield, VT 05673

K. J. Deering
The Wind Turbine Company
515 116th Avenue NE
No. 263
Bellevue, WA 98004

E. A. DeMeo
Electric Power Research Institute
3412 Hillview Avenue
Palo Alto, CA 94304

A. J. Eggers, Jr.
RANN, Inc.
744 San Antonio Road, Ste. 26
Palo Alto, CA 94303

D. M. Eggleston
DME Engineering
P.O. Box 5907
Midland, TX 79704-5907

P. R. Goldman
Acting Deputy Director
Office of Photovoltaic and
Wind Technology
Energy Efficiency & Renewable
Energy, EE-11
U.S. Department of Energy
1000 Independence Avenue
Washington, DC 20585

G. Gregorek
Aeronautical & Astronautical Dept.
Ohio State University
2300 West Case Road
Columbus, OH 43220

C. Hansen
Windward Engineering
4661 Holly Lane
Salt Lake City, UT 84117

L. Helling
Librarian
National Atomic Museum
Albuquerque, NM 87185

C. Hiel
W. Brandt Goldsworthy & Assoc.
23930-40 Madison Street
Torrance, CA 90505

S. Hock
Wind Energy Program
NREL
1617 Cole Boulevard
Golden, CO 80401

K. Jackson
Dynamic Design
123 C Street
Davis, CA 95616

G. James
University of Houston
Dept. of Mechanical Engineering
4800 Calhoun
Houston, TX 77204-4792

M. Kramer
Foam Matrix, Inc.
PO Box 6394
Malibu CA 90264

O. Krauss
Division of Engineering Research
Michigan State University
East Lansing, MI 48825

R. Lynette
Springtyme Co.
212 Jamestown Beach lane
Sequim, WA 98382

D. Malcolm
Kamzin Technology Inc.
425 Pontius Avenue North
Suite 150
Seattle, WA 98109

J. F. Mandell
Montana State University
302 Cableigh Hall
Bozeman, MT 59717

T. McCoy
RLA
425 Pontius Avenue North
Suite 150
Seattle, WA 98109

R. N. Meroney
Dept. of Civil Engineering
Colorado State University
Fort Collins, CO 80521

P. Migliore
NREL
1617 Cole Boulevard
Golden, CO 80401

A. Mikhail
Zond Systems, Inc.
13000 Jameson Road
P.O. Box 1910
Tehachapi, CA 93561

W. Musial
NREL
1617 Cole Boulevard
Golden, CO 80401

NWTC Library (5)
NREL
1617 Cole Boulevard
Golden, CO 80401

V. Nelson
Department of Physics
West Texas State University
P.O. Box 248
Canyon, TX 79016

G. Nix
NREL
1617 Cole Boulevard
Golden, CO 80401

J. W. Oler
Mechanical Engineering Dept.
Texas Tech University
P.O. Box 4289
Lubbock, TX 79409

R. G. Rajagopalan
Aerospace Engineering Department
Iowa State University
404 Town Engineering Bldg.
Ames, IA 50011

Michael Robinson
NREL
1617 Cole Boulevard
Golden, CO 80401

D. Sanchez
U.S. Dept. of Energy
Albuquerque Operations Office
P.O. Box 5400
Albuquerque, NM 87185

L. Schienbein
CWT Technologies, Inc.
4006 S. Morain Loop
Kennewick, WA 99337

R. Sherwin
Atlantic Orient
PO Box 1097
Norwich, VT 05055

Brian Smith
NREL
1617 Cole Boulevard
Golden, CO 80401

K. Starcher
AEI
West Texas State University
P.O. Box 248
Canyon, TX 79016

F. S. Stoddard
Dynamic Design-Atlantic Office
P.O. Box 1373
Amherst, MA 01004

A. Swift
University of Texas at El Paso
320 Kent Ave.
El Paso, TX 79922

R. W. Thresher
NREL
1617 Cole Boulevard
Golden, CO 80401

W. A. Vachon
W. A. Vachon & Associates
P.O. Box 149
Manchester, MA 01944

B. Vick
USDA, Agricultural Research Service
P.O. Drawer 10
Bushland, TX 79012

L. Wendell
2728 Enterprise Dr.
Richland, WA 99352

R. E. Wilson
Mechanical Engineering Dept.
Oregon State University
Corvallis, OR 97331

S. R. Winterstein
Civil Engineering Department
Stanford University
Stanford, CA 94305

M. Zuteck
MDZ Consulting
931 Grove Street
Kemah, TX 77565

M.S. 0555	B. Hansche, 9133
M.S. 0557	T. J. Baca, 9119
M.S. 0557	T. G. Carne, 9119
M.S. 0708	H. M. Dodd, 6214 (25)
M.S. 0708	T. D. Ashwill, 6214 (10)
M.S. 0708	D. E. Berg, 6214
M.S. 0708	P. L. Jones 6214
M.S. 0708	D. L. Laird, 6214
M.S. 0708	M. A. Rumsey, 6214
M.S. 0708	H. J. Sutherland, 6214
M.S. 0708	P. S. Veers, 6214
M.S. 0836	W. Wolfe, 9116
M.S. 0847	D. W. Lobitz, 9234
M.S. 0847	D. R. Martinez, 9234
M.S. 0847	K. E. Metzinger, 9117
M.S. 0958	T. R. Guess, 1472
M.S. 0958	M. Donnelly, 1472
M.S. 0619	Review & Approval Desk, 00111 For DOE/OSTI
M.S. 0899	Technical Library, 4916 (2)
M.S. 9018	Central Technical Files, 8940-2